UNIVERSIDADE DE SÃO PAULO – USP
FACULDADE DE MEDICINA DE RIBEIRÃO PRETO
DEPARTAMENTO DE GENÉTICA

CLARISSA GONDIM PICANÇO DE ALBUQUERQUE

CARACTERIZAÇÃO DO GENE *PTEN* COMO BIOMARCADOR PROGNÓSTICO NO CÂNCER DE PRÓSTATA

CHARACTERIZATION OF *PTEN* GENE AS A PROGNOSTIC BIOMARKER IN PROSTATE CANCER

RIBEIRÃO PRETO - SP
2017

CLARISSA GONDIM PICANÇO DE ALBUQUERQUE

CARACTERIZAÇÃO DO GENE *PTEN* COMO BIOMARCADOR PROGNÓSTICO NO CÂNCER DE PRÓSTATA

CHARACTERIZATION OF *PTEN* GENE AS A PROGNOSTIC BIOMARKER IN PROSTATE CANCER

Tese apresentada à Faculdade de Medicina de Ribeirão Preto da Universidade de São Paulo, como requisito para obtenção do título de Doutora em Ciências, área de concentração: Genética

Orientador: Prof. Dr. Jeremy A. Squire
Coorientador: Prof. Dr. Rodolfo Borges dos Reis

RIBEIRÃO PRETO - SP

2017

FICHA CATALOGRÁFICA

Picanço-Albuquerque, Clarissa Gondim

Caracterização do gene *PTEN* como biomarcador prognóstico no câncer de próstata. Ribeirão Preto, São Paulo, 2017.

140p. : il.; 30cm.

Tese de Doutorado apresentada à Faculdade de Medicina de Ribeirão Preto, Universidade de São Paulo. Área de concentração: Genética.

Orientador: Squire, Jeremy A.
Coorientador: Reis, Rodolfo Borges

1. Câncer de Próstata; 2. PTEN; 3. Biomarcador; 4. Recorrência de doença; 5. Microambiente tumoral.

Picanço-Albuquerque, Clarissa Gondim

Characterization of *PTEN* gene as a prognostic biomarker in prostate cancer. Ribeirão Preto, São Paulo, 2017.

140p. : il.; 30cm.

Phd thesis presented to the Medical School of Ribeirão Preto, University of São Paulo. Area of concentration: Genetics.

Supervisor: Squire, Jeremy A.
Co-supervisor: Reis, Rodolfo Borges

1. Prostate cancer; 2. PTEN; 3. Biomarker; 4. Disease recurrence; 5.Tumor microenvironment.

FOLHA DE APROVAÇÃO

CLARISSA GONDIM PICANÇO DE ALBUQUERQUE

Caracterização do gene *PTEN* como biomarcador prognóstico no câncer de próstata

Tese apresentada à Faculdade de Medicina de Ribeirão Preto da Universidade de São Paulo, como requisito para obtenção do título de Doutora em Ciências, área de concentração: Genética

Orientador: Prof. Dr. Jeremy A. Squire
Coorientador: Prof. Dr. Rodolfo Borges dos Reis

Aprovada em: _____|_____|_____

BANCA EXAMINADORA

Prof. Dr _____

Instituição:_____ Assinatura:_____

Prof. Dr _____

Instituição:_____ Assinatura:_____

Prof. Dr _____

Instituição:_____ Assinatura:_____

Prof. Dr _____

Instituição:_____ Assinatura:_____

Prof. Dr _____

Instituição:_____ Assinatura:_____

Ao meu esposo,

Emanuel Veras de Albuquerque,

Aos meus filhos, Melissa e Emanuel Jr.,

Aos meus pais, Clovis e Walewska

E aos meus queridos irmãos e cunhadas.

"Ser profundamente amado por alguém nos dá força; amar alguém profundamente nos dá coragem."

(Lao-Tsé)

AGRADECIMENTOS

Ao meu Orientador **Prof. Dr. Jeremy Squire,** minha admiração e gratidão. Obrigada por acreditar que era possível, pela oportunidade de ser sua aluna quando eu ainda estava galgando os primeiros passos nessa jornada na vida acadêmica. Seu entusiasmo pela ciência contagia a todos, nos fortalece e nos motiva a seguir em frente, sempre. Obrigada pela oportunidade, confiança e todo aprendizado pessoal e profissional.

À **Profa. Dra. Lucia Regina Martelli**, pelo imenso incentivo antes mesmo de entrar nesse universo chamado pesquisa, por abrir portas e mostrar as opções a serem trilhadas, por estar sempre ao lado, nos motivando e fazendo acreditar. Obrigada pelo espaço cedido em seu laboratório, por me guiar como se fosse sua aluna e por confiar no meu trabalho. Obrigada por todo carinho e apoio nos momentos difíceis e o meu muito obrigada pela confiança, amor e amizade construídos ao longo desses anos.

Ao **Prof. Dr. Rodolfo Reis** pela coorientação e apoio constante. Obrigada pelo planejamento do projeto, por todas as trocas de ideias, sempre construtivas e por me ajudar a compreender melhor esse universo da urooncologia, facilitando a integração da ciências básica aplicada a prática clínica.

Ao **Prof. Dr. Luciano Neder** e **Dra. Lygia Yaegashi** por todo o tempo dedicado para a revisão e seleção dos casos clínicos e em especial ao **Dr. Fabiano Saggioro** pelo apoio constante, pelo o tempo dedicado, pela paciência e por me acompanhar em todas as análises, sempre disposto a ensinar e colaborar.

Às técnicas do Banco de tumor do Hospital de Barretos, **Bia e Fabiana**, por me ajudarem na confecção dos TMAs.

Ao meu grande amigo **Ciro Silveira** que embarcou comigo nos primeiros anos dessa jornada, pessoa dedicada e muito competente no que faz, que me ensinou o passo a passo da técnica de FISH, que me ajudou a escrever as primeiras páginas desse projeto, que me acompanhou durante a viagem ao Canadá e que deixou saudades ao voltar para Salvador. A você meu amigo, meu muito obrigada e meus votos de sucesso e felicidades.

À **Jennifer Good** por me ajudar a aprimorar a técnica de FISH, por sua amizade e receptividade durante os dias de trabalho na Queen´s University, Kingston, Canada, e à **Olga Ludkovski** pela colaboração na análise do FISH.

À **Dra. Tamara Lotan**, médica patologista do Johns Hopkins e ao meu amigo **Carlos Eduardo Lima**, meu conterrâneo e na época Fellow do Serviço de Patologia do Johns Hopkins, pela troca de experiência e colaboração na execução e análise da imunohistoquímica.

Aos amigos de laboratório e grandes companheiros de trabalho **Alexandra Galvão Gomes, Carlos Henrique Grangeiro, Flávia Gaona, Juliana Dourado, Juliana Josahkian**, **Livia Ferreira**, **Victoria Cortez** por todo apoio e parceria, pelas trocas de experiências, por estenderem a mão nos momentos difíceis e por estarem presentes em todos os outros bons momentos de festividade e comemoração que a vida em comunidade nos proporciona. Um agradecimento em especial, aos meus amigos, **Tatiana Mozer**, sempre disposta a ajudar e aprender, que assumiu a bancada durante a minha primeira gestação para que eu evitasse o contato com os reagentes, que dividiu comigo intensas emoções e que se tornou uma amiga para a vida inteira, e ao meu amigo, braço direito, **Thiago Vidotto**, sempre motivado e disposto, que vibra com os desafios, que gosta de aprender e compartilhar experiências. Obrigada meu amigo, por toda sua colaboração para o desfecho desse projeto, obrigada pelo apoio técnico e moral, pela sua amizade e pelo seu tempo dedicado nesse trabalho.

Ao **Departamento de Genética** da Faculdade de Medicina de Ribeirão Preto da Universidade de São Paulo pela oportunidade e estrutura oferecida e aos órgãos de fomento, Conselho Nacional de Pesquisa **(CNPq)** e Fundação de Apoio ao Ensino Pesquisa e Assistência do HCFMRP **(FAEPA)** pelo auxílio financeiro.

A todos que fizeram e fazem parte da "Família Bloco C" pelo apoio, companhia e amizade.

Aos amigos do programa de Pós-Graduação em Genética da FMRP USP e à Susie Nalon, secretária do programa pela atenção, suporte e orientação.

Aos membros da **banca examinadora** por todas as contribuições para a melhoria deste trabalho.

Aos **docentes**, aos **colegas de trabalho** e aos **queridos residentes** do Hospital das Clínicas de Ribeirão Preto, obrigada por estarem ao meu lado desde os primeiros dias, me incentivando nessa dupla caminhada.

Aos meus pais, **Clovis** e **Walewska**, que me prepararam para alcançar os objetivos com as próprias asas e que deram suporte e fortaleza, que sempre me ensinaram que estudo e dedicação eram peças chaves para o sucesso. Obrigada por todo apoio e compreensão nos momentos em que não pude estar presente. Aos meus queridos irmãos, **João Paulo, Marcelo e Clovis Jr.**, que sempre acreditaram e me apoiaram nessa trajetória, que vibram comigo como se fossem suas próprias vitórias.

Ao meu querido esposo, **Emanuel Veras de Albuquerque** por estar ao meu lado nessa longa caminhada entre residência médica, plantões e pós graduação, pelo apoio incondicional, pelos seus sábios conselhos, pelo seu amor e serenidade, me fazendo sentir acolhida e ao mesmo tempo confiante. Obrigada por compartilhar comigo também a maior e mais desafiante experiência dessa vida, a de sermos pais. Melissa e Emanuel Jr, nos permitiram conhecer o maior amor do mundo e nos tornaram pessoas melhores. À minha pequena e linda **Mel** obrigada por tanto encanto e amor, e ao meu pequeno **Emanuel Jr.** que vive intensamente comigo a finalização desse trabalho, obrigada pela companhia diária e pelos momentos de ternura que você me traz em meio a essa avalanche de sentimentos.

À Deus por me fortalecer nessa jornada, por me mostrar o caminho e me dar forças para seguir em frente, sempre.

"De todas as direções "certas" na vida, "seguir em frente" é a que nos leva mais longe."

(Diego Vinícius)

RESUMO

PICANÇO-ALBUQUERQUE, C. G. Caracterização do gene *PTEN* como biomarcador prognóstico no câncer de próstata. 2017, 140p. Tese de Doutorado – Faculdade de Medicina de Ribeirão Preto, Universidade de São Paulo.

O gene supressor tumoral PTEN é um biomarcador promissor no câncer de próstata. Importantes evidências biológicas indicam que a sua perda de função está associada a agressividade da doença. Esse estudo tem como objetivo identificar o efeito da perda de PTEN em características clínicas em coortes distintas de câncer de próstata Gleason 7 do Brasil e dos Estados Unidos. Com isso, será possível melhorar a estratificação de risco utilizando a perda de PTEN como indicador de mau prognóstico. Além disso, estudos do nosso grupo têm identificado que a perda de PTEN está associada à alteração no perfil de infiltração de células T no microambiente tumoral. Nos pacientes brasileiros, a frequência de perda de PTEN foi avaliada em 43 indivíduos submetidos à prostatectomia radical através das técnicas de hibridação *in situ* por fluorescência (FISH) e imunohistoquímica (IHC). Na amostra americana, tivemos duas cortes distintas: uma composta por 244 casos de prostatectomia radical derivadas de uma análise *in silico* obtida do The Cancer Genome Atlas (TCGA) e outra amostra de um estudo de caso controle derivada de 111 biópsias do Johns Hopkins Medical School. Esta última análise evidenciou que a perda do PTEN por FISH e IHC foi preditivo para *upgrade* após prostatectomia radical. Nossos resultados indicaram que a frequência da perda de PTEN foi similar entre todas as coortes analisadas (~20%). Na amostra brasileira, utilizando FISH e IHC, observamos uma associação significativa entre a perda de PTEN e fatores de pior prognóstico, assim como uma tendência para recorrência bioquímica mais precoce. Na análise de variação de número de cópias das amostras Gleason 7 do TCGA, observamos alterações concomitantes no genoma em pacientes que apresentavam deleção em homozigose ou hemizigose. Além disso, na análise *in silico,* observamos uma associação entre deleção do *PTEN* e extensão extraprostática ($P = 0.05$) assim como recorrência de doença ($P = 0.03$). Também observamos uma maior frequência de deleção de *PTEN* em homens brancos quando comparados à negros e asiáticos ($P = 0.01$). Através de IHC, avaliamos a taxa de infiltração de células T CD8+ no microambiente tumoral da amostra brasileira. Observamos uma tendência para uma maior taxa de infiltração de células T CD8+ nos casos que apresentam deleção de *PTEN* em homozigose. Nesta tese, o gene *PTEN* foi caracterizado como um biomarcador informativo para estratificação de risco do câncer de próstata devido as suas diversas funções e seu alto impacto na proliferação e sobrevivência celular. Além disso, PTEN apresenta um papel emergente como biomarcador da resposta imune no microambiente tumoral.

Palavras-chaves: 1. Câncer de próstata; 2. PTEN; 3. Biomarcador; 4. Recorrência de doença; 5. Microambiente tumoral.

ABSTRACT

PICANÇO-ALBUQUERQUE, C. G. Characterization of *PTEN* gene as a prognostic biomarker in prostate cancer. 2017, 140p. Phd Thesis - Medical School of Ribeirão Preto, University of São Paulo.

The *PTEN* tumor suppressor gene is a promising biomarker for prostate cancer with strong biological evidence that its loss of function will be associated with aggressive disease. This thesis was designed to identify the association between PTEN loss and the clinical outcome in homogeneous Gleason score 7 prostate cancer cohorts from Brazil and the USA for improved stratification of the use of loss of *PTEN* as an indicator of poor prognosis. In addition, ongoing correlative studies are showing an association between PTEN loss and altered T-cell infiltration in the tumor-tissue microenvironment (TME). From the Brazilian cohort, we performed a correlative evaluation of PTEN loss from 43 patients undergoing radical prostatectomy through Fluorescence *in situ* hybridization (FISH) and immunohistochemistry (IHC). From the USA, we evaluated two cohorts: an *in silico* analysis of 244 radical prostatectomy tumors obtained from The Cancer Genome Atlas (TCGA), and a case control cohort of 111 needle biopsies from the Johns Hopkins Medical School. The analysis of the case controls showed that PTEN loss by FISH and IHC was predictive of the upgrade to in radical prostatectomy. Collectively, these studies sindicate that the frequency of PTEN loss the cohort studies, using FISH, IHC and in an *in silico* analysis of array-CGH were similar (~20%). By FISH and IHC in the Brazilian cohort, we observed a significant association between *PTEN* loss and worse prognosis and a trend for the occurrence of earlier biochemical recurrence. In the copy number landscape of the Gleason 7 patients from the TCGA cohort, we observed concomitant alterations in the genome of patients that harbored *PTEN* homozygous or hemizygous deletions. For this *in silico* analysis, we found that *PTEN* gene deletion is associated with the extraprostatic extension (*P*-value = 0.05) and with disease recurrence (*P*-value = 0.03). We also observed that *PTEN* deletion events may occur with more frequency in white men (*P*-value = 0.01) when compared to Asians and African American men. By IHC, we evaluated the rate of CD8+ T-cell infiltration in the TME of the prostate cancer samples from the Brazil cohort. CD8+ T-cell showed a trend to a significant increased CD8+ TIL infiltration in samples that harbored *PTEN* homozygous deletions. In this thesis, *PTEN* gene has been characterized as an informative biomarker for prostate cancer stratification and outcome prediction due to its functionality and impact in cell proliferation and also appearing to have an emerging role as a biomarker of immune response in the tumor-tissue microenvironment.

Keywords: 1. Prostate cancer; 2. PTEN; 3. Biomarker; 4. Disease recurrence; 5.Tumor microenvironment.

LIST OF ILLUSTRATIONS

LIST OF TABLES

LIST OF ABBREVIATIONS

aCGH - array Comparative Genomic Hybridization

APCs - Antigen-presenting cells

AR - Andrapcogen receptor

ASAP - Atypical small acinar proliferation

AUA - American Urological Association

CRPC - Castrate resistant prostate cancer

DRE - Digital rectal examination

FDA - Food and Drug Administration

FFPE - Formalin fixed paraffin embedded

FISH - Fluorescence *in situ* hybridization

HCRP - Clinical Hospital of Ribeirão Preto Medical School

HPIN - High Grade Prostatic Intraepithelial Neoplasia

IFN - Interferon

IHC - Immunohistochemistry

INCA - Brazilian National Cancer Institute

mCRPC - Metastatic castrate resistant prostate cancer

NK - natural killer T-cells

PCa - Prostate Cancer

PHTS - *PTEN* Hamartoma Tumor Syndrome

PI3K - Phosphatidylinositol-4,5-bisphosphate 3-kinase

PIN - Prostatic intraepithelial Neoplasia

PSA - Prostate-specific antigen

PTEN - Phosphatase and TENsin homolog

STAT - Signal transducer and activator of transcription

TCGA - The Cancer Genome Atlas

TMA - Tissue micro-array

TME - Tumor microenvironment

TNM - Tumor, Node invasion and metastasis

WES - Whole exome sequencing

SUMMARY

1 Introduction

1.1 Prostate Cancer

1.1.1 Epidemiology

Prostate Cancer (PCa) is the most common solid tumor in men and is the third more common cancer type in the world (Howlader et al., 2017). In the United States, it is estimated that 161,360 new PCa cases will be diagnosed in 2017. Currently, PCa is the third most common death caused by cancer in men, with lung and bronchus cancer and cancer of the colon and rectum being more common (Siegel, Miller, & Jemal, 2017) (Figure 1).

Estimated New Cases

Males				Females		
Prostate	161,360	19%		Breast	252,710	30%
Lung & bronchus	116,990	14%		Lung & bronchus	105,510	12%
Colon & rectum	71,420	9%		Colon & rectum	64,010	8%
Urinary bladder	60,490	7%		Uterine corpus	61,380	7%
Melanoma of the skin	52,170	6%		Thyroid	42,470	5%
Kidney & renal pelvis	40,610	5%		Melanoma of the skin	34,940	4%
Non-Hodgkin lymphoma	40,080	5%		Non-Hodgkin lymphoma	32,160	4%
Leukemia	36,290	4%		Leukemia	25,840	3%
Oral cavity & pharynx	35,720	4%		Pancreas	25,700	3%
Liver & intrahepatic bile duct	29,200	3%		Kidney & renal pelvis	23,380	3%
All Sites	**836,150**	**100%**		**All Sites**	**852,630**	**100%**

Estimated Deaths

Males				Females		
Lung & bronchus	84,590	27%		Lung & bronchus	71,280	25%
Colon & rectum	27,150	9%		Breast	40,610	14%
Prostate	26,730	8%		Colon & rectum	23,110	8%
Pancreas	22,300	7%		Pancreas	20,790	7%
Liver & intrahepatic bile duct	19,610	6%		Ovary	14,080	5%
Leukemia	14,300	4%		Uterine corpus	10,920	4%
Esophagus	12,720	4%		Leukemia	10,200	4%
Urinary bladder	12,240	4%		Liver & intrahepatic bile duct	9,310	3%
Non-Hodgkin lymphoma	11,450	4%		Non-Hodgkin lymphoma	8,690	3%
Brain & other nervous system	9,620	3%		Brain & other nervous system	7,080	3%
All Sites	**318,420**	**100%**		**All Sites**	**282,500**	**100%**

Figure 1. Estimate of new cancer cases and deaths by sex in the United States, 2017 (Siegel et al., 2017).

The last estimation from the Brazilian National Cancer Institute (INCA) (Instituto Nacional de Cancer José Alencar Gomes da Silva, 2016) predicted the diagnosis of 61,200 new prostate cancer cases Brazil in 2016. These values correspond to an estimated risk of 61.82 new cases for each 100,000 men. Estimations for Brazil for the years 2016 and 2017 demonstrates the occurrence of 600,000 new cancer cases. If non-melanoma skin cancer is excluded, the most frequent cancer types newly diagnosed in Brazil will be prostate (28.6%), lung (8.1%), bowel (7.8%), stomach (6.0%) and oral cavity (5.2%). These data illustrate an important clinical feature of prostate cancer: the high prevalence in the population with low mortality (Siegel et al., 2017) (Figure 2 and Figure 3).

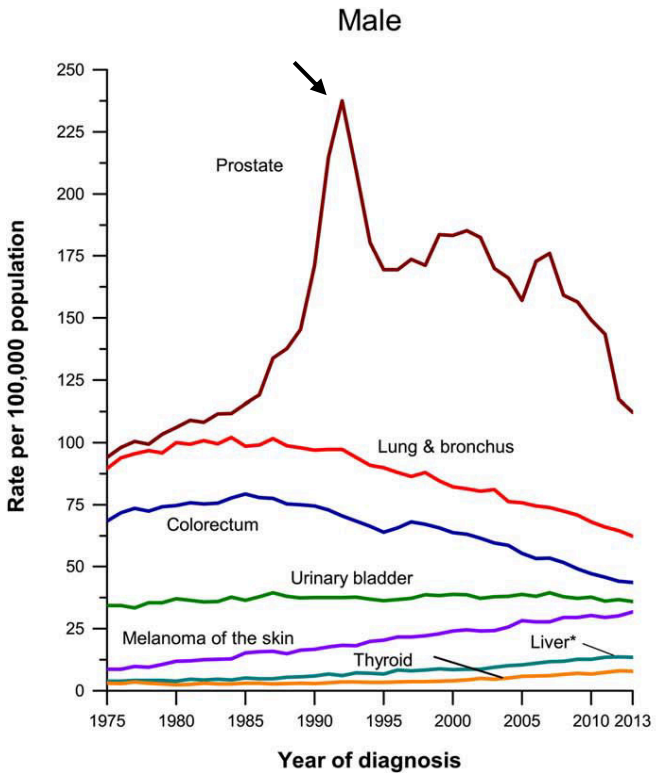

Figure 2. Incidence Rates for Selected Cancers in the United States between 1975 and 2013. *Includes intrahepatic bile duct. The arrow shows a fast increase of prostate cancer diagnosis due to the use of PSA as a biomarker during the decade of 1980 and 1990. Adapted from (Siegel et al., 2017).

PCa is strongly associated with age. Only 5% of men under the age 30 will be diagnosed with PCa, but the rate increase sharply during middle age with 59% of men >79 years (Bell, Del Mar, Wright, Dickinson, & Glasziou, 2015). Studies have also shown a large difference in disease incidence and death rates: 16-17% of men expect to be diagnosed with prostate cancer during their lifetime. However, the death risk of this disease is about 3% since the older age of men and the long duration of the disease process often mean they die from other causes. The indolence of the disease, the age of patients and tumor heterogeneity may explain this variability of incidence and mortality due to prostate cancer, suggesting that the therapeutic decision of each patient should be carefully considered (Siegel et al., 2017; Wilt et al., 2012).

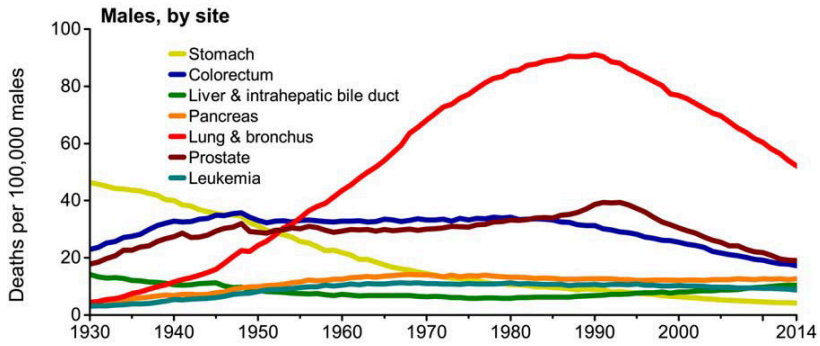

Figure 3. Death rates for malignancies in men in United States between 1930 and 2014. Due to improvements in International Classification of Diseases (ICD) coding over time, numerator data for cancers of the lung and bronchus, colon and rectum, liver, and uterus differ from the contemporary period. (Siegel et al., 2017)

1.1.2 Screening

Due to its high prevalence and cost, screening programs are increasingly discussed around the world and still remains a controversial topic (Heijnsdijk et al., 2009). Prostate-specific antigen (PSA) and digital rectal examination (DRE) are used to assess prostate cancer risk in conjunction with other clinical factors (Mottet et al., 2017).

The prostatic specific antigen is a protease of the kallikrein family that is synthesized in the prostatic epithelium and is secreted in the seminal fluid. The primary function of PSA is the liquefaction of the seminal fluid. Since the discovery of PSA in 1979 and the Food and Drug Administration (FDA) approval in 1986 as a biomarker in plasma, this protein became an important tool in the early diagnosis, treatment and follow up of the patients with malignant prostatic neoplasia. PSA levels are relevant in the patient's follow up after the radical prostatectomy and in the active surveillance of PCa. After the radical prostatectomy, biochemical recurrence is defined as the increase in PSA concentrations to 0.2ng/mL after reaching undetectable or very low (<0.04 ng/mL) levels. In this context, PSA dosage has 100% specificity and sensitivity for the disease (Reis & Cassini, 2010).

Men with abnormalities on DRE often show a great risk of presenting with prostate cancer. In this way, most urologists use PSA and DRE for prostate cancer detection. Further, PSA testing improves the positive predictive value of DRE for cancer. The positive predictive value of DRE ranges from 4% to 11% in patients having PSA levels of 0 to 2.9 ng/mL and from 33% to 83% in patients with PSA levels between 3 and 9.9 ng/mL or greater (Wein, Kavoussi, Partin, & Peters, 2016). Because DRE and PSA tests do not always detect the same cancers, the tests are complementary (Okotie et al., 2007).

The use of PSA brought benefits for the early diagnosis of PCa. However, this method also led to controversies about the overtreatment due to the indolence of some cases, suggesting that most PCa cases should be individually discussed (Carter et al., 2013; Draisma et al., 2009; Etzioni, Cha, Feuer, & Davidov, 1998). American Urological Association (AUA) recommend an informed and shared decision-making process, which should reflect the patient's understanding of the benefits and risks and should respect their preferences and values. The screening should be applied to men between 55 and 69 years of age.

1.1.3 Diagnosis and risk stratification

The diagnosis of prostate cancer is performed through the microscopic evaluation of prostate tissue obtained via needle biopsy. (Litwin & Tan, 2017). Moreover, from the biopsy, pathologists can classify pre-malignant and malignant lesions of the prostate.

Prostatic intraepithelial Neoplasia (PIN) is considered to be the most likely pre-invasive stage of adenocarcinoma, and its histological detection in biopsy is regarded as one of the most important risk factors for prostate cancer development (Bostwick & Qian, 2004; McNeal et al., 1986). The diagnosis of High Grade Prostatic Intraepithelial Neoplasia (HPIN) indicates that a repeat biopsy should be performed (Epstein & Herawi, 2006; Merrimen et al., 2009). HPIN is characterized by cellular proliferation within pre-existing ducts and glands that show cytological changes similar to cancer, including nuclear and nucleolar enlargement, usually with hyperchromatism. Unlike the adenocarcinoma of the prostate, HPIN is confined to the gland by the intact basement membrane and a well-defined basal cell layer. HPIN is detected in up to 70-80% of prostate glands that show the presence of carcinoma (Qian & Bostwick, 1995). Similar to the carcinoma, HPIN incidence increases with age and precedes cancer initiation by more than 5 years. Early pre-neoplastic genetic events in HPIN are most likely to drive the tumorigenic process in the prostate gland.

The atypical small acinar proliferation (ASAP) is also a histological finding in prostate glands. ASAP assigns different uncertain entities of the cytological and architectural features of the prostate carcinoma. Moreover, ASAP is diagnosed in 1-2% of prostate biopsies. There is a little consistency between pathologists about this criterion, but most of the glands that show glandular atypia that is not sufficient for an adequate diagnosis of prostate adenocarcinoma will be classified as ASAP. Studies have shown that 17-70% of patients that have ASAP may present adenocarcinoma in subsequent biopsies. Moreover, patients with

ASAP can be followed using PSA levels and DRE every 4-6 months with a repeat biopsy (Epstein & Herawi, 2006; Ericson et al., 2017; Lusky, 1997).

The initial histologic grade is determined on any malignant lesion, and this is the most important information from a prostate needle biopsy for planning treatment. The Gleason grading system is the most commonly used (Gleason, 1966) to classify these lesions. At low-power magnification, the Gleason score is constituted by the sum of a grade (1 to 5) assigned to the predominant pattern in the specimen and the second most common pattern of the tissue. This yields a score that ranges from 2 to 10 (Gleason & Mellinger, 1974; Mellinger, Gleason, & Bailar, 1967) (Figure 4). The architectural patterns of the glands are classified by considering their level of differentiation with 1 being the most differentiated and 5 being undifferentiated. Currently, the most common and second most common grades were combined and the Gleason system was updated to consider the *most common* and *highest-grade* patterns on a given core (Epstein, Allsbrook, Amin, Egevad, & ISUP Grading Committee, 2005).

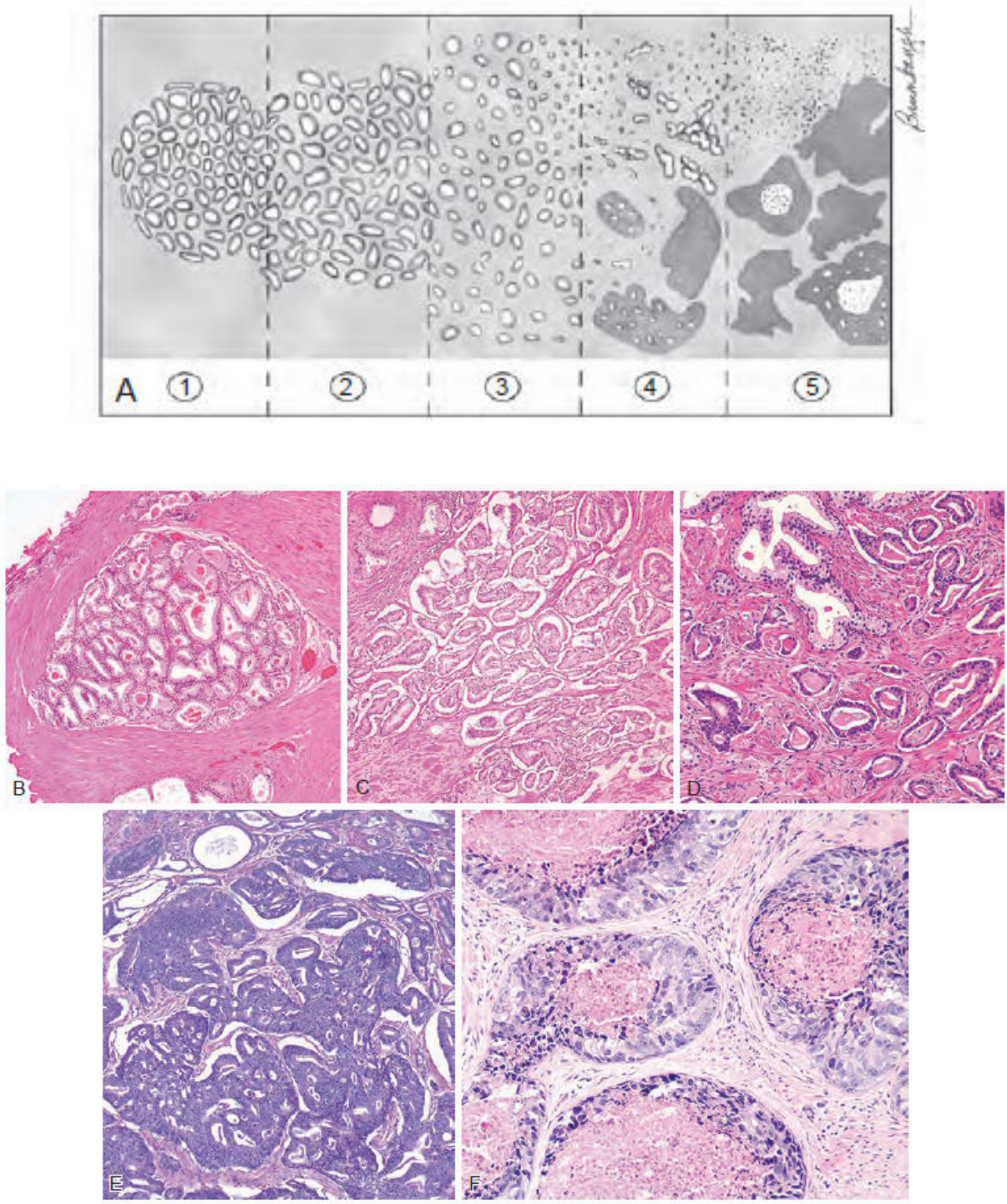

Figure 4. The Gleason grading system. A. Schematic diagram of the Gleason grading system. B, Gleason pattern 1: well-circumscribed nodule of closely packed glands. C, Gleason pattern 2: nodule with more loosely arranged glands. D, Gleason pattern 3: small glands with an infiltrative pattern between benign glands. E, Gleason pattern 4: large irregular cribriform glands. F, Gleason pattern 5: solid nests of tumor with central comedonecrosis (Wein et al., 2016).

The clinical staging of prostate cancer considers pre-treatment parameters to predict the extent of disease, prognosis and appropriate treatment. (Wein et al., 2016). The diagnosis and staging of the disease are assessed through DRE, serum PSA levels, needle biopsy findings, and imaging. Pathological staging, however, is determined after radical prostatectomy and involves histologic analysis of the prostate, seminal vesicles, and pelvic lymph nodes. Pathologic staging is more accurate and estimates the real disease burden and predicts the outcome prediction (Pound, Partin, Epstein, & Walsh, 1997). Biochemical recurrence-free survival and cancer-specific survival are both inversely related to the pathologic stage of disease (Roehl, Han, Ramos, Antenor, & Catalona, 2004).

Currently, the clinical staging is based on the Tumor, Node invasion and metastasis (TNM) classification system (Table 1). This system was first adopted by the American Joint Committee on Cancer (AJCC) in 1975 and has undergone numerous modifications since then (Edge & Compton, 2010). In the most recent version, the TNM staging is combined with PSA levels and Gleason score of the diagnostic biopsy to classify newly diagnosed prostate cancer tumors into prognostic groups. The Gleason score at biopsy provides the only pathological information if a non-surgical treatment modality is chosen, since there will be no tumor available for more accurate Gleason evaluation provided by prostatectomy (see section 1.1.5). Several classification schemes were proposed that correlate with clinical outcomes. D'Amico et al. (2001) (Table 2) demonstrated that the stratification of the disease into low-risk (T1 to 2a, PSA <10 ng/mL and Gleason score ≤6), intermediate-risk (T2b or PSA ≥10 but <20 ng/mL or Gleason score 7), and high-risk disease (T2c, or PSA ≥20 ng/mL or Gleason score 8 to 10) significantly correlated with freedom from disease at 10 years after radical prostatectomy for 83% for low-risk, 46% for intermediate-risk, and 29% for high-risk disease. Other validated classification methods were developed and included the Cancer of the Prostate Risk Assessment (CAPRA) score (Cooperberg et al., 2005, 2006; May et al., 2007).

Moreover, due to the heterogeneity of prostate cancer and the common occurrence of indolent cases, the pre-treatment risk stratification using multiple parameters is useful for patient counseling.

Table 1. Tumor Node Metastasis (TNM) classification prostate cancer.

T - Primary Tumour		
TX	Primary tumour cannot be assessed	
T0	No evidence of primary tumour	
T1	Clinically inapparent tumour that is not palpable	
	T1a	Tumour incidental histological finding in 5% or less of tissue resected
	T1b	Tumour incidental histological finding in more than 5% of tissue resected
	T1c	Tumour identified by needle biopsy (e.g. because of elevated prostate-specific antigen (PSA) level)
T2	Tumour that is palpable and confined within the prostate	
	T2a	Tumour involves one half of one lobe or less
	T2b	Tumour involves more than half of one lobe, but not both lobes
	T2c	Tumour involves both lobes
T3	Tumour extends through the prostatic capsule[1]	
	T3a	Extracapsular extension (unilateral or bilateral) including microscopic bladder neck involvement
	T3b	Tumour invades seminal vesicle(s)
T4	Tumour is fixed or invades adjacent structures other than seminal vesicles: external sphincter, rectum, levator muscles, and/or pelvic wall	
N - Regional Lymph Nodes[2]		
NX	Regional lymph nodes cannot be assessed	
N0	No regional lymph node metastasis	
N1	Regional lymph node metastasis	
M - Distant Metastasis[3]		
M0	No distant metastasis	
M1	Distant metastasis	
	M1a	Non-regional lymph node(s)
	M1b	Bone(s)
	M1c	Other site(s)

[1]Invasion into the prostate apex or into (but not beyond) the prostate capsule is not classified as T3, but T2.
[2]Metastasis no larger than 0.2cm can be designated pNmi.
[2]T2a to c only exist for clinical (cT2). For pathological T2 they are no longer present in the 2017 TNM. Only pT2 exists.
[3]When more than one site of metastasis is present, the most advanced category is used. (p)M1c is the most advanced category.

https://uroweb.org/guideline/prostate-cancer/#4

Table 2. D'Amico et al risk stratification for clinically localized prostate cancer.

Low risk	Diagnostic PSA < 10 ng/mL *and* highest biopsy Gleason score ≤ 6 *and* clinical stage T1c or T2a
Intermediate risk	Diagnostic PSA ≥ 10.0 but < 20 ng/mL *or* highest biopsy Gleason score = 7 *or*clinical stage T2b
High risk	Diagnostic PSA ≥ 20 ng/mL *or* highest biopsy Gleason score ≥ 8 *or* clinical stage T2c/T3

1.1.4 Treatment

The complexity of treating this complex disease is well-documented in prostate cancer therapeutic studies (Okotie et al., 2007; Roehl et al., 2004; Venderbos et al., 2015). The populations of patients are often heterogeneous and not comparable due to their different stratification and due to a lack of standardization of outcome measurements (e.g. different definitions for relapse, such as biochemical recurrence, after surgery or radiotherapy). Prostate cancer is very diverse, varying from indolent disease to a highly aggressive cancer that metastasizes to different organs. Physicians are advised to evaluate the need of treatment together with the assessment the preferences of each patient (Wein et al., 2016).

There are various treatment options for prostate cancer patients, including surgery; radiation; hormonal therapy; chemotherapy; targeted therapy, and immunotherapy. To reduce overtreatment of indolent disease, active surveillance has emerged as a viable management option for men with low-risk prostate cancer (Welty, Cooperberg, & Carroll, 2014). However, in the decision for surgery, patients with PCa have their prostate, seminal vesicles and, when necessary, lymph nodes removed. The radical prostatectomy can be performed through an open, laparoscopic or robotic approach. Most radical prostatectomies require nerve spanning,

which sometimes may be invaded by the neoplastic lesion (Quaranta, Marks, & Anscher, 2004).

PSA measurement is a key element during follow-up after local treatment. Furthermore, PSA recurrence often precedes clinical recurrence. A single, elevated, serum PSA levels should be confirmed before deciding for second-line therapy (Horwitz et al., 2005; Stephenson et al., 2006). After a successful radical prostatectomy, PSA levels are expected to be undetectable within six weeks. Elevated persistent PSA levels in patients treated with radical prostatectomy may indicate the presence of residual cancer, either micro- metastases or residual pelvic disease (Stamey et al., 1989).

Radiotherapy is efficient due to its specific damaging effects on DNA in proliferating cells so that cancer cells accumulate mutations and DNA breakages over time, and undergo apoptosis leading to cell death. Radiation treatments are often guided by CT scans and are unique for each PCa case (Wein et al., 2016).

Hormonal therapy is based on testosterone deprivation through luteinizing hormone-releasing hormone (LHRH) or androgen receptor (AR) blockade (Pagliarulo et al., 2012). Once cells of the prostate require testosterone to grow, the deprivation of this hormone will lead to reduced cell growth and proliferation. Hormonal therapy, however, leads to a series of side effects, such as urinary and sexual dysfunction, together with the loss of muscle mass, bone density, reduced metabolism, weight gain and even depression (Wein et al., 2016).

During hormonal therapy, some patients exhibit tumor growth despite the treatment with testosterone deprivation (Figure 5). These patients often show an increase in AR receptors or AR gain of function mutations that show high activity even in small concentrations of testosterone. PCa disease, in this case, is designed as castrate resistant prostate cancer (CRPC). CRPC may be present as one or any combination of a continuous increase in serum PSA levels, progression of the pre-existing disease, or appearance of new

metastases. Bone metastases are present in 90% of men with CRPC, leading to significant morbidity, including fractures, bone pain, bone marrow failure and spinal cord compression. Other effects, such as anemia, weight loss, fatigue, hypercoagulability, and increased susceptibility to infection are also observed (Mottet et al., 2017).

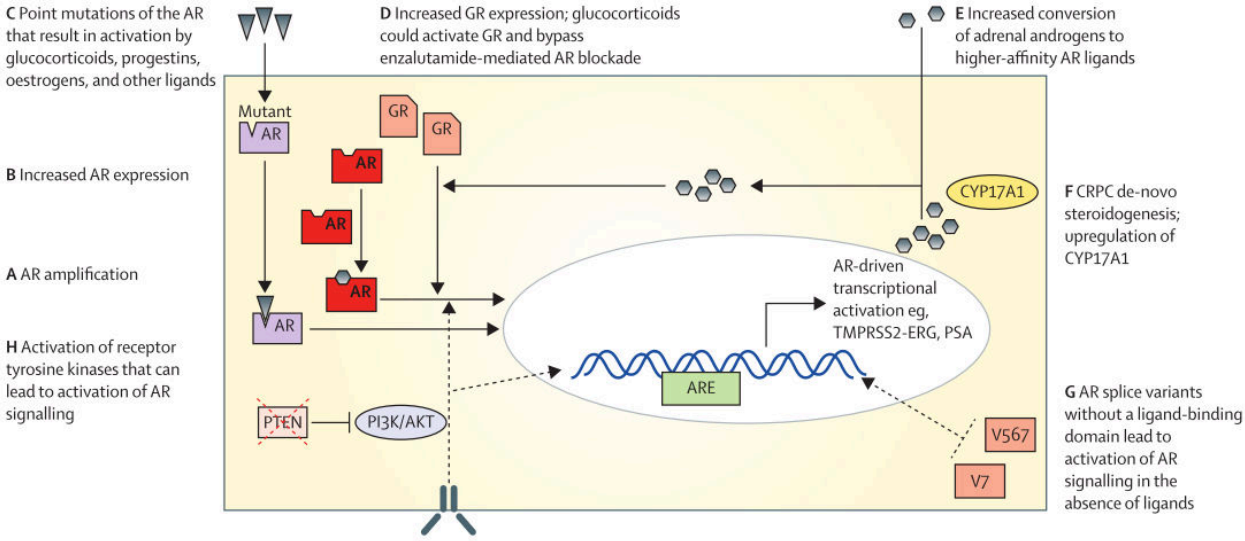

Figure 5. Mechanisms that underlie CRPC. Different genomic markers in prostate cancer may impact castration resistance disease due to their direct effect on androgen receptors, such as *PTEN*, as well as other mutational processes that occur in AR that promotes its activation even in the absence of testosterone (Attard et al., 2016).

Patients with CRPC exhibit more aggressive patterns of the disease and are treated with super castration chemotherapies, such as abiraterone, which blocks AR synthesis in the testicles and adrenal gland and enzalutamide, which is an ultra-androgen receptor blocker. Both drugs can provoke side-effects such as fatigue and seizures. However, unfortunately many patients with CRPC treated with hormone deprivation therapies still experience relapse and progression to metastatic CRPC (mCRPC). There are some new chemotherapeutic agents being developed to treat patients with mCRPC, and the most promising treatments are based on the activation of the natural anti-tumor activities of the immune system of the patient. These treatments are designed as immunotherapies (Ciccarese et al., 2017; Gerritsen, 2012; Wein et al., 2016).

1.1.5 Challenges in Therapeutic Decision

Prostate cancer varies from an indolent disease that might not cause symptoms during a patient's lifetime to a highly aggressive malignancy that presents early metastasis and causes terrible suffering and premature death. As discussed in section 1.1.3 the clinical tools currently available to help guide therapeutic treatment decisions in the USA include PSA level, number of positive core biopsies, percent of cores involved by tumor, and Gleason score (Cooperberg et al., 2005, 2006; May et al., 2007). However, the Gleason score of the initial positive biopsy sample, which remains the most powerful prognostic marker, is inaccurate in a large percentage of patients especially when only a small volume tumor is sampled during biopsy. Gleason score 6 detected in biopsy cores is particularly problematic as it is one of the low group parameters, but it has the highest likelihood for upgrading to a higher score after radical prostatectomy sample (Garnett, Oyasu, & Grayhack, 1984). Likewise, clinical stage poorly estimates the final pathological stage, which is also one of the most important predictors of clinical outcome. There is thus an urgent need for biomarkers that can clearly distinguish aggressive from indolent forms of prostate cancer. Such biomarkers could help the clinician who manages patients with prostate cancer to advise on effective treatment in those for whom treatment is necessary. Biomarkers may also provide information on the pathways that are active and actionable in patients with more aggressive disease.

In this way, improvements in prostate imaging, biomarker discovery, tumor genetic profiling and immunotherapies will very likely change the approach to management of men diagnosed with prostate cancer.

1.2 PTEN

1.2.1 Biology and structure of the *PTEN* tumor suppressor

Phosphatase and TENsin homolog (*PTEN*) is located in 10q23.31 and is the most common somatically mutated tumor suppressor gene in a variety of human malignancies (reviewed in Wise 2017). The *PTEN* gene consists of 9 exons and encodes 403 amino acids (PTPs) (Song, Salmena, & Pandolfi, 2012) (Figure 6).

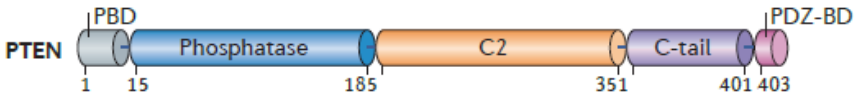

Figure 6. Structure of the *PTEN* tumor suppressor. The domain structure of phosphatase and tensin homologue (*PTEN*). *PTEN* is a 403 amino acid protein that is composed of five functional domains: a phosphatidylinositol-4,5-bisphosphate (PtdIns(4,5)P2)-binding domain (PBD), a phosphatase domain, a C2 domain, a carboxy-terminal tail and a PDZ-binding domain (Song et al., 2012).

The PTEN protein acts as a dual-specificity phosphatase and a direct antagonist of PI3K signaling by reverting the second messenger phosphoinositol- 3,4,5-trisphosphate (PIP3) into PIP2, which does not activate downstream signaling (Maehama & Dixon, 1998a). Loss and/or inactivating mutation of the *PTEN* gene leads to activation of the phosphatidylinositide 3-kinases (PI3K) signaling pathway, which is up-regulated in 30–50% of prostate cancers cases (Hopkins, Hodakoski, Barrows, Mense, & Parsons, 2015; Pulido, 2015). The PI3K family is complex and the encoded proteins fall into three classes (I, II, III) based on the genes, their distinct structures and isoform substrate preference. There are four members in class I, with the subdivisions of PI3Kα, PI3Kβ and PI3Kδ into class IA and PI3Kγ into class IB. The PI3K pathway is activated by different receptor tyrosine kinases, including platelet-derived growth factor receptor (PDGFR), epidermal growth factor receptor (EGFR) and insulin-like growth factor receptor (IGFR) (Figure 7).

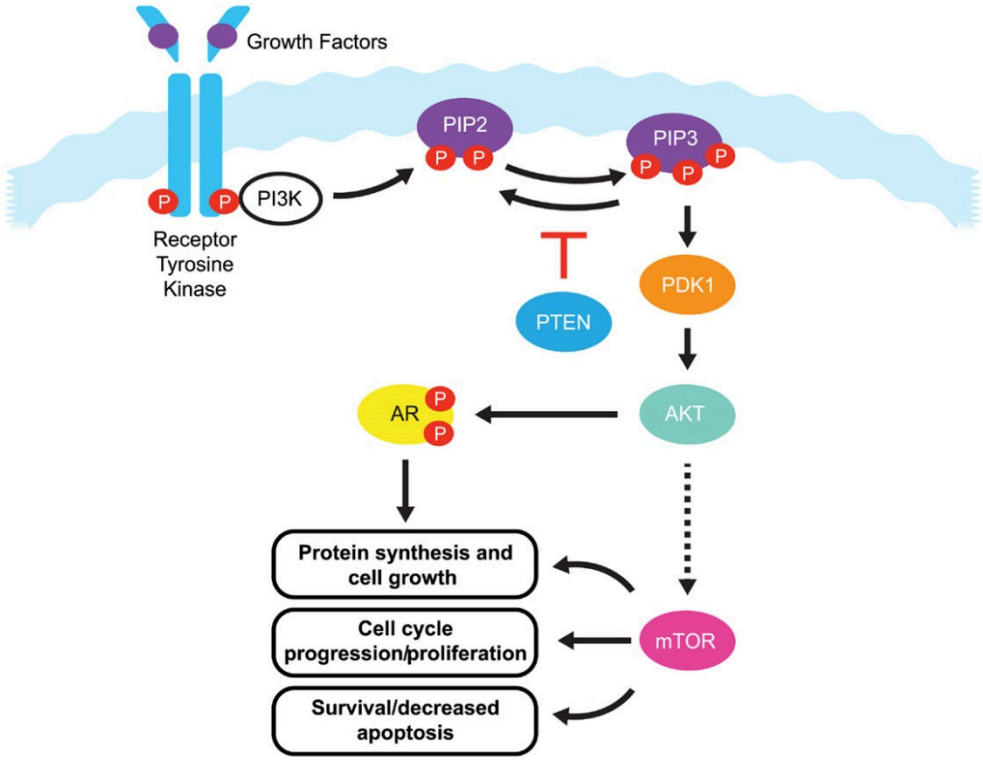

Figure 7. The PI3K/PTEN/Akt pathway. The activation of tyrosine kinase receptors by growth factors recruits and activated PI3K, which regulates the PDK1 mediated Akt phosphorylation by converting PIP2 to PIP3. Akt, when phosphorylated, targets mTOR, which is associated with cell grown, proliferation and survival. Moreover, activated Akt interacts with AR in an androgen-independent manner, leading to over-activation of AR signaling pathway. *PTEN* is a tumor suppressor gene that negatively regulates Akt activation by converting PIP3 to PIP2. In this way, PTEN loss leads to increased cell proliferation, growth, and survival. In addition, PTEN loss is associated with CRPC due to the maintained AR activation even in the absence of testosterone (Phin, Moore & Cotter, 2013).

These receptors, when activated, phosphorylate PI3K at the cell membrane. The phosphorylated PI3K then phosphorylates phosphatidylinositol-4,5-diphosphate (PIP2), leading to the accumulation of phosphatidylinositol-3,4,5-triphosphate (PIP3). Then, PIP3 recruits the Akt protein and phosphoinositide dependent protein kinase 1 (PDK1) to the cell membrane, where Akt is phosphorylated by PDK1. When phosphorylated, the Akt protein activates different substrates, such as the mammalian target of rapamycin (mTOR) (Lee et al., 1999), which is a serine/threonine kinase that regulates cell growth, survival, and proliferation. Phosphorylated Akt also interacts with the AR, leading to the over-activation of the AR signaling pathway.

PTEN also shows other Akt/PI3K/mTOR independent functions in cells, including DNA stability regulation and cell cycle maintenance. *Pten*-null mice show increased genomic

and chromosomal instability, leading to extensive centromere breakage, chromosomal translocations, and spontaneous DNA double-strand breaks through an Akt/PI3K/mTOR independent manner. Further, *PTEN*189 mutation (lacking C-terminus region) leads to significant increase in chromosomal aberrations, with transfected *PTEN189* cells showing a high frequency of aneuploidy. This mechanism of centromere instability is physically regulated by PTEN interactions with the centromere protein, together with Rad51 that regulate double-strand break repair machinery (W. H. Shen et al., 2007) through homologous recombination (Kass, Moynahan, & Jasin, 2016). Additionally, PTEN loss downregulates the DNA repair mechanisms by acting together with BRCA1 (Minami, Nakanishi, Ogura, Kitagishi, & Matsuda, 2014). In this way, PTEN protein is also an important regulator of genomic stability maintenance in the nucleus (Hopkins, Hodakoski, Barrows, Mense, & Parsons, 2014) (Figure 8).

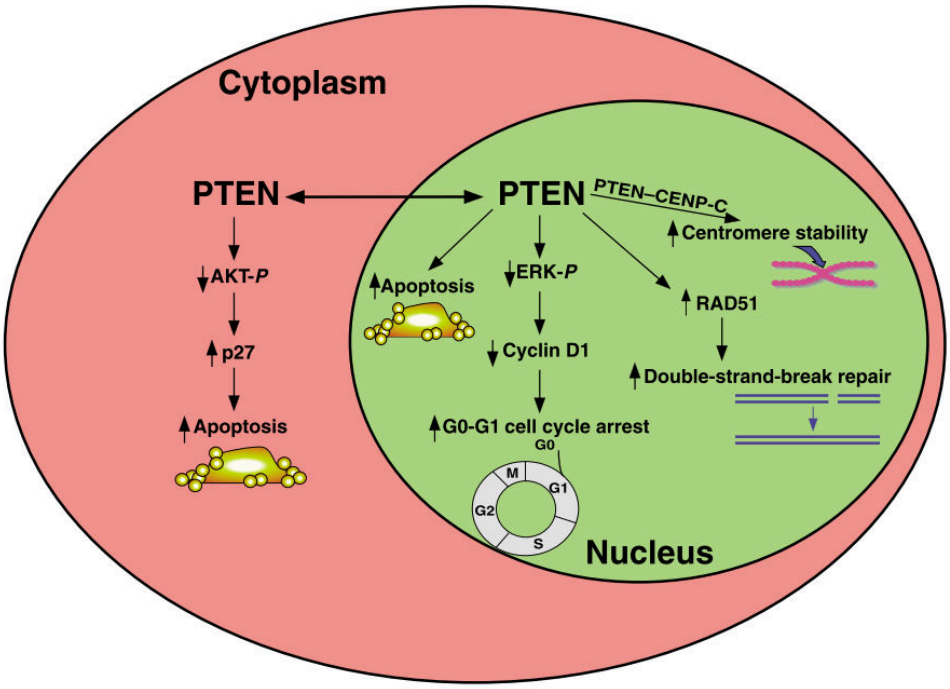

Figure 8. PTEN nuclear and cytoplasmic signaling regulation. PTEN function was firstly depicted on the cytoplasm and included the downregulation of AKT pathway. In contrast, nuclear PTEN can downregulate MAPK (ERK), promoting the G0-G1 arrest due to cyclin 1 regulation. Moreover, PTEN promotes the upregulation of RAD51 expression, being associated with double-stranded-break repair. PTEN can also interact with CENP-C to enhance centromere stability and overall genomic stability (Planchon, Waite, & Eng, 2008).

Recently, PTEN was described to regulate the degradation of the DNA-binding factor CHD1. CHD1 depletion suppresses cell proliferation, survival and tumorigenic potential in PTEN-deficient prostate and breast cancers. The authors demonstrate that PTEN deficiency stabilized CHD1, which promotes the activation of the TNF-NFKB gene network (Zhao et al., 2017). In addition, PTEN and CHD1 are mutually exclusive in prostate cancer samples. In this way, tumors with *PTEN* deletions may show increased proliferation and cell survival through another Akt/PI3K/mTOR-independent way (Figure 9).

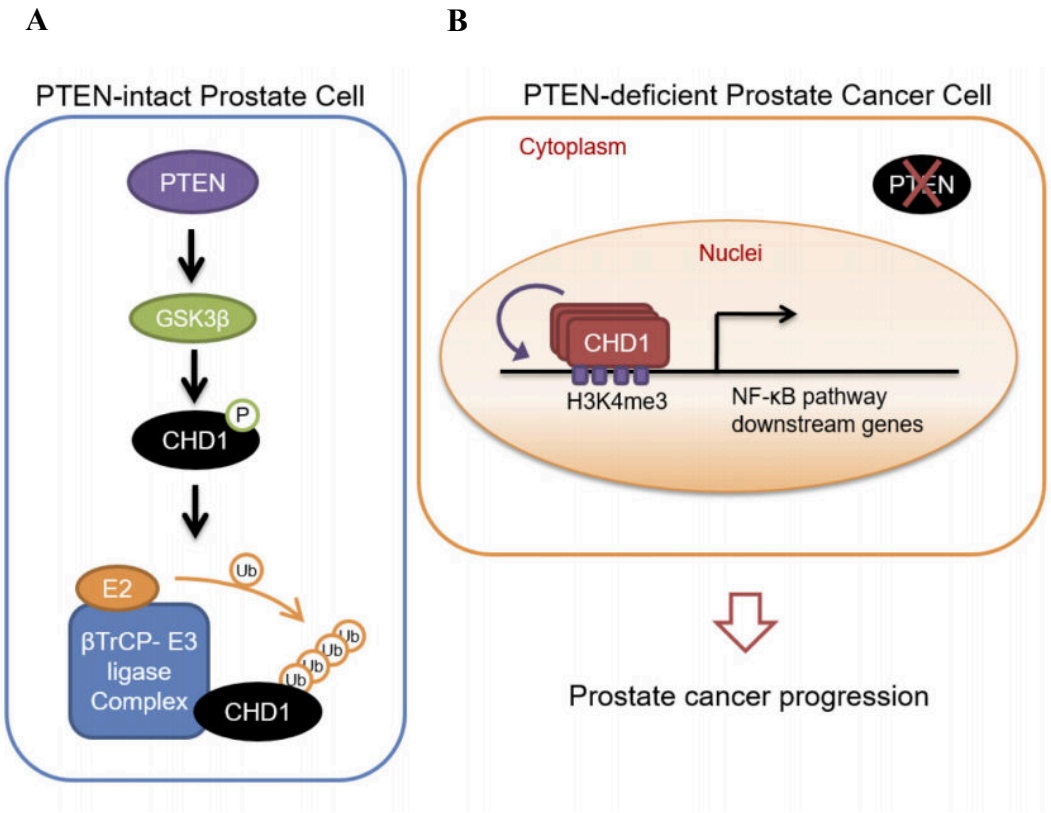

Figure 9. Schematic representations of the role of CHD1 in prostate cancer. **A.** In PTEN-intact prostate cells, GSK3β is activated by PTEN through inhibition of AKT and phosphorylates CHD1, which stimulates its degradation through the β-TrCP-mediated ubiquitination– proteasome pathway. **B.** However, in PTEN-deficient prostate cancer cells, accumulated CHD1 interacts with and maintains H3K4me3, followed by transcriptional activation of genes downstream of NF-κB, leading to disease progression. Zhao et al., 2017.

Additionally, PTEN physically regulates the minichromosome maintenance complex component 2 (MCM2), which is essential for DNA replication. PTEN loss results in unrestrained fork progression, suggesting that PTEN is essential for prevention of

chromosomal aberrations in cells under replication stress (Feng et al., 2015). Collectively, these findings evidence the role of PTEN on the maintenance of genomic instability in newly described functions for this protein. This suggests that PTEN loss is a pivotal event in cancer progression due to the numerous nuclear and cytoplasmic functions that PTEN have in cells.

The essential role of PTEN regulated pathways show increased potential for therapeutic targeting, including the specific characterization of *PTEN* null tumors for regulation of downstream molecules that PTEN is directly associated, including MCM2, CDH1, and RAD51 (Figure 10).

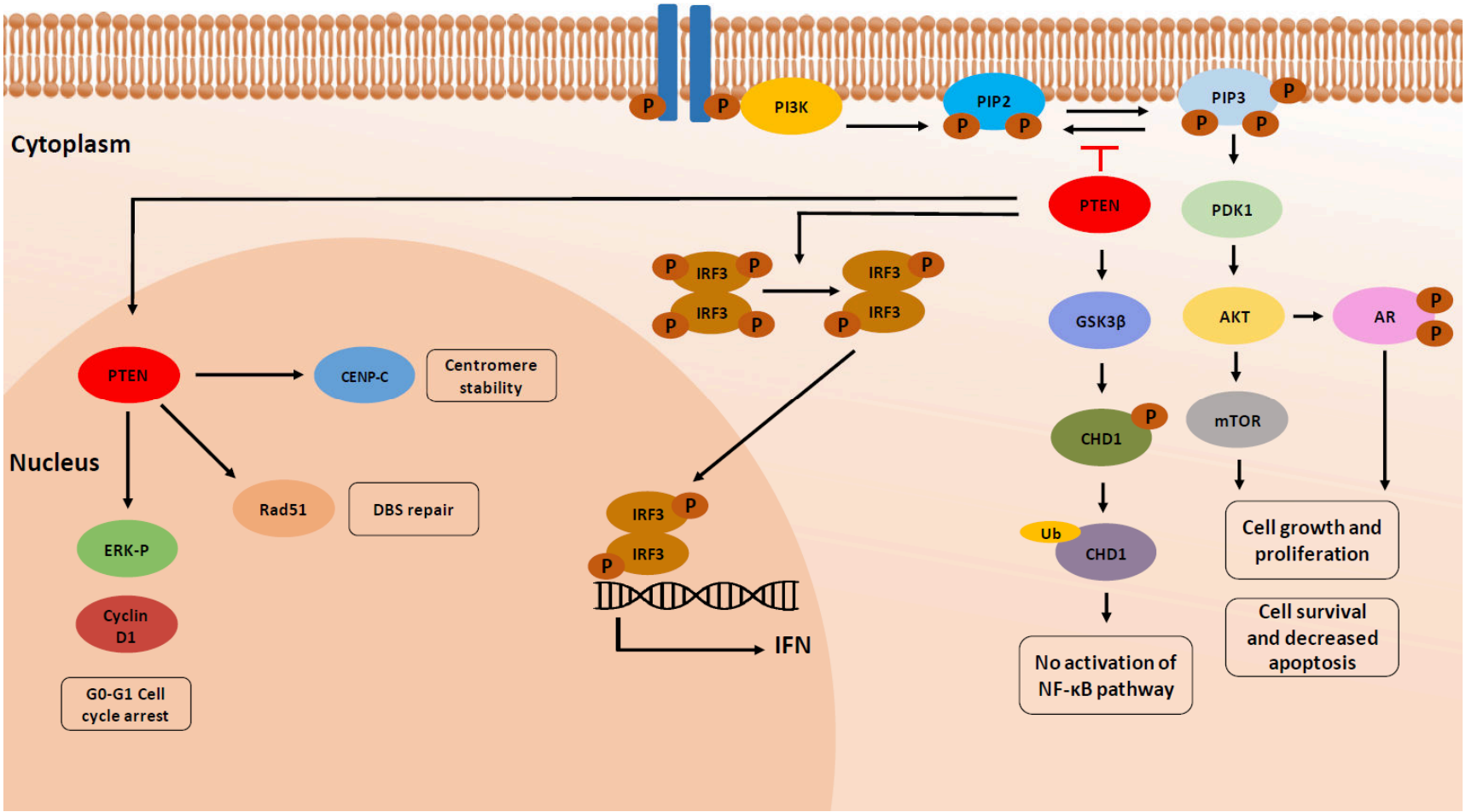

Figure 10. PTEN functions in the cytoplasm and nucleus. In the cytoplasm, PTEN acts dephosphorylating PIP3, which leads to decreased cell survival, growth and proliferation through the AKT/mTOR axis. PTEN also directly regulates interferon (IFN) signaling pathways by dephosphorylating the Ser97 of interferon regulatory factor 3 (IRF3) transcription factor. Once dephosphorylated, active IRF3 migrates to the nucleus and promotes the transcription of IFN response-related genes. This observation may explain why PTEN-deficient tumor cells are more permissive to IFN-sensitive oncolytic viruses and demonstrate possible targets for immunotherapy in patients that harbor PTEN losses. In the cytoplasm, PTEN also activates GSK3β that phosphorylates CHD1. Once CHD1 is phosphorylated, the β-TrCP-mediated ubiquitination– proteasome pathway degrades CHD1. In PTEN-deficient prostate cancer cells, the accumulation of CHD1 maintains H3K4me3, which promotes the transcription of downstream genes from NF-κB signaling pathway. The activation of NF-κB pathway then leads to disease progression. In the nucleus, PTEN can downregulate MAPK (ERK-P), promoting the G0-G1 arrest due to cyclin 1 regulation. Moreover, PTEN promotes the upregulation of RAD51 expression, which promotes double-stranded-break repair. PTEN can also interact with CENP-C to enhance centromere stability and overall genomic stability.

1.2.2 Germline mutations

Soon after the identification of *PTEN* as a tumor suppressor, heterozygous mutations in the *PTEN* gene were identified in patients suffering from the familial multi-system cancer syndromes, Cowden syndrome, and its pediatric presentation, Bannayan–Riley–Ruvalcaba syndrome (Liaw et al., 1997; Marsh et al., 1997). Later, the discovery of inherited *PTEN* mutations associated with clinical manifestations as Lhermitte Duclos syndrome (or cerebellum dysplastic hamartoma) (Padberg, Schot, Vielvoye, Bots, & De Beer, 1991) juvenile polyposis of infancy (Olschwang, Serova-Sinilnikova, Lenoir, & Thomas, 1998), segmental overgrowth (Caux et al., 2007) or autism spectrum disorder with macrocephaly (Butler et al., 2005; Eng, 2003) highlighted the complex relationship between genetic changes which impair the functions of the PTEN protein and patient phenotype. More recently, the term *PTEN* Hamartoma Tumor Syndrome (PHTS) has been used to encompass the range of symptoms identified in *PTEN* mutation carriers and broader diagnostic criteria have been proposed(M S Orloff & Eng, 2008; Pilarski et al., 2013).

Early literature estimated that about 80% of individuals with a diagnosis of Cowden syndrome had a germline *PTEN* mutation (Marsh et al., 1997). A study by Tan and colleagues (M. H. Tan et al., 2011) investigated a diverse cohort of individuals with Cowden syndrome and found that about 25% of affected individuals present germline *PTEN* mutations. For clinicians, it is important to consider the wide spectrum of clinical features of PHTS to differentiate a diagnosis of PHTS from other hereditary cancer syndromes (J. L. Mester, Moore, & Eng, 2013; Jessica L Mester, Tilot, Rybicki, Frazier, & Eng, 2011; M.-H. Tan et al., 2012).

Over the last decade, many patients with classic Cowden syndrome were classified as not having germline *PTEN* mutations. Recent research have shown several other germline

susceptibility genes for such individuals. Approximately 10% of the affected patients with classic Cowden syndrome or Cowden syndrome-like phenotypes have germline heterozygous variants in the genes that encode the subunits of succinate dehydrogenase (SDHx) or mitochondrial complex II (Ni et al., 2008). *KLLN* gene, present on 10q23 region, encodes *KILLIN* and shares a promoter with *PTEN*. Approximately 30% of individuals with Cowden syndrome or Cowden syndrome-like phenotypes without germline mutations of *PTEN* or SDHx, were recently found to have germline *KLLN* promoter hypermethylation (Bennett, 2010). Another 9% of these patients have found to have germline *PIK3CA* mutations and 2% harbored germline *AKT1* mutations (Mohammed S. Orloff et al., 2013). Moreover, germline heterozygous gain-of-function mutations in *SEC23B* gene were identified in approximately 5% of Cowden syndrome patients and enriched in apparently sporadic thyroid cancer individuals (Yehia et al., 2015). Gain-of-function germline mutations of *EGFR* gene were identified in a unique Cowden syndrome Family with Lhermitte-Duclos disease (Colby et al., 2016). The *KLLN* gene map close to *PTEN* loci in chromosome 10 the other associated genes mentioned above participate in the *PTEN* cellular pathway (Ngeow, Sesock, & Eng, 2017).

As *PTEN* is considered one of the most important tumor suppressor genes, several groups studied the phenotypes of large cohorts of carriers of *PTEN* mutations. This analysis revealed a diversity of other symptoms (Bubien et al., 2013; Nicholas R. Leslie & Longy, 2016; Nieuwenhuis et al., 2014; M.-H. Tan et al., 2012), as well as a lifetime cancer risk of over 80%. This risk is higher in women than it is in men. Prostate cancer has been reported in one man with an inherited *PTEN* gene mutation (Barbosa, Henrique, Pinto-Basto, Claes, & Soares, 2011), but at the present time there is insufficient data to determine if the presence of a germline mutation increases the risk of prostate cancer in carriers.

1.2.3 Frequency of PTEN inactivation in human prostate tumors

The 10q23 region that contains the *PTEN* gene exhibits high rates of loss in many human malignancies, including breast, glioma, melanoma, and prostate cancer (Song et al., 2012). The first descriptions of *PTEN* genomic deletion in prostate cancer were reported almost two decades ago (Maehama & Dixon, 1998b; Steck et al., 1997). Later studies of *PTEN* gene mutations in PCa focused on small changes in DNA and somatic point mutations that led to the inactivation of PTEN protein function (Rahdar et al., 2009). In addition, mate-pair sequencing demonstrated that 5% of prostate cancer patients harbored *PTEN* point mutations (Murphy et al., 2016) (Table 3). Recent whole genome sequencing approaches have demonstrated that *PTEN* is the most commonly lost tumor suppressor gene in primary PCa (Abeshouse et al., 2015; Barbieri et al., 2012; Berger et al., 2011). The vast majority of prostate tumors inactivate *PTEN* by genomic deletion (Abeshouse et al., 2015; Berger et al., 2011). Depending on the type of cohort examined, material preparation, and the methodology used, the reported rate of *PTEN* gene deletions in prostate cancer varies widely, in large part because the frequency of *PTEN* deletion is highly correlated with increasing Gleason grade and tumor stage (Table 3).

Table 3. Review of prostate cancer studies that depict PTEN loss by fluorescence *in situ* hybridization (FISH), immunohistochemistry (IHC) and array comparative genomic hybridization (aCGH), together with *PTEN* mutational profile through Sanger and whole genome and exome sequencing.

	TECHNIQUE	COHORT	PTEN STATUS	FEATURES	CITATION
***PTEN* MUTATION**	Whole exome sequencing	61 PCa Autopsy	**8% (5/61) of mutations** **1.5% (1/61) in High Grade PCa** **6.5% (4/61) in mCRPC**	11 High Grade PCa 50 mCRPC	Grasso et al., 2012
	Whole exome sequencing	150 mCRPC	**40.7% (61/150) of mutations**	mCRPC	Robinson et al. 2015
	Whole genome sequencing	333 PCa Radical Prostatectomy	**2% (7/333) of mutations**	GS 4-9; pT2a-pT4	Abeshouse et al., 2015
	Whole genome sequencing	126 PCa Radical Prostatectomy	**5% (6/126) of mutations**	GS 6-9; pT2a-pT3b	Murphy et al., 2016
	Sanger sequencing	97 PCa Radical Prostatectomy	**7% (7/97) of mutations**	71 (GS 4-9; pT2a-pT4) 26 CRPC	Krohn et al., 2012
***PTEN* COPY NUMBER VARIATION**	FISH (Four color)	59 CRPC	**77% (82/330) Loss** (43% Homozygous, 34% Hemizygous)	CRPC	Sircar et al., 2009
	FISH (Two color)	322 PCa Transurethral resection (TURP)	**17% (56/322) Loss** (Pooled hemi- and homozygous deletions)	GS 6-10; T1-T3	Reid et al., 2010
	FISH (Four color)	330 PCa 298 Radical Prostatectomies 32 Transurethral resection (CRPC)	**37.5% (112/298) Loss** (15% Homozygous, 25% Hemizygous) **62% (20/32) CRPC** (34% Homozygous, 28% Hemizygous)	298 (GS 4-9; pT2-pT3) 32 CRPC	Yoshimoto et al., 2012a
	FISH (Four color)	612 PCa Radical Prostatectomy	**18% (112/612) Loss** (9.3% Homozygous, 9% Hemizygous)	GS 6-10; pT1-pT4	Troyer et al., 2015
	FISH (Two color)	37 Transurethral Ressection (TURP)	**40% (15/37) Loss** (21% Homozygous, 19% Hemizygous)	10 (pT3-pT4) 27 CRPC	Verhagen et al., 2006
	FISH (Four color)	220 PCa Radical Prostatectomy	**36% (70/193) Loss** (13% Homozygous, 23% Hemizygous)	GS 3-9; pT2-pT4	Bismar et al., 2010
	FISH (Two color)	2266 PCa Radical Prostatectomy	**20% (458/2266) Loss** (12% Homozygous, 8% Hemizygous)	2217 (GS 4-9; pT2a-pT4) 49 CRPC	Krohn et al., 2012
	FISH (Two color)	643 PCa Transurethral resection (TURP)	**16% (104/643) Loss**	GS 6-9	Cuzick et al., 2013

	FISH (Two color)	13 PCa included Radical Prostatectomy	**30% (4/13) Loss in progressive disease**	6 non-progressive 7 progressive disease	Heselmeyer-Haddad et al., 2014
	FISH (Four color)	111 PCa Radical Prostatectomy	**17.2% (19/111) Loss** (13.6% Homzygous, 3.6% Hemizygous)	GS 7	Picanço-Albuquerque et al, 2016
	FISH (Four color)	731 PCa Radical Prostatectomy	**18% (145/810) Loss** (9.1% Homozygous, 8.9% Hemizygous)	GS 4-9; pT2-pT4	Lotan et al., 2016
	FISH (Two color)	160 PCa Radical Prostatectomy	**17% (27/160) Loss**	GS 6-9; pT2-pT4	Qu et al., 2016
	aCGH	77 PCa Radical Prostatectomy	**18% (14/77) Loss**	GS 4-9; pT2a-pT4	Krohn et al., 2012
	aCGH	61 PCa Autopsy	**40% (25/61) of loss** **33% (20/61) in mCRPC** **7% (5/61) in High Grade PCa**	11 High Grade PCa 50 mCRPC	Grasso et al., 2012
	aCGH	333 PCa Radical Prostatectomy	**15% (50/333) Homozygous Loss**	GS 4-9; pT2a-pT4	Abeshouse et al., 2015
	Whole genome sequencing	126 PCa Radical Prostatectomy	**20% (26/126) of loss**	GS 6-9; pT2a-pT3b	Murphy et al., 2016
PTEN PROTEIN LOSS	IHC anti-PTEN Clone 6H2.1 (Cascade Bioscience)	38 PCa Transurethral Ressection (TURP)	**39% (15/38) protein loss**	11 (pT3-pT4) 27 CRPC	Verhagen et al., 2006
	IHC anti-PTEN #ab31392 (Abcam)	3320 PCa Radical Prostatectomy	**29.7% (986/3320) protein loss**	GS 4-9; pT2a-pT4	Krohn et al., 2012
	IHC anti-PTEN 138G6 (Cell Signaling)	675 PCa Transurethral resection (TURP)	**18% (119/675) protein loss**	GS 4-9; pT2a-pT4	Cuzick et al., 2013
	IHC anti-PTEN 138G6 (Cell Signaling)	282 PCa Radical Prostatectomy	**15% (42/282) protein loss** 45% (55/122) CRPC protein loss 61% (19/31) mCRPC protein loss 14% (19/135) Gleason 7 protein loss	GS 4-9; pT2a-pT4	Leinonen et al., 2013
	IHC anti-PTEN D4.3 XP (Cell Signaling)	174 PCa Radical Prostatectomy	**11% (20/174) protein loss** 18.3% (13/71) Gleason 7 7% (7/103) Gleason 6	GS 6 - 7; pT2-pT3b	Lotan et al., 2014
	IHC anti-PTEN PREZEON assay	77 PCa Needle Biopsy	**12% (9/77) protein loss**	GS 4-9; pT1-pT3	Mithal et al., 2014

	IHC anti-PTEN D4.3 XP (Cell Signaling)	731 PCa Radical Prostatectomy	**22% (158/731) protein loss**	GS 4-9; pT2-pT4	Lotan et al., 2016
	IHC anti-PTEN D4.3 XP (Cell Signaling)	111 PCa Radical Prostatectomy	**16.3% (18/111) protein loss**	GS 7	Picanço-Albuquerque et al., 2016
	IHC anti-PTEN D4.3 XP (Cell Signaling)	126 PCa Radical Prostatectomy	**33% (35/107) protein loss**	GS 6-9; pT2a-pT3b	Murphy et al., 2016
	IHC anti-PTEN D4.3 XP (Cell Signaling)	7813 PCa Radical Prostatectomy	**24.2% (1890/7813) protein loss**	GS 4-9; pT2-pT4	Lotan et al., 2017

In early studies using microsatellite analysis, loss of heterozygosity (LOH) at the *PTEN* locus was reported in 10-55% of primary and advanced tumors from surgical cohorts (Feilotter, Nagai, Boag, Eng, & Mulligan, 1998; Pesche et al., 1998; Steck et al., 1997). In addition, fluorescence *in situ* hybridization (FISH) studies demonstrate that the deletion of at least one *PTEN* allele has been identified in as few as 17% of patients with tumors that were incidentally discovered on transurethral resection (TURP). Nonetheless, *PTEN* allelic loss has been reported in up to 68% of primary tumors from various historical surgical cohorts (Attard et al., 2009; Sircar et al., 2009; Verhagen et al., 2006; M Yoshimoto et al., 2007; Maisa Yoshimoto et al., 2006). More recent studies analyzing larger cohorts are reporting PTEN loss rates of around 20% in surgically treated men (Ahearn et al., 2016; Lotan et al., 2016; Troyer et al., 2015). Similarly, large scale recent whole exome sequencing efforts have reported ~20% of primary prostate cancer cases with *PTEN* gene loss (Abeshouse et al., 2015).

The frequency in which *PTEN* is inactivated by somatic point mutations appears to be quite low in many cancers. Sequencing studies reported a high rate of mutations in the *PTEN* promoter region. However, it is likely that some of these studies were confounded by the existence of a *PTEN* pseudogene (*PTENP1*) that harbors a high rate of mutations (L Poliseno et al., 2010; Zysman, Chapman, & Bapat, 2002). Whole exome sequencing (WES) studies have shown the presence of mutation around 5% in primary prostate tumors, with many samples having hemizygous deletions of the second allele (Barbieri & Tomlins, 2014; Berger et al., 2011; Grasso et al., 2012; Robinson et al., 2015). The most common mutation types are truncating mutations, with a relatively low rate of missense mutations.

Althought the variations in reported rates of genomic *PTEN* loss, a nearly universal finding is that loss of one *PTEN* allele is significantly more frequent than loss of both *PTEN* alleles in surgical cohorts (Abeshouse et al., 2015; T. a. Bismar et al., 2011). Consistent with the strong correlation with tumor stage, *PTEN* loss is more common in prostate cancer metastases than in

primary tumors, with rates of loss reported near 50% in most studies (Grasso et al., 2012; Liu et al., 2009; Min-Han Tan et al., 2011). Recent data from a castrate resistant prostate cancer (CRPC) cohort showed deep (likely homozygous) deletions in ~30% of patients, with truncating mutations and gene fusions in an additional 10% of the cases studied (Robinson et al., 2015).

Somatic and germline mutations in *PTEN* present similar a pattern, as shown in Figure 11. The phosphatase domain DSPc comprised by the exons 3, 4 and 5 is a hotspot for point mutations, showing about one-half of the mutations in *PTEN*. The mutations enriched in exon 5 are mostly pathogenic due to the inactivation of PTEN protein (Ngeow et al., 2017). Moreover, recent findings from our group showed that *PTEN* deletions in PCa may have different sizes. Most deletions occur within 10q23.2 and 10q23.33 regions and they appear to be associated with a more aggressive PCa phenotype (Vidotto, Tiezzi & Squire, 2017, unpublished data). Chromosome 10 deletions that comprise *PTEN* gene include flanking genes that are used as markers for a recently developed four-colour probe FISH assay (Maisa Yoshimoto et al., 2012). *WAPAL* and *FAS* genes are used as deletion controls together with a centromere probe that together reduce the effect of truncation in tissue cells of a histological section.

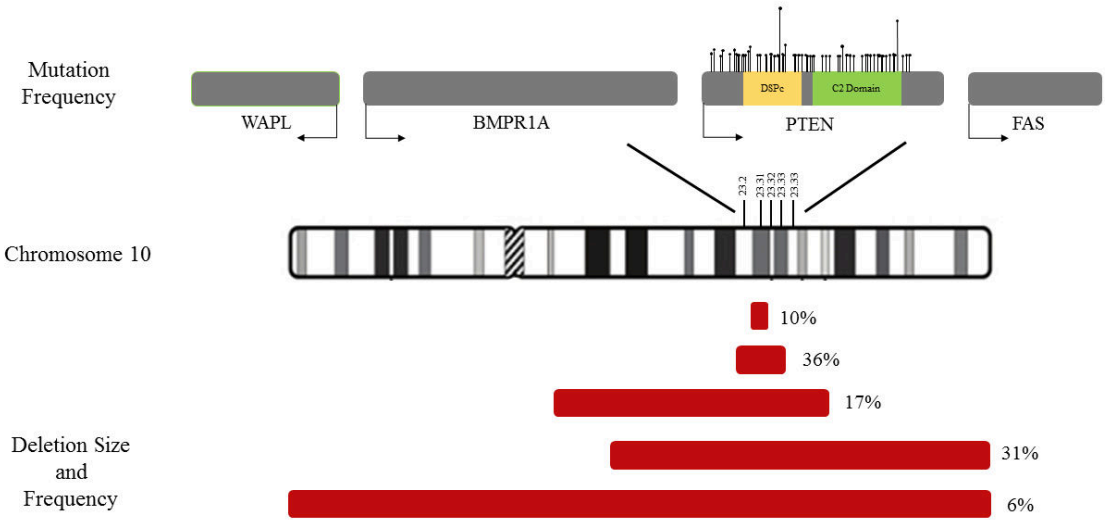

Figure 11. Diagram showing *PTEN* deletion sizes and mutational profile in prostate cancer**.**

The four-color FISH probe design (Figure 12 and Figure 13) was validated in various cohorts and showed high sensitivity and specificity to predict worse outcomes in PCa (Picanço-Albuquerque et al., 2016; Troyer et al., 2015; Maisa Yoshimoto et al., 2012). Additionally, this assay demonstrated a high predictive value for PCa cases that undergo needle core biopsies and are misclassified as low-risk (Lotan et al., 2014; Picanço-Albuquerque et al., 2016). Our recent study used this 4-color FISH assay to examine the association between *PTEN* deletion by FISH and the odds of upgrading from biopsy (Gleason 3+3) to prostatectomy (Gleason 7+). Both FISH and immunohistochemistry were concordant, showing consistent positive associations between PTEN loss and upgrading Gleason score. Moreover, we show that in some situations FISH provided a more precise approach to the examination of areas of cancer with heterogeneous staining when immunohistochemistry was uncertain (Picanço-Albuquerque et al., 2016).

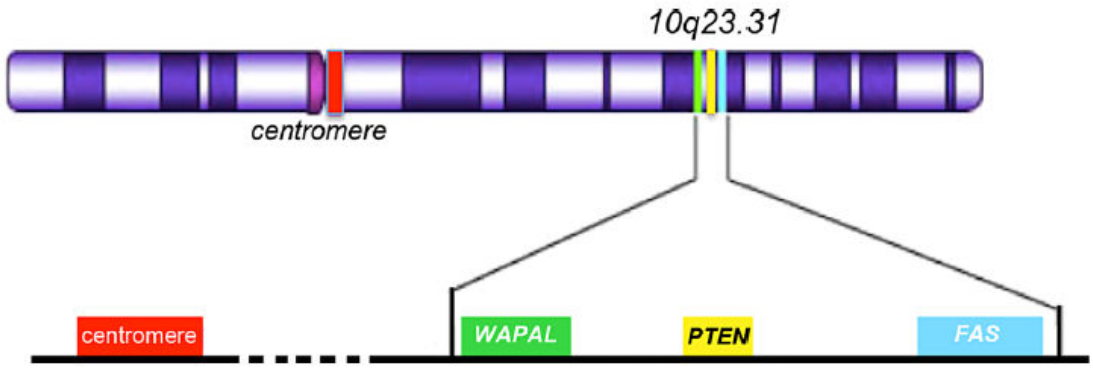

Figure 12. Schematic diagram of chromosome 10 showing genomic locations and respective positions of the four-color FISH probe used (Troyer et al., 2015).

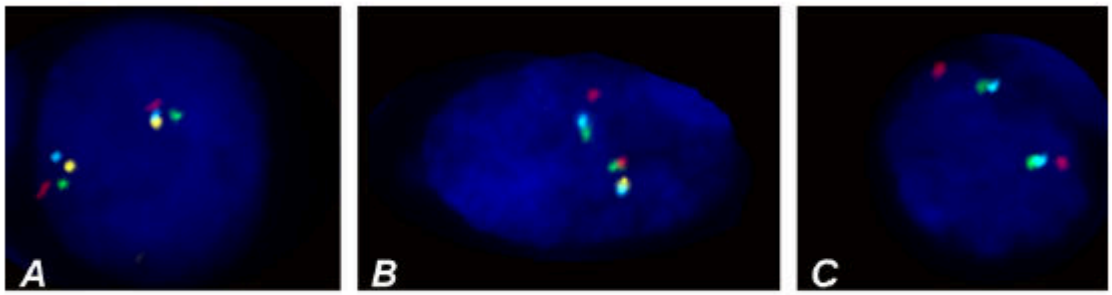

D

PTEN status	Signal configuration Centromere WAPAL PTEN FAS
PTEN Intact by FISH (two copies)	
Hemizygous PTEN deletion (one copy)	
Homozygous PTEN deletion (no copies)	

Figure 13. Examples of *PTEN* deletions by four-color FISH assay. **A**. Representative signal pattern observed when the *PTEN* gene is intact and two copies of the gene and all chromosome 10 probes are present as two copies. **B**. Nuclear signal pattern observed for *PTEN* hemizygous deletions. **C**. Homozygous *PTEN* deletion (both copies lost). **D**. Scoring schema used to classify FISH signals present in interphase nuclei based on the colored labels used for each probe. The schema only shows examples with simple interstitial deletions affecting the *PTEN* gene (yellow spot loss) only. In some tumors, larger deletions extending from WAPAL (green) to FAS (blue) were detected.

1.2.4 Epigenetic and RNA mechanisms of *PTEN* suppression

PTEN gene expression can also be downregulated by epigenetic events such as promoter methylation (Nguyen et al., 2000). *PTEN* silencing may also occur by genomic rearrangements and complex DNA alterations involving *PTEN* and nearby genes (Murphy et al., 2016; A. H. M. Reid et al., 2012). *PTEN* promoter methylation is also a mechanism by which functional loss of the gene may occur. In many tumor types, loss of PTEN protein by promoter hypermethylation is well documented. However, few studies have investigated

PTEN hypermethylation in primary prostate cancers, and most have reported negative results (Konishi et al., 2002).

In prostate cancer, *PTEN* also appears to be inactivated by miRNA and non-coding RNA (lncRNA, long non-coding RNA). The *PTEN* pseudogene PTENP1 mRNA that has growth- and tumor-suppressive properties, can act as competing endogenous RNAs (ceRNAs) to microRNAs that regulate *PTEN* function (Tay et al., 2011). The microRNAs miR-22 and the miR-106b-25 cluster that regulate *PTEN* expression are aberrantly overexpressed in human tumors can initiate prostate tumorigenesis in vitro and in vivo (Laura Poliseno et al., 2010). Moreover, lncRNAs act as microRNA sponges that compete for microRNA binding to protein-coding transcripts. The downregulation of such lncRNAs (TUG1 and CTB-89H12.4) have shown to increase prostate cancer cell proliferation in vitro (Laura Poliseno et al., 2010). After translation, PTEN protein can also be regulated by phosphorylation, oxidation, ubiquitylation, acetylation, proteosomal degradation, as well as protein-protein interactions (Nick R. Leslie & Foti, 2011). A number of studies have indicated that posttranslational modifications such as phosphorylation and ubiquitination decrease PTEN protein levels, while oxidation and acetylation reduce PTEN activity (Salmena, Carracedo, & Pandolfi, 2008). However, the frequency with which such inactivation events occur in human prostate tumors remains unclear.

As *PTEN* is commonly deleted in primary tumors and evidences show that PTEN loss events occur in the beginning of the disease progression. Sequencing studies in autopsy cohorts have shown that *PTEN* deletion occurs in at least a subset of tumor cells from the primary and all or most sampled metastases (Gundem et al., 2015). In contrast, *TMPRSS2-ERG* gene fusion events are less heterogeneous within the primary tumor when compared to *PTEN* deletions(Gumuskaya et al., 2013; Krohn et al., 2014a). These data are corroborated by the relatively low frequency of PTEN loss observed in PIN samples, which is a premalignant lesion of the prostate (Lotan et al., 2012; Morais et al., 2015, 2016).

1.2.5 Murine models of *Pten* and prostatic tumorigenesis

Mouse models have been used to demonstrate the effects of *Pten* loss in other genomic events, as well as its influence in signaling pathways in human prostate cancer. In mice, *Pten* hemizygous gene loss ($Pten^{+/-}$) induces the occurrence of PIN without leading to invasive prostatic carcinoma (Di Cristofano, Pesce, Cordon-Cardo, & Pandolfi, 1998; Trotman et al., 2003). In contrast, bi-allelic ablation of *Pten* in mice ($Pten^{-/-}$), a common event in aggressive prostate cancer, leads to the development of invasive and more rarely metastatic prostate carcinoma (Z. Chen et al., 2005; Wang & Dai, 2015). In mice, prostate tumors harboring *Pten* deletions are less sensitive to castration therapy, supporting that *Pten* loss might have at least a partial effect on castration resistance (Jiao et al., 2007; M. M. Shen & Abate-Shen, 2007). Moreover, in animal models, the mechanism of castration resistance appears to occur through the down-regulation of androgen receptor levels due to the feedback between PI3K activation and AR (Carver et al., 2011). This regulation has also been demonstrated in human prostate tumors (T. A. Bismar et al., 2012; Carver et al., 2011; Choucair et al., 2012).

1.2.6 PTEN loss and the inflammatory tumor microenvironment

The relatively long time of the prostate cancer disease process provides opportunities for immunotherapy clinical trials designed, to trigger specific antitumor immune responses (Drake, 2010). Moreover, there is emerging data suggesting that in addition to its established role as a tumor suppressor, PTEN loss may also impact the tumor microenvironment (TME) in an immunosuppressive manner (L. Chen & Guo, 2017).

In pre-symptomatic prostate cancer, chronic inflammation findings are often accompanied by the presence of PIN (Marzo et al., 2007). The tumor microenvironment of

prostate cancers shows increased infiltration of immune cells, such as CD4+, CD8+, natural killer (NK) T-cells and antigen-presenting cells (APCs) (Strasner & Karin, 2015). I addition, the ratios of each cell subtype of NK and APC are associated with different prognoses. For example, increased NK T-cell infiltration is associated better outcome due to its strong antitumor response (Gannon et al., 2009). Conversely, CD4+ T-cell infiltration which can be regulatory T-cells (T_{reg} cells) induces the suppression of the immune responses, leading to a worse prognosis (Si, Wang, & Guo, 2013). PTEN loss has also been shown to be involved in the repression of interferon (IFN) response signaling pathways by regulating the migration of interferon regulatory factor 3 (IRF3) transcription factor to the nucleus (Li et al., 2015). The authors show that PTEN-depleted cells or PTEN-deficient cancer cells have a low level of type I IFN responses and thus are more sensitive to viral infections. These alterations in IFN signaling pathways in tumors may lead to a pro-tumorigenic effect in the immediate microenvironment. These observations may explain why PTEN-deficient tumor cells are more permissive to IFN-sensitive oncolytic viruses and demonstrate possible targets for immunotherapy in patients that harbor PTEN losses (Champion, Fisher, & Seymour, 2016).

Based on collaborative work performed recently in our laboratory (Vidotto et al., 2017 - submitted) and other studies (Pencik et al., 2015), the role of PTEN in the immune response of prostate cancers with *PTEN* deletions probably occurs through the activation of the signal transducer and activator of transcription (STAT) protein family in prostate cancer. PTEN dephosphorylates IRF3 transcription factor and affects its nuclear translocation, leading to reduced expression of IFN1 response genes (L. Chen & Guo, 2017). Downstream targets of IRF3 include IFNα/β28, both of which activate the STAT1 and STAT3 transcription factors. STAT proteins are key to both Type I and Type II IFN responses, such as the induction of chemokines that recruit immune cells into the tumor microenvironment (Yu, Pardoll, & Jove, 2009). Both cancer and immune cells synthesize interferon that impacts the overall immune

response in the prostate tumor microenvironment. Since PTEN can regulate cellular interferon responses and IL-6 synthesis, reduced expression of STAT proteins in the tissue microenvironment could be a PTEN-mediated effect.

The development of effective immunotherapies based on the dynamic interaction between *PTEN* deleted tumors and the immune signaling response of the tumor microenvironment is promising. Pten knockout prostate cancer mouse models showed increased secretion of senescence-associated cytokines that were immunosuppressive in the tumor microenvironment (Pencik et al., 2015). Interestingly these investigators also showed that by pharmacologically inhibiting the Jak2/Stat3 pathway there was reactivation of senescence-associated cytokine network, leading to an antitumor immune response that enhanced sensitivity to chemotherapy. These data suggest that if the immune surveillance of senescent PTEN null tumors is suppressed, it may be possible to use specific pharmacological interventions that could restore immunogenicity to tumors.

The emerging relationship between *PTEN* deletions and the immune and inflammatory responses is very complex and covers both pro- and anti-tumorigenic cascades that are exclusive for each cell phenotype (Vidotto et al., 2017 – submitted). More studies are needed to take advantage of how PTEN-dependent changes, such as reduced type I interferon response and cytokine signaling to the tumor microenvironment can be exploited for effective immunotherapy in prostate cancer.

1.2.7 Role of *PTEN* as a prognostic biomarker in prostate cancer

As discussed above (see 1.1.2) the widespread dosage of serum PSA in the late 1980s led to a marked increase in the number of new cases of prostate cancer. These data were interpreted as overdiagnosis by PSA screening that resulted in the overtreatment of patients

with clinically insignificant prostate tumors (Moschini et al., 2017). However, the distinction between indolent from aggressive prostate cancer is still challenging.

Patients with low risk prostate cancer are often eligible for active surveillance. This treatment is prescribed based on biopsy pathology variables, such as Gleason score and PSA levels (Bruinsma et al., 2016). However, 30% of men on active surveillance will present disease progression to a more aggressive disease and will require further intervention (Tosoian et al., 2015). Among biopsy parameters, the Gleason grade is the most used as a prognosticator of the disease (Epstein, Allsbrook, Amin, & Egevad, 2006). However, the tumor morphology analysis has limitations for disease stratification. In this way, there is a need validate tissue-based prognostic biomarkers such as *PTEN* to better characterize a potentially aggressive prostate cancer, once PTEN participates in prostate cancer tumorigenesis and progression (Figure 14).

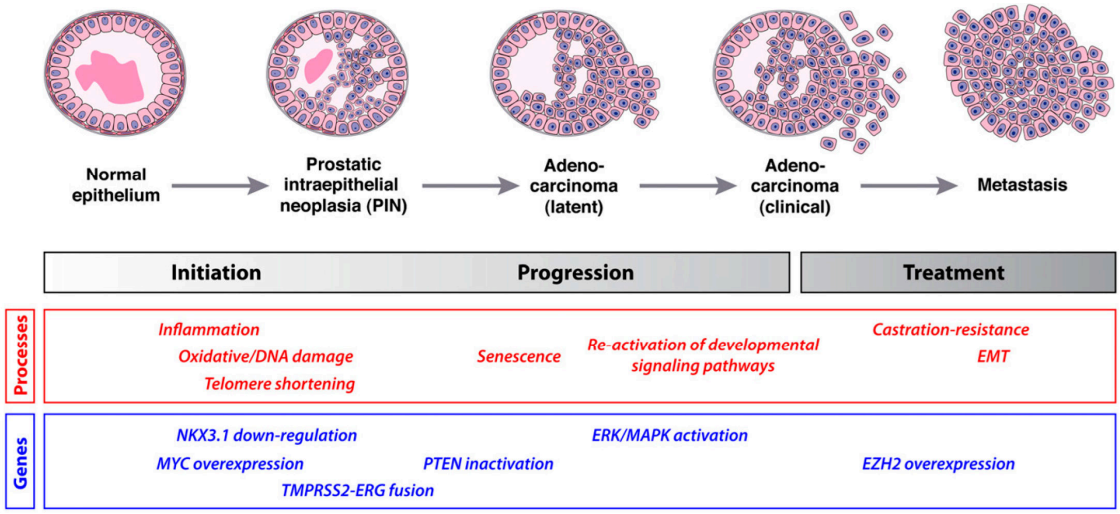

Figure 14. Pathway for prostate cancer progression (Adapted from Abate-Shen & Shen, 2000).

RNA-based commercial assays have been applied in this context (Ross, D'Amico, & Freedland, 2015). However, DNA-based biomarkers are more stable and less prone to variation in tissue pre-processing, such as tissue fixation and age. Of all recent prognostic

DNA biomarkers from analysis of prostate cancers, *PTEN* gene loss is probably one of the most promising and it is relatively inexpensive and easy to perform. PTEN inactivation in prostate tumors is associated with adverse outcome in several surgical cohorts, such as earlier biochemical recurrence after radical prostatectomy, higher tumor grade and stage, metastasis, prostate cancer specific death and CRPC progression (Ahearn et al., 2016; T. a. Bismar et al., 2011; Lotan et al., 2011). A recently published multicenter study confirmed the strong association between *PTEN* genomic deletion worse prognosis features, such as higher Gleason score and higher probability of extraprostatic extension (Troyer et al., 2015). Moreover, PTEN loss is clearly associated with an increased chance of biochemical recurrence after prostatectomy in numerous large studies (Krohn et al., 2012). Most importantly, *PTEN* was found to be an independent prognostic indicator of prostate cancer-specific death in both conservatively treated and surgically treated patients (Reid et al., 2010). When compared to animal models that show a prediction of *Pten* inactivation with development of CRPC, PTEN loss in human prostate cancer has also been associated with decreased response androgen deprivation therapies, including abiraterone (Ferraldeschi et al., 2015). These studies evidence the use of PTEN loss as an early biomarker of aggressive prostate cancer on clinical biopsy samples.

2 Justification

Prostate cancer is a clinically heterogeneous disease and often presents many challenges for therapeutic decision when first diagnosed. *PTEN* is a promising new biomarker for prostate cancer with strong biological evidence that its loss of function will be associated with aggressive disease. However, there is a lack of strong evidence that PTEN loss is an independent and reproducible biomarker suited for routine clinical applications. This project is designed to characterize of *PTEN* deletions and protein loss in clinical cohorts from Brazil and the USA, to consolidate the use of loss of *PTEN* as a biomarker for improved stratification of this disease. An emerging biological effect of PTEN loss seems to lead to an altered inflammatory response in the tumor microenvironment. A second aim of this project is to investigate immunological changes that may be elicited by loss of PTEN in tumors. In this way, *PTEN* characterization may be used to better stratify prostate cancer in the clinic to improve the decision-making process between the clinician and the patient.

3 Hypothesis

We hypothesize that PTEN loss is associated with a worse prognosis and biochemical recurrence in prostate cancer, in a way that the evaluation of PTEN status through FISH and immunohistochemistry may be sufficient for its consolidation as an informative biomarker for making clinical decisions in prostate cancer. In addition, there is an emerging role for PTEN as a mediator of inflammation in the tissue microenvironment of prostate cancer. We postulate that the deletion of *PTEN* could be associated with altered tumor-tissue microenvironment regulation leading to distinct differences in CD8+ tumor infiltrating lymphocyte infiltration.

4 Aims

4.1 General Aim

Identify the association between PTEN loss and the clinical outcome in homogeneous prostate cancer cohorts from Brazil and the USA designed to help stratify the use of loss of PTEN as (1) an indicator of poor prognosis; and (2) to be associated with altered T-cell infiltration in the tumor-tissue microenvironment.

4.2 Specific Aims

Identify the presence of PTEN loss through Fluorescence *in situ* hybridization (FISH) and immunohistochemistry (IHC) in the selected Brazilian prostate cancer cases;

Compare the *PTEN* gene expression levels through IHC with the presence of *PTEN* gene loss by FISH in the selected Brazilian prostate cancer cases;

Compare the association between PTEN loss by FISH and IHC with prostate cancer clinical outcome in the selected Brazilian prostate cancer cases;

Compare the association between *PTEN* deletions by array Comparetive Genomic Hybridization (aCGH) in a public USA domain cohort with prostate cancer outcome through *in silico* analysis;

Evaluate the influence of *PTEN* loss in the immune and inflammatory response by immunohistochemistry of tumor infiltrating CD8+ T-cells in the selected Brazilian prostate cancer cases.

5 Materials

5.1 Cohort descriptions

5.1.1 Clinical Hospital of Ribeirão Preto Medical School Cohort

We evaluated 50 representative prostate cancer cases collected after radical prostatectomy between 2009 and 2010 for this cohort study. The prostate cancer samples were randomly chosen from the database of cases consented for research from Medical Data of the Clinical Hospital of Ribeirão Preto Medical School (HCRP). Samples were fixed in formalin, embedded in paraffin and were obtained from the archive of the Pathology Service from the HCRP. All cases selected for biochemical recurrence analysis were followed up for up to five years after radical prostatectomy in the ambulatory of Uro-oncology from the HCRP.

All selected cases were initially revised by two pathologists to confirm the pathological stage and Gleason score. The pathologists also selected three areas that contained tumor and one benign adjacent region for each sample. The benign adjacent region was used as a control of the study. The selected regions were used for the construction of tissue micro-arrays (TMAs).

5.1.2 Inclusion Criteria

Samples were included for analysis when showed histopathological Gleason score grading of 7(3+4) or 7(4+3).

5.1.3 Exclusion Criteria

Samples that showed Gleason scores different of 7(3+4) or 7(4+3) after the evaluation of the radical prostatectomy tumors by two independent pathologists were excluded from the study. Cases that presented loss of follow up and death were also removed from the study. Patients unavailable tumor blocks were also removed from this research.

5.2 TCGA Cohort

The Cancer Genome Atlas (TCGA) prostate cancer cohort is composed by 500 prostate cancer samples and 50 benign adjacent tissue samples characterized by genome, proteome, transcriptome and methylome with all data publicly available for download. We downloaded Level 3 normalized aCGH (Affymetrix Genome-wide SNP Array 6.0), SNV, RNAseq, and clinical data for 500 prostate cancer cases and 50 matching benign adjacent gland cases. Downloads were performed on February 2016 from the TCGA Data Portal (http://TCGA-portal.nci.nih.gov). From the 500 cases downloaded, nine had data only for RNAseq or aCGH and were excluded from the analysis, resulting in 491 cases. Only data from primary tumors were used.

5.2.1 Inclusion Criteria

We selected patients with Gleason score 7(3+4) or 7(4+3) after radical prostatectomy for analysis. This selection resulted in 244 prostate cancer samples that showed Gleason score 7 after radical prostatectomy. These samples were used for investigation of PTEN loss and its

effects on clinical endpoints, such as extraprostatic extension, biochemical recurrence, pathological and clinical staging, bone metastasis, and treatment outcome.

5.2.2 Exclusion Criteria

Samples that showed Gleason scores different of 7(3+4) or 7(4+3) were excluded from the study.

6 Methods

6.1 Tissue microarray (TMA)

TMA is a microarray technique for analysis of formalin fixed paraffin embedded (FFPE) tissue samples that permits the evaluation of many molecular targets in hundreds of tissue samples at one time. The TMAs can be used for DNA, RNA and protein analysis, such as histological characterization, immunohistochemistry and fluorescence *in situ* hybridization (FISH).

For the construction of the TMA, we used the Manual Tissue Arrayer (MTA-1 – Beecher Instruments, Silver Spring, MD, USA) device. Each perforation unit (core) of the TMA had 1mm diameter. We obtained at least four cores per patient (case). The first and the second cores were obtained from two regions of the tumor that presented the most prevalent Gleason grade. The third was obtained from a tumor region that presented the second most prevalent Gleason grade. The fourth core was an adjacent benign area from the gland, used as a control. Other cores were added to investigate other pathological characteristics, such as margin invasion, vesicle invasion, perineural invasion and extracapsular invasion. The regions marked by the pathologists were placed at the base of the TMA device and the first needle was guided to the region of interest. Then, the perforation in the donor block (sample) was made. We then inserted the tissue sample in the receiver block. Two TMA blocks were constructed, one with 21 cases (TMA1 - 103 cores) and one with 22 cases (TMA2 - 105 cores) (Figure 15).

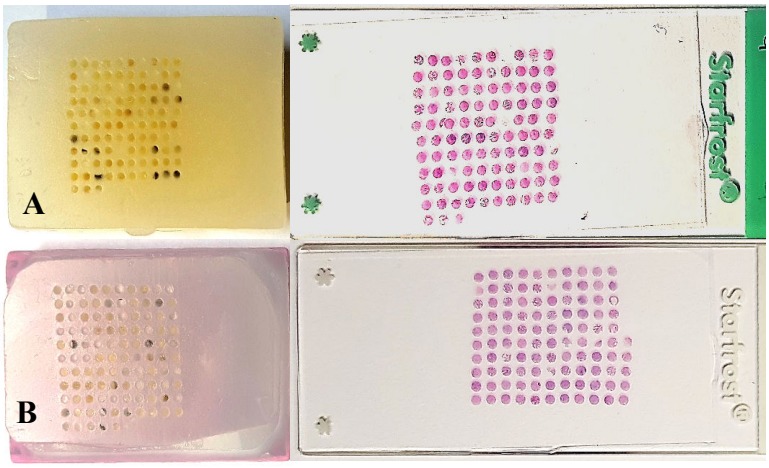

Figure 15. TMA blocks and slides. A. TMA1 with 103 cores. B. TMA 2 with 105

The TMA blocks were constructed in collaboration with the Pathology Department of Barretos Cancer Hospital (Figure 16).

Each TMA was used for the preparation of histological slides and HE staining. The pathologist used the HE staining to detect the presence of tumor tissues in the cores for the cases.

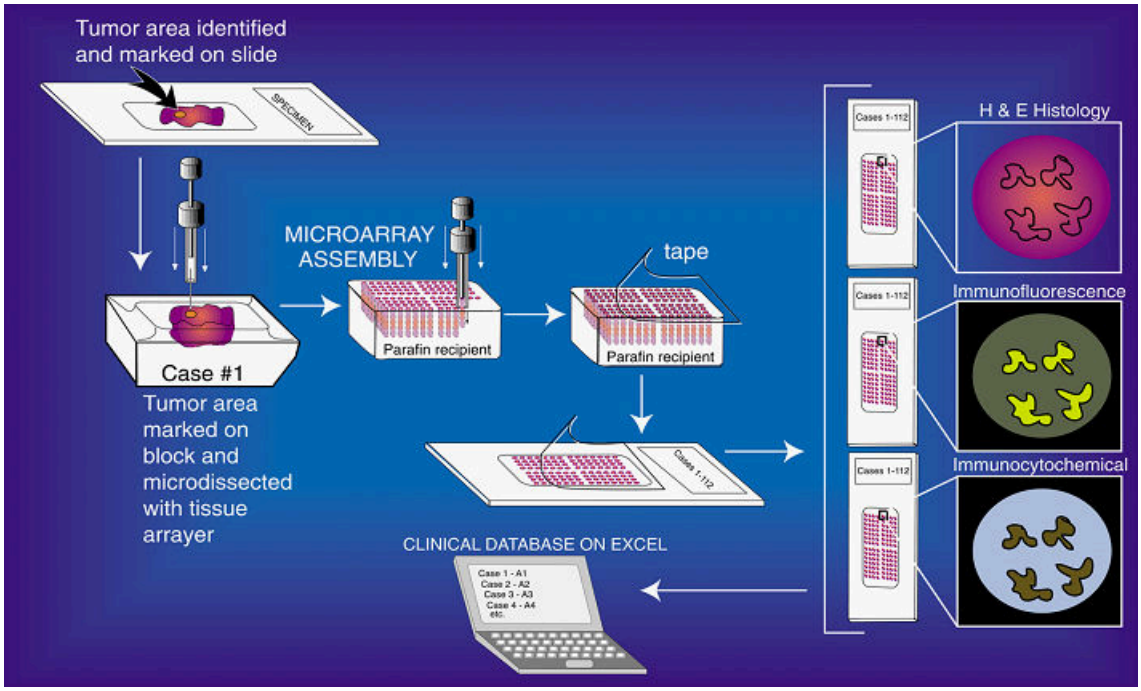

Figure 16. Scheme for TMA construction for FFPE tissues

6.2 Fluorescence *in situ* Hybridization (FISH)

The FISH analysis was conducted following the FISH protocol for prostate cancer established by the Laboratory of Dr. Jeremy Squire from the Department of Pathology and Molecular Medicine of Queen's University, Kingston, Canada. The protocols and technical considerations are available in Attachment A.

The histological preparations were previously deparafinized with xylol, sodium citrate and then were treated with pepsin for enzymatic digestion of the membrane and cytoplasm. After this, the slides were washed in 2x SSC and then incubated in ethanol gradient for dehydration. After dehydration, 10uL of the hybridization solution of the probe Four-Color *PTEN* FISH (CymoGen DX) was applied in each TMA slide. The DNA from the tissue and the probe were codenaturated in Thermobrite Hybridization Instrument (Abbot Cat# 07J91-010) at 82ºC. After denaturation and hybridization, the slides were kept in a wet chamber at 37ºC for 16 hours. We then washed the slides with 2xSSC and Igepal 0.3% to remove the excess of probes in the histological preparations.

For analysis, we used an epifluorescence microscope Olympus BX-40 connected in a computer in the Laboratory of Cytogenetics from HCRP. For hybridization analysis, we used the software FISH Review EXPO (ASI Ltda, Israel).

Areas of interest selected by the pathologist using an adjacent hematoxylin and eosin section were analyzed by FISH considering the areas that were was tumor rich, nuclei had a regular shape and uniform DAPI staining, nuclei did not have evidence of digestion damage such as "doughnut-like" appearance with empty epicentres, nuclei were not covered by cloudy typically yellowish layer or obscured by auto-fluorescence structures, and nuclei have hybridization signals with uniform intensity and similar patterns of granularity.

We counted the presence of each probe in up to 100 cells for each core. For some tumors there may be more than one type of clone. If possible, 100 cells were scored for each clone individually and the location of the clone within the core was marked on the hematoxylin and eosin slide map. When homozygous and hemizygous clones were present in the tumor glands, the cases were classified as having homozygous deletions. Samples were considered as harboring *PTEN* hemizygous deletion when at least 50% of the cells showed one specific signal for *PTEN* and homozygous deletion when at least 30% of the cells presented the complete loss of *PTEN* signal.

6.3 Immunohistochemistry for PTEN

The IHC technique was performed in collaboration with the Department of Pathology at the Johns Hopkins School of Medicine. We used the anti-PTEN antibody D4.3 XP® (Cell Signaling) diluted 1:50 in the TMA samples. Briefly, the TMAs were treated with H_2O_2 and methanol for 30 minutes before the recuperation of the antigen in the EDTA solution (1mM, pH 8.0) for 15 minutes. After blockade with the protein free serum (Dako Cytomation) and incubation with the primary antibody for 90 minutes, the TMAs were treated with biotinylated secondary antibodies (Dako Cytomation) and streptavidin-peroxidase (Dako Cytomation). The reaction product was then revealed with diaminobenzidine (Dako Cytomation) and the nuclei were contrasted with hematoxylin Harris (Sigma-Aldrich, MO, USA). The negative control was performed with fetal bovine serum instead of the primary antibody.

The immunohistochemistry were analyzed by two independent pathologists based on a previously validated dichotomous scoring system (Lotan et al., 2011). Cases with extremely weak signal or cases with more than 10% of the tissue showing no reactivity when compared to an adjacent benign gland (internal control) were classified as negative for PTEN protein

expression. Samples that presented stained cytoplasm and nuclei in the tumor areas were classified as positive for PTEN protein expression. Samples were classified as indeterminate when immunohistochemistry failed, in the absence of internal control or tumor tissue.

6.4 Immunohistochemistry for CD8+ T-cells

The immunohistochemistry for the presence of CD8+T-cells was performed in 10 cases that were previously analyzed through *PTEN* four-color FISH assay. We selected four patients that presented *PTEN* intact, three patients that harbored hemizygous loss of *PTEN* gene and three patients that harbored homozygous *PTEN* gene deletions.

Whole histological sections of the prostate glands were used for CD8+ T-cells analysis. Briefly, the slides were deparaffinised and rehydrated with xylene and alcohol. Then, we blocked the endogenous peroxidases using diluted hydrogen peroxide and an antigen retrieval step was performed in boiling Target retrieval solution pH 9 (Dako). Staining with anti-CD8 (Novus Biological, 4B11, 1/40) primary antibody was performed with a BenchMark XT automated stainer (Ventana Medical System Inc.). Revelation was performed with the UltraView universal DAB detection kit (Ventana Medical System Inc.) and slides were stained with hematoxylin, dehydrated and mounted. Further, the slides were imaged using the automated slides scanner VS-110 (Olympus).

Scoring of the CD8+ T-cells for the ten patient samples was conducted in a 3mm² area around the core perforation. Two independent and double-blinded observers manually counted the number of the CD8+ T-cells present in both stroma and tumor regions for each patient case. After counting, we averaged the two scores from the observers and dichotomized the number of CD8+ T-cells as high, when the number of cells counted for the case was above average, and as low, when the number of the cells for the case was below average.

6.5 In silico analysis of TCGA cohort

The 244 prostate cancer samples from the TCGA cohort were analyzed through Nexus Copy Number, v8.0 (BioDiscovery, Santa-Clara, CA, USA). The software was used for normalization, segmentation and identification of corresponding copy number events, gene expression analysis and mutational profile of all sample data from the TCGA cohort using build 37 (human genome 18) of the genome as the common scaffold for all tumor profiles. Specific settings to define *PTEN* deletion status have been published previously (Williams et al 2014). PTEN RNAseq analysis and mutational profiling were established in our laboratory in recently finished studies (Vidotto, Tiezzi & Squire, in preparation).

Samples were then characterized by their *PTEN* genomic status as homozygous (both copies of *PTEN* were deleted), hemizygous (one copy of *PTEN* was deleted) and *PTEN* intact (both copies of *PTEN* preserved). Then, samples were classified according to their *PTEN* gene expression through RNAseq data. PTEN levels showing expression values below the standard thresholds from Nexus Copy Number 8.0 were considered as showing decreased gene expression.

Mutational profiling of *PTEN* was performed, which included frame-shift, missense, and splice-site mutations. Samples were considered as having *PTEN* mutations when at least one nucleotide resulted in an altered protein due to a codon change.

After identification of the status of *PTEN* loss in the 244 samples, we evaluated the effects of *PTEN* loss and *PTEN* mutations in clinical parameters, such as disease recurrence, pathological and clinical staging, and treatment outcome.

6.6 Data Analysis

Data were analyzed through IBM SPSS Statistics 19.0.0. We performed one-way ANOVA and Chi-square tests to identify possible associations between clinical parameters

and *PTEN* status. We also performed survival cox regression models together with Kaplan Meier curves for biochemical recurrence prediction. The tests showed significant associations when *P*-value was above or equal to 0.05.

7 Ethics Committee Approval

The FFPE prostate cancer specimens were obtained from radical prostatectomy of 50 patients treated at the Archive of the Pathology Service at the Clinics Hospital (HCRP) of the Medicine School of Ribeirão Preto between 2009 and 2010. An informed consent form was signed by every patient before surgery approving the use of the tumor samples for research purposes. The TCLE was not applied in this study due to the current status of the use of FFPE blocks for research purposes. Moreover, the patient´s folder was evaluated preserving the anonymity of each patient. This study was approved by the HCRP Ethics Committee under protocol number 9499/2015.

8 Results

8.1 Clinical features of HCRP and TCGA cohorts

The HCRP cohort was reviewed by two pathologists to confirm the pathological stage and Gleason score 7. The cases were selected from a list of 50 patients with Gleason 7 that undergone radical prostatectomy in 2009 and 2010. One case was excluded because showed Gleason score different from 7, four cases presented insufficient tumor area, and 2 cases had unavailable paraffin blocks. The case selection resulted in 43 patients. We observed that the average age at diagnosis of the patients was 63 years (ranging between 49 and 74 years). The average preoperative PSA for this cohort was 9.88 ng/mL (ranging between 2.68 and 29.10 ng/mL) (Table 4). We also observed that 7/40 (17.5%) of the patients presented biochemical recurrence with an average of 30.14 months (ranging between 6 and 49 months) for detection of this event. Three cases were excluded from the analysis of biochemical recurrence because they died in the first month after surgery, two of cardiac disease and one unknown cause. Other important prognostic features observed were extraprostatic extension, present in 18.6% of the patients, and Gleason score upgrade after radical prostatectomy in 53.5% (Table 4).

Table 4. Clinical and pathological features of the 43 patients from the HC cohort.

Clinical Feature	Frequency	%
Age at diagnosis (years) (mean, range)	63 (49-74)	
Time to biochemical recurrence* (months) (mean, range)	30.14 (6-49)	
Preoperative PSA (ng/mL) (mean, range)	9.89 (2.68-29.10)	
Preoperative testosterone (ng/mL) (mean, range)	373 (140-817)	
Positive fragments from biopsy (percentage) (mean, range)	36 (8-100)	
Gland weight (grams) (mean, range)	41 (25-74)	
Capsular invasion		
No	29	67.4
Yes	14	32.6
Perineural invasion		
No	19	44,2
Yes	24	55,8
Angiolymphatic invasion		
No	29	67.3
Yes	3	7
Missing	11	25.6
Extraprostatic extension		
No	35	81.4
Yes	8	18.6
Vesicle invasion		
No	39	90,7
Yes	4	9,3
Positive margin		
No	29	67,4
Yes	14	32,6
Biochemical recurrence*		
No	33	83,7
Yes	7	16,3
Missing	3	7
Gleason score upgrade		
No	20	46,5
Yes	23	53,5
Pathological stage		
pT2a	2	4.7
pT2b	2	4.7
pT2c	31	72.1
pT3a	4	9.3
pT3b	4	9.3
Hormonal therapy*		
Yes	3	7.0
No	37	86.0
Missing	3	7.0
Radiotherapy*		
Yes	7	16.3
No	33	76.7
Missing	3	7.0

***** Data available for 40 patients.

For the validation of our results, we used the TCGA cohort, which is primarily composed by 491 patients. After the selection of cases with Gleason score 7, the cohort was established with 244 patients. We observed that the disease recurrence was present in 9% (22/242) of the patients in this cohort, which showed an average of 26 months for detection of this event. The TCGA cohort presented a heterogeneous follow-up time for the patients. This may justify the low frequency of disease recurrence detected. Moreover, extraprostatic extension was present in 45.9% (115/241) of the patients (Table 5).

Table 5. Clinical and pathological features of 244 patients from the TCGA cohort.

Clinical Feature	Frequency	%
Age at Diagnosis (mean; range)	60 (43-77)	
Months to Disease Recurrence (mean; range)	26 (4-71)	
Extraprostatic Extension		
No	126	51.6
Yes	115	47.1
Missing	3	1.2
Pathological Stage		
T2a	8	3.3
T2b	4	1.6
T2c	114	46.7
T3a	84	34.4
T3b	28	11.5
T4	3	1.2
Missing	3	1.2
N0	193	79.1
N1	13	5.3
Missing	38	15.6
Disease Recurrence*		
No	220	90.2
Yes	22	9
Missing	2	0.8
Race		
Asian	2	0.8
Black or African American	4	1.6
White	106	43.4
Missing	132	54.1

*Disease recurrence was defined the presence of at least one of the following events after radical prostatectomy surgery: distant metastasis, local metastasis, biochemical recurrence, or new primary tumor.

8.2 Concordance between FISH and IHC techniques in HCRP Cohort

The analysis of *PTEN* copy number through FISH was conclusive for 95% (41/43) of the patients. Two cases remained inconclusive due to poor quality probe hybridization. For the IHC, the results were conclusive for 90% (39/43) of the patients. The inconclusive cases presented technique failures, absence of internal control in the core or absence of tumor in the core.

Through FISH, we observed *PTEN* deletion in 18.9% (8/41), being that *PTEN* hemizygous deletions in 11.6% (5/41) and *PTEN* homozygous deletions in 7.3% (3/41) of the study cases. Moreover, by IHC, we detected PTEN protein loss in 16.3% (7/39) of the patients (Table 6).

The identification of *PTEN* gene deletions was performed through the four-color *PTEN* FISH assay, which permits the analysis of chr10 aberrations without interference of truncated nuclei in the tumor cells (Figure 17). PTEN protein expression by immunohistochemistry is shown in Figure 18.

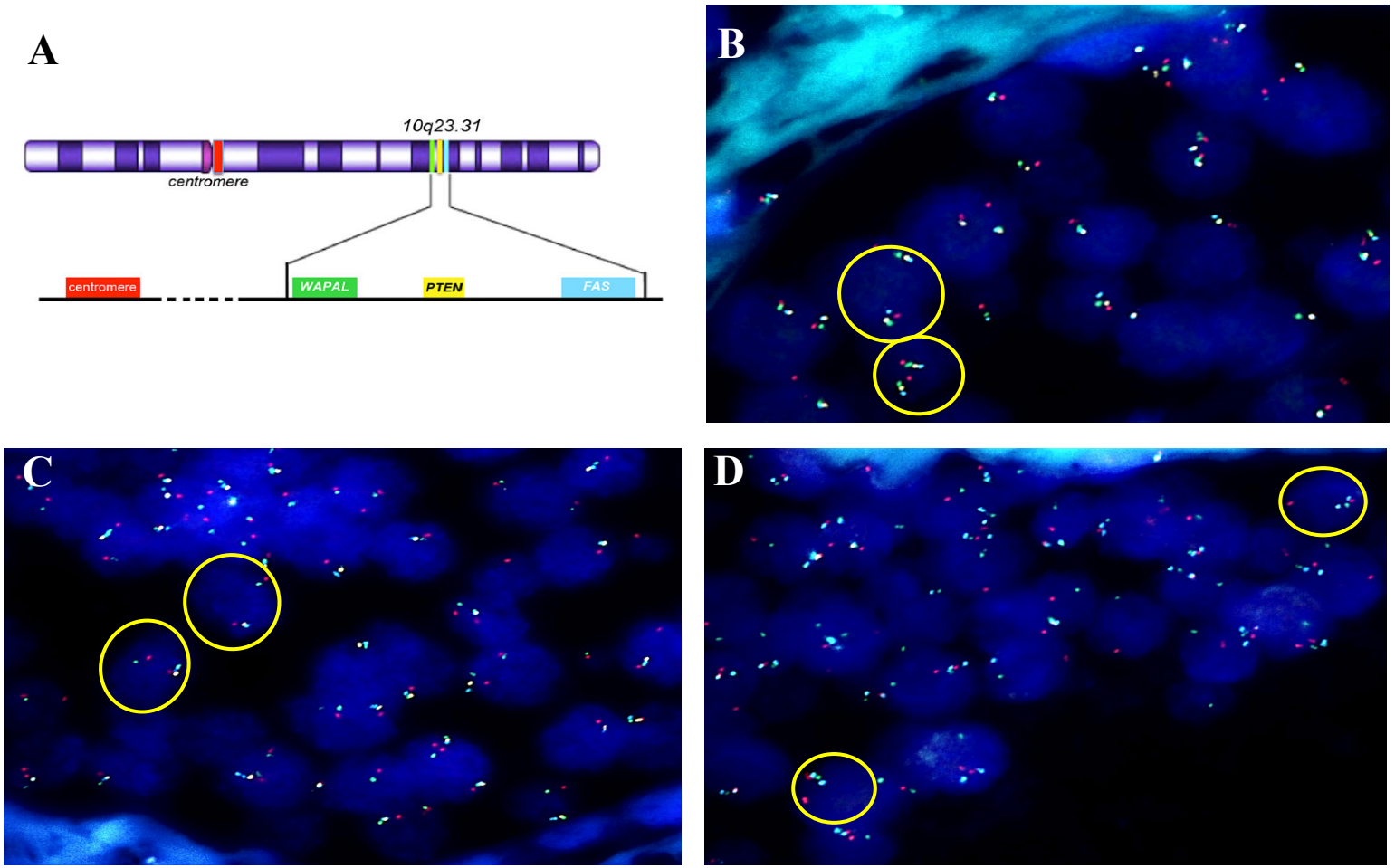

Figure 17. *PTEN* deletion by FISH from HCRP cohort. **A**. Four-color *PTEN* FISH probe. **B**. Representative FISH image for a tumor with both copies of PTEN gene. PTEN four-color FISH image (×63 magnification) showing a normal chromosome 10 disomy pattern—two copies of PTEN. Note that *PTEN* intact (yellow) as well as pericentromic control probes (CEPs) (red) and flanking gene probes WAPAL (green) and FAS (aqua) are intact in all untrucated cells. The yellow circled nuclei has two clusters of signals in which all probes are represented, consistent with a normal undeleted PTEN FISH pattern. **C**. *PTEN* FISH image (×63 magnification) showing hemizygous *PTEN* and FAS deletions. The yellow circled nuclei has one intact chromosome 10 with four signs (red, green, yellow and aqua) and the other chromosome with hemizygous PTEN and FAS deletions showing two signals (red and green). **D**. *PTEN* FISH image (×63 magnification) showing homozygous PTEN deletions (yellow signals missing). The yellow circled nuclei has one chromosome 10 showing CEP (red), WAPAL (green) and FAS (aqua), and the second chromosome 10 showing CEP (red) and FAS (aqua).

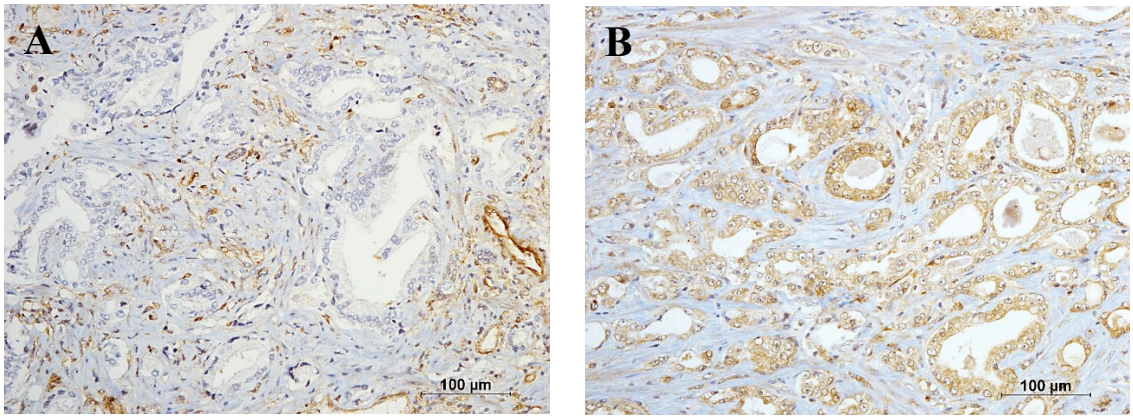

Figure 18. Immunohistochemistry for PTEN from HCRP cohort (20x magnification). **A.** PTEN protein loss is evident in tumor glands, while shows positive bening internal control in the tissue. **B.** PTEN protein intact in the tumor glands.

Table 6. Comparison of the findings for FISH and IHC for PTEN for all 43 patients from the HCRP cohort.

IHC	FISH				
	***PTEN* Deletion**		**No *PTEN* deletion**	**Failure**	**Total**
	Homozygous	**Hemizygous**			
PTEN loss	3 (7%)	1 (2.3%)	3 (7%)	0	7 (16.3%)
PTEN intact	0	3 (7%)	27 (62.8%)	2 (4.6%)	32 (74.4%)
Indeterminate	0	1 (2.3%)	3 (7%)	0	4 (9.3%)
Total	3 (7%)	5 (11.6%)	33 (76.7%)	2 (4.6%)	43 (100%)

The comparison between FISH and IHC showed that both assays were highly concordant, with 90% (27/30) showing protein intact and undeleted *PTEN* by FISH (Table 7).

Table 7. Concordance between techniques.

IHC	FISH			
	***PTEN* Deletion**		**No *PTEN* deletion**	**Total**
	Homozygous	**Hemizygous**		
PTEN loss	3 (8%)	1 (3%)	3 (8%)	7 (19%)
PTEN intact	0	3 (8%)	27 (73%)	30 (81%)
Total	3 (8%)	4 (11%)	30 (81%)	37* (100%)

* The total number of patients that had available data for both FISH and IHC was 37.

We also observed that PTEN FISH and IHC analysis are strongly concordant for the prediction of biochemical recurrence events in the patients. Moreover, in cases of technical failure or complexity in interpretation, the assays are complementary. The IHC for PTEN protein is useful for the quantification of the gene expression when *PTEN* was hemizygously deleted in tumor samples.

8.3 Association between PTEN loss and clinical endpoints for HCRP cohort

We evaluated the effect of PTEN loss by FISH, IHC and both techniques in clinical features of the patients with prostate cancer. The PTEN loss characterization through FISH and IHC were combined to provide more sensitivity for the diagnosic test. Clinical endpoints used were capsular invasion, perineural invasion, angiolymphatic invasion, extraprostatic extension, vesicular invasion, biochemical recurrence, Gleason score upgrade after radical prostatectomy, pathological stage, age at diagnosis, recurrence free survival (months) and preoperative PSA levels.

8.4 FISH for HCRP cohort

Chi-square test was performed for the categorical variables and we observed a significant association between *PTEN* loss and worse prognosis for the presence of capsular invasion (*P*-value = 0.04), angiolymphatic invasion (*P*-value = 0.03), and a strong trend to extraprostatic extension (*P*-value = 0.06) (Table 8). We observed no significant association between *PTEN* gene loss and perineural invasion (*P*-value = 0.41), vesicle invasion (*P*-value = 0.29), and biochemical recurrence (*P*-value = 0.77). We also did not observe an association

between *PTEN* gene deletion and Gleason score upgrade after radical prostatectomy (*P*-value = 0.90) and pathological stage (*P*-value = 0.58).

One-way ANOVA with Bonferroni posthoc test was applied to identify the differences between *PTEN* deletions for the continuous parameters. We did not observe any association between *PTEN* homozygous and hemizygous deletions for age of diagnosis (*P*-value = 0.67), months to biochemical recurrence (*P*-value = 0.47) or pre-operatory PSA levels (*P*-value = 0.38) (Table 8).

Table 8. Comparison between the PTEN gene and protein evaluation methods for clinical endpoints of the HCRP cohort.

	FISH (n=41)				IHC (n=39)		
	Homo loss	Hemi loss	*PTEN* Intact	***P*-value**	PTEN protein loss	PTEN Intact	***P*-value**
Age at diagnosis (years; mean, range)	63 (62-66)	65 (61-71)	63 (49-74)	**0.67**	63 (59-71)	63 (49-74)	**0.81**
Time to Biochemical Recurrence[#] (months; mean, range)	6 (6)	36 (36)	34 (7-49)	**0.47**	27 (6-49)	43 (36-48)	**0.41**
Preoperative PSA (ng/mL; mean, range)	13.96 (7.98-18.4)	11.66 (3.32-16.2)	9.39 (2.68-29.1)	**0.38**	10.53 (3.32-18.4)	9.77 (2.68-29.1)	**0.77**
Capsular Invasion							
No	0	4	23	**0.04***	3	23	**0.14**
Yes	3	1	10		4	9	
Perineural Invasion							
No	2	1	12	**0.41**	5	10	**0.04***
Yes	1	4	21		2	22	
Angiolymphatic Invasion							
No	1	5	22	**0.03***	4	21	**0.45**
Yes	1	0	1		1	2	
Extraprostatic Extension							
No	1	5	27	**0.06**	4	28	**0.05***
Yes	2	0	6		3	4	
Vesicle Invasion							
No	2	5	30	**0.29**	6	30	**0.47**
Yes	1	0	3		1	2	
Biochemical Recurrence[#]							
No	2	4	25	**0.77**	5	26	**0.21**
Yes	1	1	5		2	3	
Gleason Score Upgrade							
No	1	2	15	**0.90**	2	16	**0.30**
Yes	2	3	18		5	16	
Pathological Stage							
pT2a	0	0	2	**0.58**	0	2	**0.35**
pT2b	0	0	2		0	2	
pT2c	1	5	23		4	24	
pT3a	1	0	3		2	2	
pT3b	1	0	3		1	2	

*Significant *P*-value.

[#] Data available for 40 patients

Furthermore, Log Rank analysis and Kaplan Meier plots were generated to evaluate the effect of *PTEN* gene deletion in predicting earlier biochemical recurrence events. We observed a trend for the occurrence of earlier biochemical recurrence when *PTEN* gene is deleted (*P*-value = 0.65) (Figure 19).

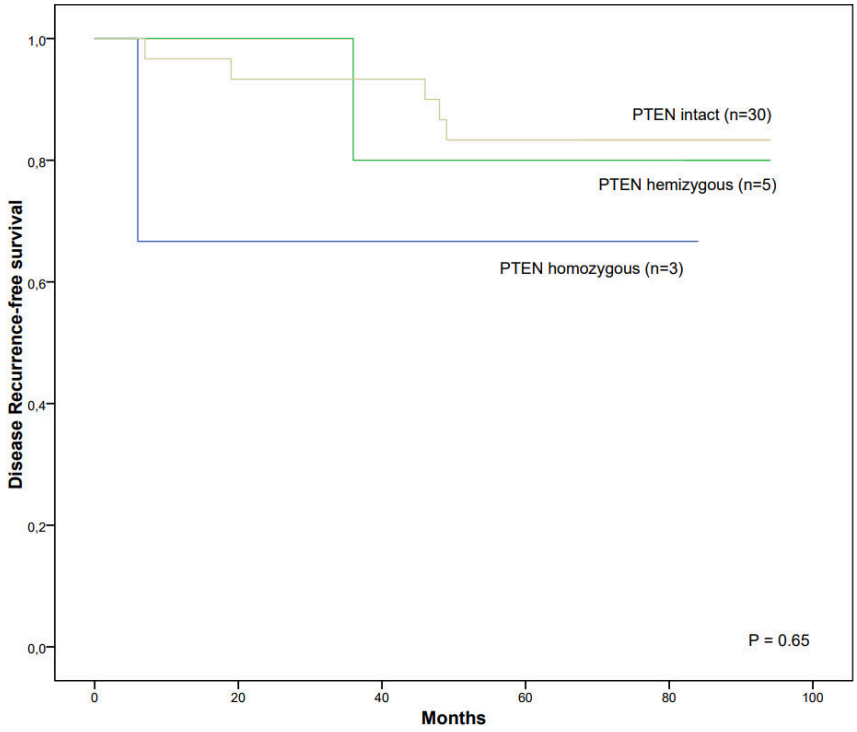

Figure 19. Kaplan-Meier plot for biochemical recurrence based on *PTEN* deletion.

8.5 IHC for HCRP cohort

We observed significant association between PTEN protein loss and perineural invasion (*P*-value = 0.04), extraprostatic extension (*P*-value = 0.05), but we observed no significant association between PTEN protein loss and capsular invasion (*P*-value = 0.14), angiolymphatic invasion (*P*-value = 0.45), vesicular invasion (*P*-value = 0.47), and biochemical recurrence (*P*-value = 0.21). We also did not observe an association between

PTEN protein loss and Gleason score upgrade after radical prostatectomy (*P*-value = 0.30) (Table 8).

One-way ANOVA test was applied to identify the effect of PTEN protein loss in the age of diagnosis, recurrence free survival (months) and pre-operatory PSA levels. We did not observed any association between PTEN protein loss and age of diagnosis (*P*-value = 0.81) or pre-operatory PSA levels (*P*-value = 0.77) and months to biochemical recurrence (*P*-value = 0.41) (Table 8 and Table 9).

In addition, Log Rank analysis and Kaplan Meier plots were generated to evaluate the effect of PTEN protein loss in predicting earlier biochemical recurrence events. We also observed a trend for the occurrence of earlier biochemical recurrence in patients that showed PTEN protein loss (*P*-value = 0.20) (Figure 20).

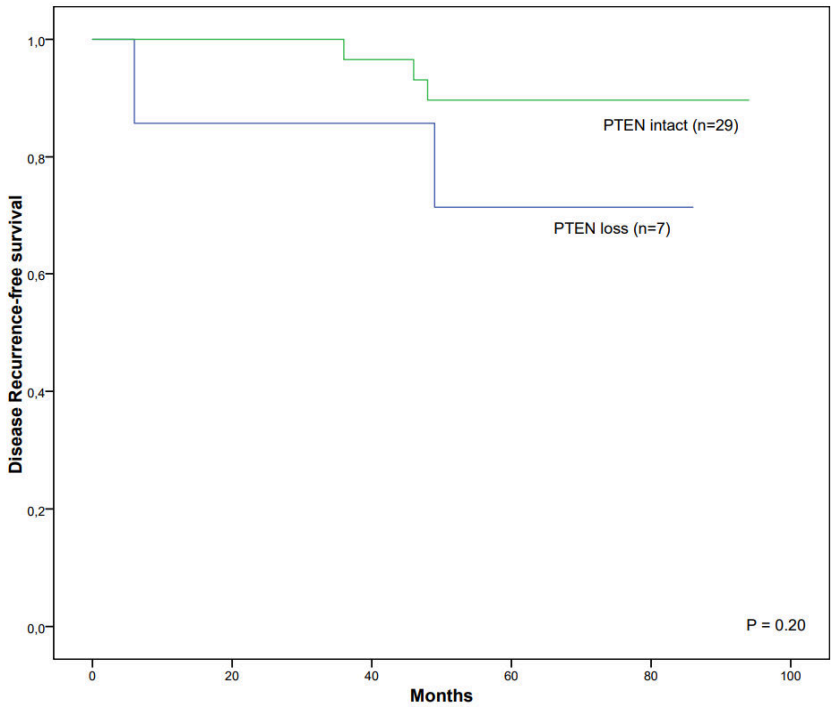

Figure 20. Kaplan-Meier plot for biochemical recurrence based on PTEN protein loss.

8.6 *In silico* analysis of TCGA cohort

We performed an *in silico* validation of the results obtained from TCGA cohort with patients presenting exclusively Gleason score 7 after radical prostatectomy. Somatic copy number alterations (SCNAs) of 244 patients was performed and showed a distinct pattern of gains and loss events throughout the genome. We observed that 20.9% (51/244) patients harbored *PTEN* deletions, being 5.7% (14/244) patients presenting homozygous deletions of *PTEN* gene and 15.2% (37/244) presenting hemizygous deletions of *PTEN* gene. An overview of the copy number alterations from the 244 prostate cancer cases is pictured in Figure 21.

In the copy number landscape of the Gleason 7 patients from the TCGA cohort, we observed concomitant alterations in the genome of patients that harbored *PTEN* homozygous or hemizygous deletions. In addition, we detected significant differences in 10q23.31 region and 17p when the copy number events were compared between samples that harbored *PTEN* hemizygous loss with samples that showed *PTEN* intact (Figure 22). The region 17p comprises the TP53 gene, which is an important tumor suppressor gene that is often mutated and deleted in prostate cancer and other malignancies.

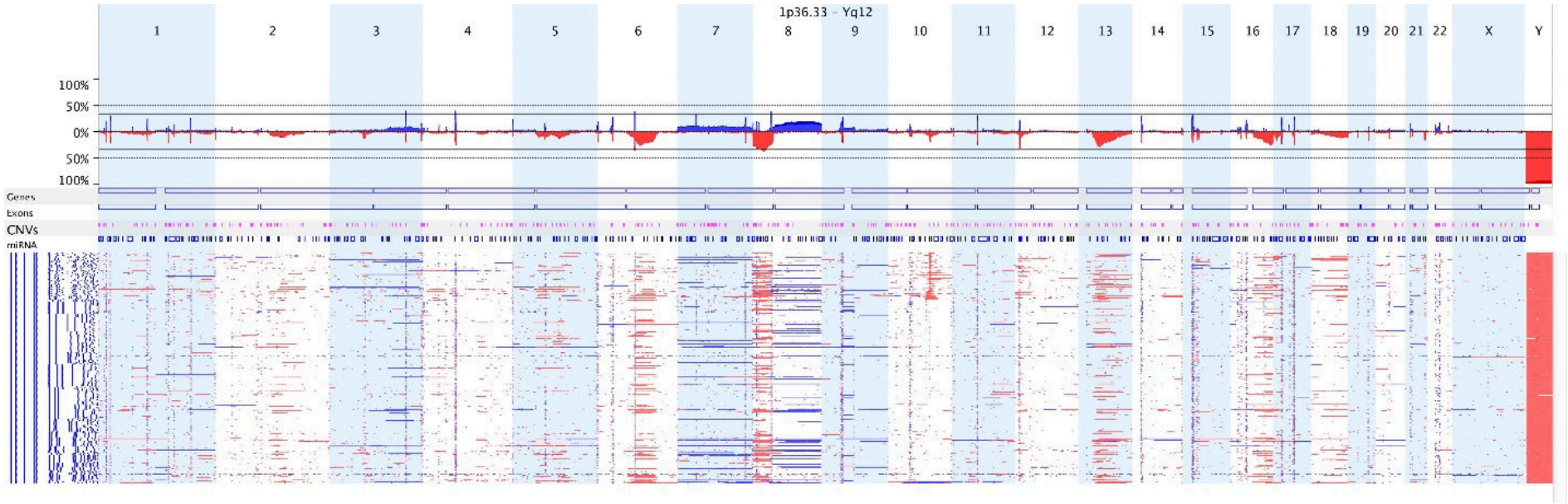

Figure 21. Genome-wide overview of copy number changes for the 244 patients Gleason 7 from the TCGA cohort. Red indicates losses and blue indicate gains. The top bar shows the percentage of copy number calls for all patients. The list below depicts the copy number alterations for each patient. Recurrent copy number alterations can be identified in chromosome 6, 7, 8, 13, 16 and 17 for the patients of this cohort.

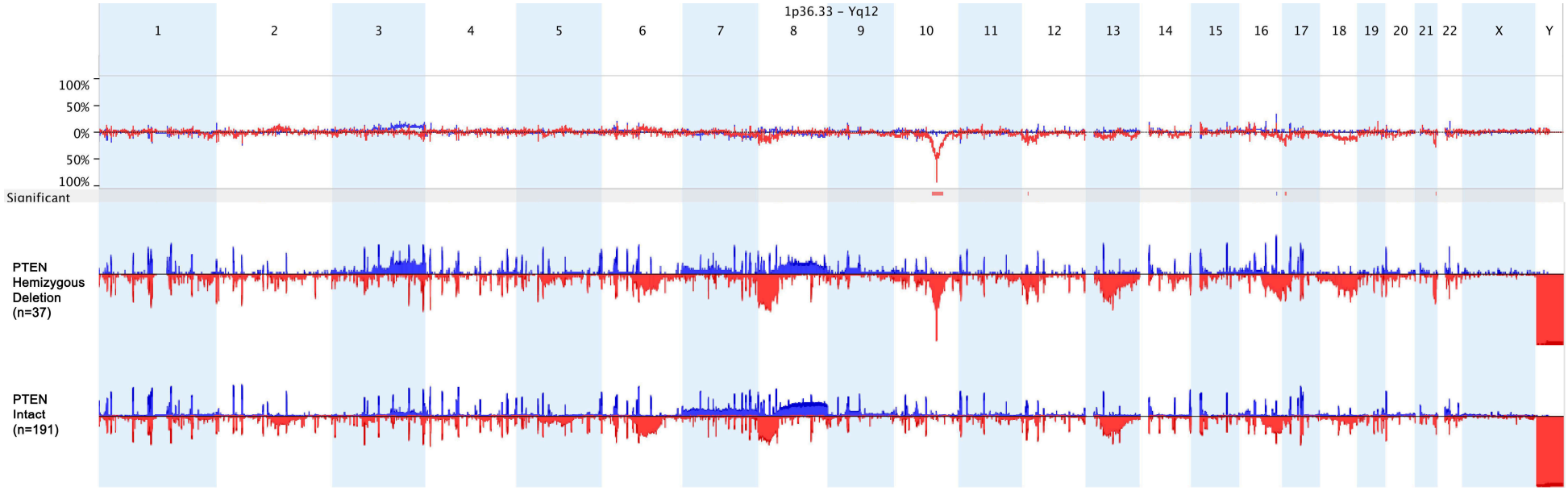

Figure 22. Comparison between samples with PTEN hemizygous (upper bar, n=37) deletion and PTEN intact (lower bar, n=191). The upper-lined graph shows the difference between the groups, while the "significant" bar shows the regions that are differentially gained or lost between the cases. Red indicates losses and blue indicate gains. We only observed copy number alterations for this comparison at chromosome 17p, which shows an increased loss rate in samples that harbor PTEN hemizygous deletions.

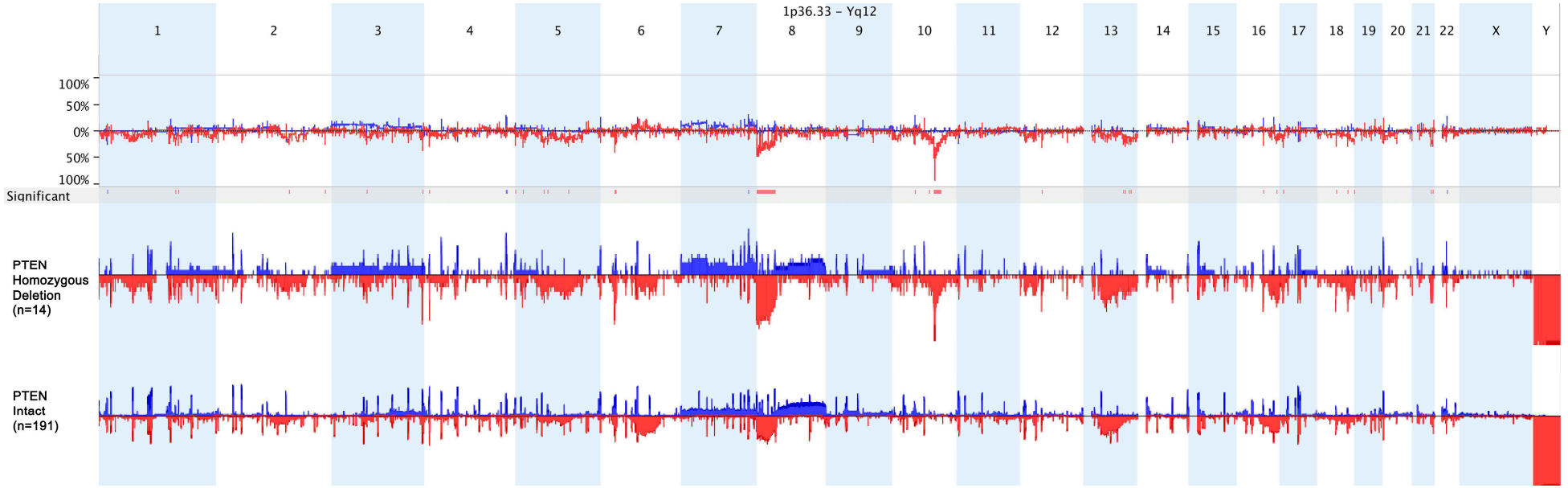

Figure 23. Comparison between samples with PTEN homozygous deletion (upper bar, n=14) and PTEN intact (lower bar, n=191). The upper-lined graph shows the difference between the groups, while the "significant" bar shows the regions that are differentially gained or lost between the cases. Red indicates losses and blue indicate gains. We observed copy number alterations for this comparison at chromosomes 3p, 5q, 8p, 13q, 17p and 21q.

Moreover, samples that harbored *PTEN* homozygous loss showed increased loss rates in 3p, 5p, 8p, 13q and 17p when compared to *PTEN* intact samples (Figure 23). We also observed an increased rate of *TMPRSS2-ERG* gene fusions due to 21q deletions in patients that harbored *PTEN* homozygous deletions. Additionally, we identified that PTEN gene expression is homogeneously decreased when PTEN is either homozygously and hemizygously deleted.

To select for genes more strongly associated with cancer, we used the Cancer Gene Sensus list (Nexus Copy Number 8.0). This list selects genes that are significantly correlated with cancer present in the regions of copy number alterations obtained by comparing patients with loss of both copies of PTEN and PTEN intact. This analysis showed that *TP53* (chr17), *WHSC1L1, WRN, PCM1*, and *NGR1* (chr8), and *ERG* and *TMPRSS2* (chr21) were the most affected cancer-related genes.

Further, we aimed to characterize the PTEN mutational profile of the prostate cancer patients from the TCGA cohort. SNV data was available for 85 of the 244 samples evaluated. Mutational analysis of PTEN gene of 85 patients of the TCGA cohort showed that 10/85 (4.1%) of the patients harbored a missense mutation in PTEN gene. We observed that 7/10 (70%) of the mutations in PTEN occurred in patients that harbored PTEN hemizygous deletions and 3/10 (30%) in patients that had PTEN intact.

8.7 *In silico* clinical analysis

We performed statistical analysis to identify and validate our results through FISH and IHC by using SCNA data from array-CGH experiments in the TCGA cohort. Clinical endpoints evaluated were age at diagnosis, time to disease recurrence, the presence of extraprostatic extension, pathological stage, disease recurrence, characterized by the presence

of at least one of the following events after radical prostatectomy surgery: distant metastasis, local metastasis, biochemical recurrence, or new primary tumor.

Chi-square test was used to identify significant associations between *PTEN* copy number and clinical endpoints. We observed that *PTEN* gene deletion is associated with the extraprostatic extension (*P*-value = 0.05) and a trend for disease recurrence (*P*-value = 0.07). We also observed that *PTEN* deletion events may occur in more frequency in white men (*P*-value = 0.01) when compared to Asians and African American men (Table 9).

Table 9. Association between *PTEN* genomic deletions with clinical features of 244 patients of the TCGA cohort.

Clinical Features	***PTEN* SCNA**			
	Homozygous Loss (n= 14)	**Hemizygous Loss (n=37)**	***PTEN* Intact (n= 193)**	***P*-Value**
Age at Diagnosis (years) (mean) (range)	60 (50-67)	61 (46-74)	60 (43-77)	0.63
Months to Disease Recurrence (mean) (range)	33 (15-42)	36 (23-54)	22 (4-71)	0.28
Extraprostatic Extension (frequency)				
No	5	14	107	0.05*
Yes	9	23	83	
Pathological Stage (frequency)				
T2a	0	1	7	0.50
T2b	1	0	3	
T2c	4	13	97	
T3a	7	17	60	
T3b	2	5	21	
T4	0	1	2	
Missing	0	0	3	
N0	12	32	149	0.64
N1	1	1	11	
Missing	1	4	33	
Disease Recurrence (frequency)				
No	10	34	176	0.03*
Yes	4	3	15	
Missing	-	-	2	
Race (frequency)				
Asian	0	2	0	0.01*
Black or African American	0	0	4	
White	7	20	79	
Missing	7	15	110	

* Significant *P*-value.

One-way ANOVA was performed to identify the associations between *PTEN* deletion and age at diagnosis and months to disease recurrence. We did not observe associations with months to disease recurrence (*P*-value = 0.54) and age at diagnosis (*P*-value = 0.63). Binary logistic regression analysis was performed with extraprostatic extension and disease recurrence endpoints to detect the hazard ratio of these events for the patients from the TCGA cohort. We observed that hemizygous deletions may significantly predict extraprostatic extension events in Gleason 7 patients (*P*-value = 0.04, Hazard Ratio [HR] = 2.118, Confidence Interval [CI] = 1.027-4.367), while homozygous deletions showed only a trend for a significant prediction of this pathological endpoint (*P*-value = 0.14, HR = 2.320, CI = 0.749-7.185). For disease recurrence, we observed that *PTEN* homozygous deletions significantly predicts this event (*P*-value = 0.02, HR = 3.519, CI = 1.159-10.685). We did not observe any association between *PTEN* hemizygous deletions and disease recurrence (*P*-value = 0.98, HR = 1.009, CI = 0.292-3.490).

Log rank test and Kaplan Meier curves were generated to test the association between *PTEN* gene deletion and disease recurrence. We observed a significant association between the occurrence of earlier disease recurrence events for cases with *PTEN* deletions (*P*-value = 0.05) (Figure 24).

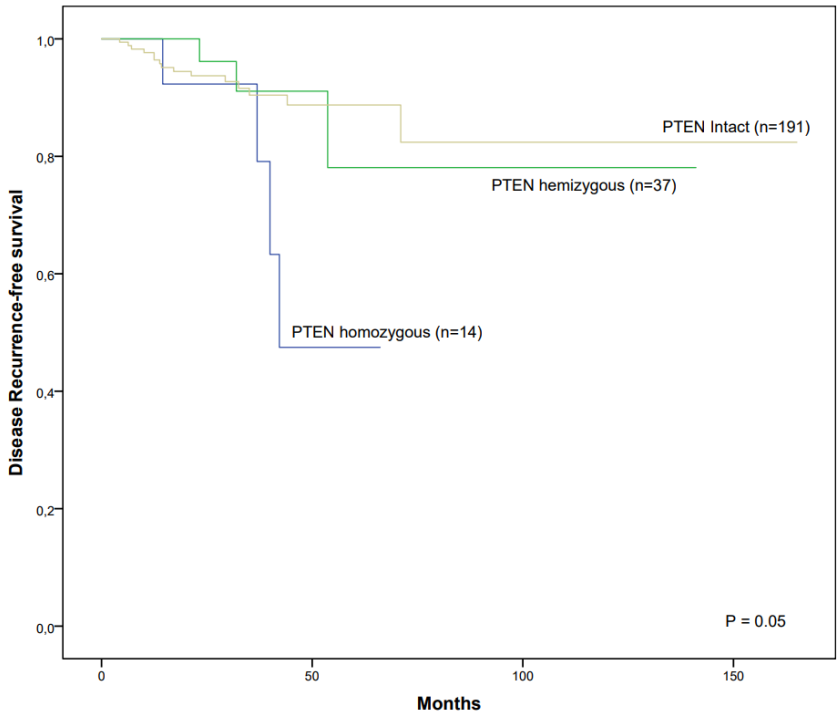

Figure 24. Kaplan-Meier plot for biochemical recurrence based on *PTEN* genomic deletion.

8.8 Analysis of immune infiltrates in prostate cancer samples

We conducted immunohistochemistry experiments to evaluate the rate of CD8+ T-cell infiltration in the TME of the prostate cancer samples from the HCRP cohort. We compared the rates of CD8+ T-cell infiltration for PTEN FISH and IHC analyses.

CD8+ T-cell showed a trend to a significant increased CD8+ TIL infiltration in samples that harbored *PTEN* homozygous deletion (3/10; 30%) when compared to *PTEN* hemizygous deletion (2/10; 20%) and *PTEN* intact (1/10; 10%) (*P*-value = 0.12). In addition, we observed a significant difference between low and high CD8+ T-cell infiltration rates when we considered PTEN protein loss by IHC (*P*-value = 0.03), which presented an increase CD8+ TIL infiltration in samples that harbored PTEN protein loss (4/10; 40%) when compared to PTEN intact (2/10; 20%) (Table 10; Figure 25).

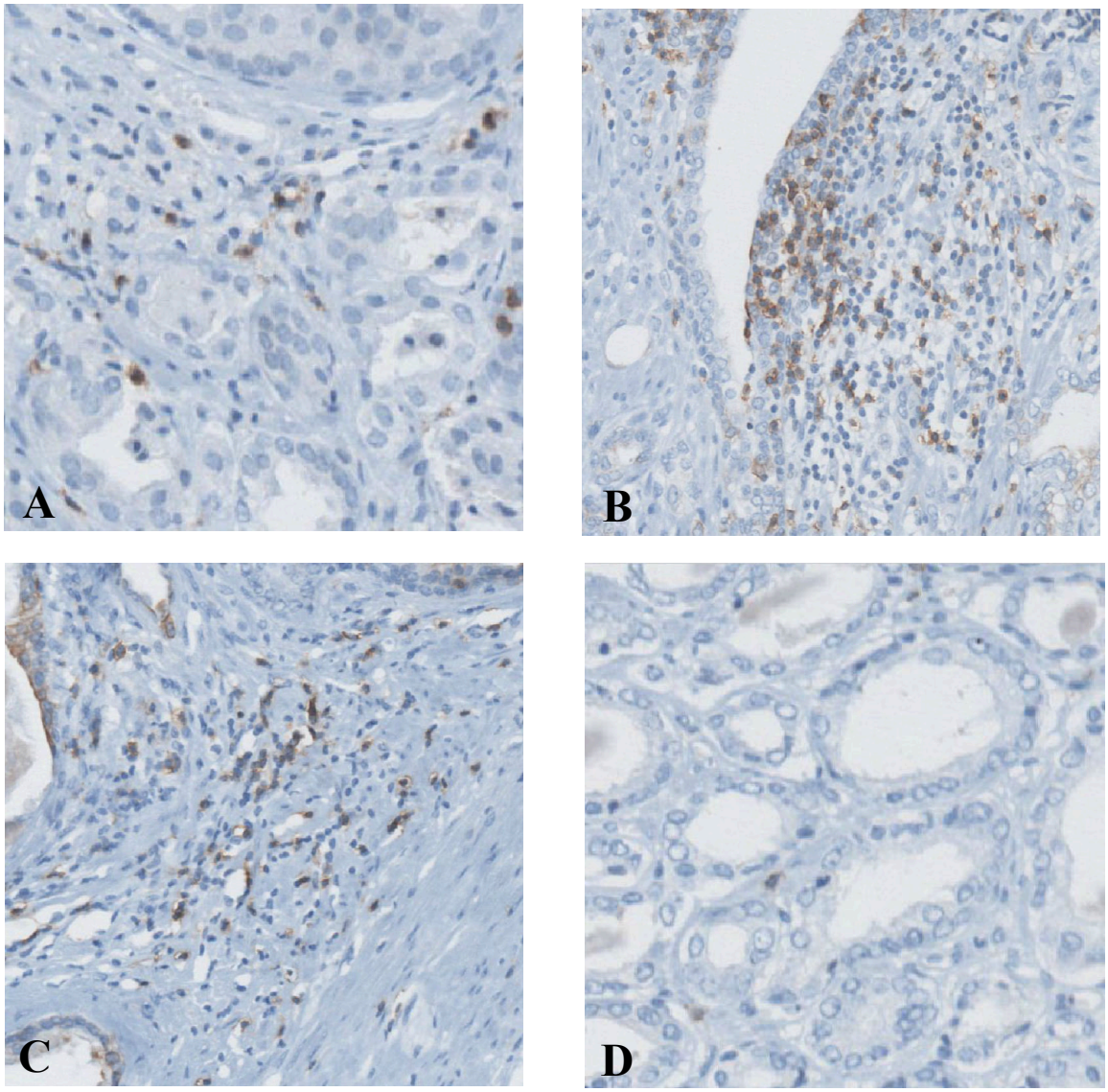

Figure 25. Representative image of the CD8+ T-cell infiltration in the prostate cancer cases from the HCRP cohort. **A**. Intermediate CD8+ T-cell infiltration in a patient that showed *PTEN* hemizygous deletion and PTEN protein loss. **B**. High CD8+ T-cell infiltration in a patient that presented both copies of *PTEN* gene deleted and PTEN protein loss. **C**. High CD8+ T-cell infiltration in a patient with *PTEN* homozygous deletion and PTEN protein loss. **D**. Low CD8+ T-cell infiltration in a patient with both copies of *PTEN* and protein intact. The scoring of the CD8+ T-cell infiltration was performed through the absolute number count of a 3mm² region around the core removal for TMA construction. We then dichotomized the samples according to the values above the mean infiltration and below the mean infiltration.

Table 10. Frequency of high and low scores for CD8+ T-cell infiltration according to the assay.

CD8+ T-cell Infiltration	***PTEN* FISH**				**PTEN IHC**		
	Homo	Hemi	Intact	***P*-value**	Loss	Intact	***P*-value**
Low	0	1	3	0.12	0	4	0.03
High	3	2	1		4	2	

Log rank test and Kaplan Meier curves were generated to test the association between the rates of CD8+ TIL infiltration and biochemical recurrence. We observed a trend for the occurrence of disease recurrence when CD8+ TIL infiltration rates are increased (*P*-value = 0.22) (Figure 26).

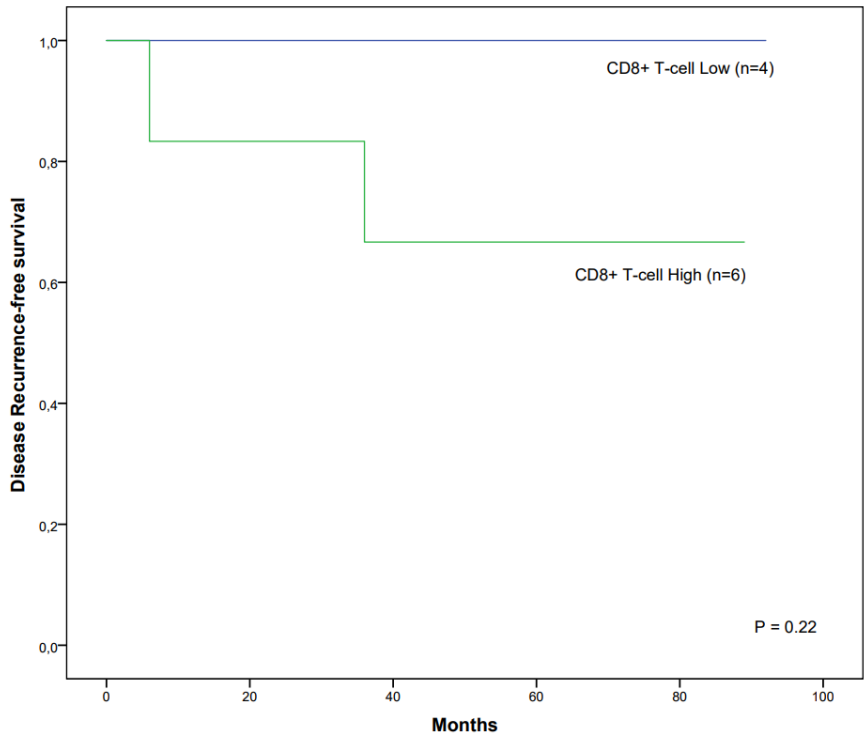

Figure 26. Kaplan Meier plot for time to biochemical recurrence by CD8+ T-cell infiltration for the HCRP cohort.

9 Discussion

9.1 PTEN loss and clinical outcome

Deciding the best treatment of newly diagnosed intermediate risk prostate cancer is still challenging for urologists. Moreover, prostate cancer risk stratification, such as Gleason score from biopsy, preoperative PSA, and clinical stage, are still not sufficient to distinguish more aggressive tumors from those projected to have an indolent disease course, so that overtreatment often occurs. From the clinical features, the Gleason score from biopsy is the most powerful and strongly associated with extraprostatic extension, but is less predictive in patients with Gleason score 7. In this way, the intensive investigation for biomarkers that may facilitate the management of prostate cancer patients is still in progress. Several *PTEN* gene and protein investigations have demonstrated increasing evidence that this biomarker can be used for the prediction of non-organ confined disease and disease recurrence (Cuzick et al., 2013; Krohn et al., 2012; Lotan et al., 2011; Mithal et al., 2014; Murphy et al., 2016; Qu et al., 2016; Troyer et al., 2015; Maisa Yoshimoto et al., 2012).

In our study, we evaluated the impact of *PTEN* deletions by FISH and PTEN protein loss by IHC in the prognosis of a homogeneous cohort of Gleason 7 prostate cancer patients. We observed that *PTEN* deletion was detected in 18.9% for the patients of the HCRP cohort, which is highly concordant with other studies that evaluated *PTEN* deletions by FISH in Gleason score 7. Picanço-Albuquerque et al. (2016) showed that 17.2% of the Gleason 7 patients harbored *PTEN* deletions by FISH. Moreover, our *in silico* analysis of array-CGH data showed that Gleason score 7 patients presented *PTEN* gene deletion in 20.9% (51/244) of the cases, being also highly concordant with our FISH results. PTEN protein analysis by IHC

showed that 16.3% of the patients harbored protein loss, which is highly concordant for another Gleason score 7 cohort study by IHC (18.3%) (Lotan et al., 2014).

Through FISH, we observed *PTEN* hemizygous deletions in 5/41 (11.6%) and *PTEN* homozygous deletions in 3/41 (7.3%) of the study cases. PTEN protein was lost in 7/39 (16.3%) and was expressed in 32/39 (82%) of the evaluated samples. Our results are concordant with the literature, that shows that *PTEN* deletions can be detected by FISH in 16-37% of patients (Picanço-Albuquerque et al., 2016; Sircar et al., 2009; Troyer et al., 2015). Further, PTEN protein loss can be identified in 11-30% of prostate cancer cases (Cuzick et al., 2013; Krohn et al., 2014b; Lotan et al., 2016). The range of the percentage of *PTEN* deletions by FISH and IHC is observed due to different scoring methodologies, variation of probe/antibody, material quality, pathological stage of the sample, and material type (biopsy, TURP, radical prostatectomy, CRPC, and metastasis).

The comparisons between PTEN FISH and IHC showed that all patients that harbored *PTEN* homozygous deletions concomitantly presented total PTEN protein loss. This finding is in keeping with the observation of complete deletion of both alleles of *PTEN* gene, which led to total protein loss. In addition, we observed that three patients that presented *PTEN* hemizygous deletions still had apparently normal levels of PTEN protein expression through IHC, indicating that one copy of *PTEN* gene was enough to maintain PTEN protein expression in the prostate gland. In contrast, three patients with both copies of *PTEN* gene presented PTEN protein loss. The patients that showed *PTEN* gene intact but PTEN protein loss possibly underwent point mutations, submicroscopic deletion, epigenetic alteration, or miRNA silencing that led to absence of PTEN protein expression.

The mutational profile of *PTEN* gene was accessed in the TCGA cohort showing that 4.1% of the patients harbored *PTEN* missense point mutations. From these, 70% of the mutations were detected in patients that harbored *PTEN* hemizygous deletions. Studies show

that *PTEN* mutations are found between 2-8% of prostate cancer cases (Abeshouse et al., 2015; Grasso et al., 2012; Krohn et al., 2012). In addition, in more aggressive prostate cancer cases, such as CRPC and mCRPC, *PTEN* mutations are more frequent and are present around 40% (Robinson et al., 2015). The high frequency of *PTEN* point mutations detected in the patients with hemizygous deletions may be associated with increased genomic and chromosomal instability generated by PTEN protein loss (Murphy et al., 2016; W. H. Shen et al., 2007). Hemizygous deletions that harbor proliferation inhibitory genes are preferentially selected during tumor development (Solimini, 2013). Furthermore, genomic instability has a critical role in the creation of variants within tumor cell populations, leading to clonal evolution, inter- and intratumoral heterogeneity and therapeutic resistance (Tapia-Laliena, Korzeniewski, Hohenfellner, & Duensing, 2014). In mice, *Pten* haploinsufficiency promotes progression of prostate cancer (Kwabi-Addo et al., 2001). Further, the haploinsufficiency of tumor suppressor genes leads to increased cell proliferation rates that consequently will promote mutational and SCNA accumulations in the genome (Davoli et al., 2013).

PTEN deletions are strongly associated with worse prostate cancer outcome. In our study, we evaluated the clinical impacts of PTEN loss in two cohorts of prostate cancer cases. The examined cohorts presented differences for the number of evaluated patients and other clinical features, such as the presence of extraprostatic extension, which was present in 47.1% of the patients from the TCGA cohort and 18.6% for the patients from the HCRP cohort. A study conducted with 45 Gleason 7 patients showed that 31.8% of the patients present extraprostatic extension (Picanço-Albuquerque et al., 2016).

By FISH, IHC and array-CGH, we found similar results showing a statistically significant increase in extraprostatic extension frequency when PTEN is lost. For the patients from the HCRP cohort, we observed that 25% cases with extraprostatic extension presented *PTEN* deletions by FISH, whereas 18% of the patients without *PTEN* deletions presented

extraprostatic extension. For the TCGA cohort, we observed that 62% and 43% cases with extraprostatic extension harbored either *PTEN* homo- or hemizygous deletions and both copies of *PTEN*, respectively. Troyer et al. (2015) evaluated the presence of *PTEN* deletions by FISH in 612 and detected that 40% of the patients with either *PTEN* homo- or hemizygous deletions presented extraprostatic extension. Moreover, homozygous deletions presented increased frequency of non-organ confined disease in all studies evaluated. In addition, we detected significant differences between cases with *PTEN* deletions and *PTEN* intact for capsular invasion, showing that 50% of the patients that harbored *PTEN* deletions presented capsular invasion, while 30% of the patients with both copies of the gene showed this feature. These observations are consistent with the findings that indicate that *PTEN* deletions by FISH are strong predictors of an aggressive prostate cancer disease.

The IHC analysis of the HCRP cohort, we observed that 42% of the patients that harbored PTEN protein loss showed extraprostatic extension. A study conducted with 260 prostate cancer patients with variable Gleason score showed that 52% of the patients presented extraprostatic extension when PTEN was lost by IHC (Guedes, Tosoian, Hicks, Ross, & Lotan, 2017).

When considering the occurrence of biochemical recurrence of the prostate cancer patients, we observed that 25% of the patients with *PTEN* deletions by FISH presented biochemical recurrence. Similarly, by IHC, we found that 28% of the patients that presented PTEN protein loss showed biochemical recurrence. In the TCGA cohort, we found that 38% of the patients with *PTEN* deletions presented disease recurrence. This association was statistically significant (*P*-value=0.03). Our log-rank analysis for the HCRP cohort did not show statistically significant association between PTEN gene and protein loss with earlier biochemical recurrence. However, the TCGA cohort showed a significant association with earlier biochemical recurrence events. Logistic regression of the TCGA cohort showed that

PTEN homozygous deletions significantly predict the occurrence of biochemical recurrence (*P*-value=0.02, HR=3.51).

Biochemical recurrence is associated with *PTEN* gene deletion in many studies (Murphy et al., 2016; Troyer et al., 2015; M Yoshimoto et al., 2007). In a prostate cancer cohort with patients presenting variable Gleason scores, Qu et al. (2016) showed that biochemical recurrence is found in 28% of the patients that harbor *PTEN* deletions by FISH. Moreover, the authors found a statistically significant value for prediction of this event when *PTEN* is deleted (*P*-value=0.008, HR=3.58) (Krohn et al., 2012). In the same way, Troyer et al. (2015) observed that *PTEN* homozygous deletions were significantly associated with the occurrence of biochemical recurrence events. Conversely, a PTEN protein analysis conducted with 77 prostate cancer needle biopsies demonstrated any significant association between protein loss and biochemical recurrence events, but significantly predicted CRPC, metastasis and prostate cancer specific-mortality (Mithal et al., 2014).

9.2 *In silico* genomic investigation of *PTEN* deletions

For validation and a more in-depth analysis of the genomic events associated with *PTEN* deletions, we performed an *in silico* analysis of public domain data of 244 Gleason 7 prostate cancer cases. The comparison between cases with *PTEN* deletions and *PTEN* intact presented a distinct copy number profile. *PTEN* homozygous deletions showed increased impact in the copy number profile, showing significantly associated losses in chromosomes 3p, 5q, 8p, 10q, 13q, 17p and 21q. This copy number profile is concordant with the findings from a meta-analysis of 662 prostate cancer cases that also shows concomitant genomic events in *PTEN* deleted samples (Williams, Greer, & Squire, 2014). Moreover, our findings are concordant with the literature, suggesting that *PTEN* homozygous deletions leads to an

increased instability of the genome due to greater proliferative rates together with the downregulation of apoptosis (Armstrong et al., 2016; Simpson & Parsons, 2001). We also observed that hemizygous deletion samples show reduced levels of SCNA profile, being concordant with the hypothesis that the loss of one allele of tumor suppressor genes may influence tumor progression in earlier stages of tumor development (Davoli et al., 2013; Solimini, 2013).

We also identified that patients with hemizygous deletions of *PTEN* also presented significant increase in TP53 deletions. These concomitant loss events are concordant with the observations that regions with tumor suppressor genes are commonly hemizygously lost (Solimini, 2013). Further, reduced p53 expression due to genomic loss events leads to dysregulation in cellular programs, such as apoptosis and DNA damage repair, consequently enabling tumor progression through acquisition of additional genetic changes (Kluth et al., 2014).

In addition, we observed that 35% of the samples that harbored *PTEN* homozygous deletions showed *TMPRSS2-ERG* rearrangements. Many studies have shown the association between *PTEN* loss and *TMPRSS2-ERG* rearrangements (Squire, 2009). In addition, the presence of *TMPRSS2-ERG* rearrangements have shown to influence prostate cancer outcome, being associated with bone metastasis (Deplus et al., 2016; Squire, 2009). However, *ERG* gene rearrangement itself does not portend an altered prognosis in most surgical cohorts (Pettersson et al., 2012). Investigations on the interaction of *PTEN* and *ERG* with respect to prostate cancer outcome prostate cancer has been complex. Based on animal models that demonstrate the synergy between *Pten* and *Erg* for prostate cancer progression, and early studies of the interaction of *PTEN* and *ERG* with respect to biochemical recurrence, it was initially understood that patients with combined *ERG* gene rearrangement and *PTEN* inactivation may exhibit worst prognosis compared to all other groups (Yoshimoto et al., 2008). However additional, larger studies using biochemical recurrence as an outcome

measure have found that patients with *PTEN* loss did similarly poorly, regardless of *ERG* status (Steurer et al., 2014).

Interestingly, we observed that racial ancestry may have an impact on *PTEN* deletions. All African-American patients showed *PTEN* intact, while European American and Asians harbored *PTEN* deletions. However, due to limited clinical information on racial ancestry of the TCGA cohort patients, our observations may be inconclusive. In the same way, the definition of the enrichment of *PTEN* deletion types for the three racial ancestry groups in this study cannot show significant differences. Indeed, primary prostate tumors arising in African-Americans have reduced rates of PTEN loss compared to tumors arising in matched patients of European-American ancestry (Khani et al., 2014; Lindquist et al., 2016; Tosoian et al., 2017). Moreover, the association of PTEN loss with poor prognosis appears to be independent of racial ancestry (Tosoian et al., 2017).

Our main findings suggest that *PTEN* homozygous deletions show increased impact on prognosis of prostate cancer patients when compared to hemizygous deletions. Moreover, PTEN protein loss showed sufficient specificity to detect worse prognosis in the cases from our cohort. Studies of prostate cancer samples are often very heterogeneous at their clinical and pathological staging. Our cohort is exclusively composed by patients with pathological Gleason score 7, which is an unique group for therapeutic decision. The characterization of PTEN deletion or protein loss could be helpful for disease stratification, once we observed that our patients showed a trend for earlier biochemical recurrence events through FISH, IHC and array-CGH techniques.

9.3 *PTEN* loss and CD8+ T-cell infiltration

We also evaluated the impact of *PTEN* gene deletion and PTEN protein loss in the infiltration of CD8+ T-cells in the TME of prostate cancer samples. We observed that PTEN

protein loss demonstrated increased CD8+ T-cell infiltration in the TME of the patient samples. Some studies have shown an inverse association with *PTEN* gene and protein loss with CD8+ T-cell infiltration. *PTEN* deletions inhibits the development of CD8+ T-cells by downregulating IL-17 in the TME (Hand et al., 2010).

We also observed that increased infiltration of CD8+ T-cells in the prostate cancer samples show a trend for earlier biochemical recurrence events. Indeed, CD8+ T-cell infiltration is an independent predictor factor of earlier biochemical recurrence (Ness et al., 2014). However, other studies indicate that increased CD8+ T-cell infiltration shows controversial association with biochemical recurrence in prostate cancer (Fridman, Zitvogel, Sautès–Fridman, & Kroemer, 2017).

CD8+ T-cells demonstrate great importance in the promotion of tumor cell specific death, being also promising option for prostate cancer immunotherapies. The most common immunotherapy for prostate cancer is the treatment with sipuleucel-T, a personalized immune system booster that promotes malignant cell death by the host lymphocytes. This treatment consists in obtaining white blood cells from the patients and their activation through their exposition to a prostate cancer protein (PAP) antigen. Cells are then stimulated by granulocyte-macrophage colony-stimulating factor (GM-CSF) and then reinjected in the patient. Immunotherapies are currently being combined with other treatments, such as hormonal therapy, radiotherapy, and chemotherapy (Gerritsen, 2012).

Other promising treatment consists in reactivating CD4+ and CD8+ T-cells of the tumor microenvironment. When present in the TME, the T-cells may exhibit no lytic function due to the interaction their cytotoxic-T-lymphocyte-associated protein 4 (CTLA-4) receptors with B7 family molecules present in antigen presenting cells (APC). In this way, the treatment with anti-CTLA-4 has shown a significant decrease of tumor volume of malignant prostate lesions (Drake, 2010). However, some patients experience a resistance to immune blockers,

suggesting that a combinatory treatment would be more efficient in these cases. Currently, the treatment of myeloid-derived suppressor cells (MDSCs) combined with anti-CTLA-4 showed a robust synergistic response in an mCRPC mouse model (Lu et al., 2017).

In melanoma, PTEN loss promotes reduced CD8+ T-cell infiltration and leads to an increased expression of immunosuppressive cytokines in the TME. *Pten* null melanoma mouse models showed a better response to treatment with anti-PD1 and anti-CTLA-4 when simultaneously treated with PI3K-beta inhibitors (Peng et al., 2016). In prostate cancer, PTEN protein loss are associated with decreased CD8+ T-cell infiltration (Vidotto et al., 2017, submitted). Moreover, PTEN loss showed to influence the immune response through interferon type I and II responses, leading to a reduced expression and activation of STAT1 and pSTAT3, two downstream effectors of IFN type I and II responses. These findings collectively suggest that genomic alterations may impact the TME and also influence patients response to immunotherapy.

10 Conclusion

This study shows that the frequency of PTEN loss in prostate cancer both in a cohort study, using FISH (18.9%), IHC (16.3%) and in an *in silico* analysis of array-CGH (20.9%) were similar and concordant with other studies.

Moreover, we found a statistically significant increase in extraprostatic extension frequency when PTEN is lost. We also detected other worse prognosis features, including a trend for earlier biochemical recurrence in patients that harbored *PTEN* deletions and PTEN protein loss.

We observed that PTEN protein loss in tumors was associated with increased $CD8^+$ T-cell infiltration in the tumor microenvironment, and these patients also had a trend for earlier biochemical recurrence.

In this thesis, *PTEN* gene has been characterized as an informative biomarker for prostate cancer stratification and for outcome prediction due to its functionality and impact in cell proliferation and also its role in the tumor microenvironment.

11 References

Abeshouse, A., Ahn, J., Akbani, R., Ally, A., Amin, S., Andry, C. D., … Zmuda, E. (2015). The Molecular Taxonomy of Primary Prostate Cancer. *Cell*, *163*(4), 1011–1025. https://doi.org/10.1016/j.cell.2015.10.025

Ahearn, T. U., Pettersson, A., Ebot, E. M., Gerke, T., Graff, R. E., Morais, C. L., … Lotan, T. L. (2016). A Prospective Investigation of PTEN Loss and ERG Expression in Lethal Prostate Cancer. *Journal of the National Cancer Institute*, *108*(2), 1–9. https://doi.org/10.1093/jnci/djv346

Armstrong, C. W. D., Maxwell, P. J., Ong, C. W., Redmond, K. M., Mccann, C., Neisen, J., … Waugh, D. J. J. (2016). PTEN deficiency promotes macrophage infiltration and hypersensitivity of prostate cancer to IAP antagonist/radiation combination therapy. *Oncotarget*. https://doi.org/10.18632/oncotarget.6955

Attard, G., Swennenhuis, J. F., Olmos, D., Reid, A. H. M., Vickers, E., A'Hern, R., … De Bono, J. S. (2009). Characterization of ERG, AR and PTEN gene status in circulating tumor cells from patients with castration-resistant prostate cancer. *Cancer Research*, *69*(7), 2912–2918. https://doi.org/10.1158/0008-5472.CAN-08-3667

Barbieri, C. E., Baca, S. C., Lawrence, M. S., Demichelis, F., Blattner, M., Theurillat, J.-P., … Garraway, L. a. (2012). Exome sequencing identifies recurrent SPOP, FOXA1 and MED12 mutations in prostate cancer. *Nature Genetics*, *44*(6), 685–9. https://doi.org/10.1038/ng.2279

Barbieri, C. E., & Tomlins, S. a. (2014). The prostate cancer genome: Perspectives and potential. *Urologic Oncology: Seminars and Original Investigations*, *32*(1). https://doi.org/10.1016/j.urolonc.2013.08.025

Barbosa, M., Henrique, M., Pinto-Basto, J., Claes, K., & Soares, G. (2011). Prostate cancer in Cowden syndrome: somatic loss and germline mutation of the PTEN gene. *Cancer Genetics*, *204*(4), 224–5. https://doi.org/10.1016/j.cancergen.2010.12.011

Bell, K. J. L., Del Mar, C., Wright, G., Dickinson, J., & Glasziou, P. (2015). Prevalence of incidental prostate cancer: A systematic review of autopsy studies. *International Journal of Cancer*, *137*(7), 1749–1757. https://doi.org/10.1002/ijc.29538

Bennett, K. L. (2010). Germline Epigenetic Regulation of KILLIN in Cowden and Cowden-Like Syndromes. *Jama*, *304*(24), 2724. https://doi.org/10.1001/jama.2010.1877

Berger, M. F., Lawrence, M. S., Demichelis, F., Drier, Y., Cibulskis, K., Sivachenko, A. Y., … Garraway, L. A. (2011). The genomic complexity of primary human prostate cancer. *Nature*, *470*(7333), 214–220. https://doi.org/10.1038/nature09744

Bismar, T. A., Yoshimoto, M., Duan, Q., Liu, S., Sircar, K., & Squire, J. A. (2012). Interactions and relationships of PTEN, ERG, SPINK1 and AR in castration-resistant prostate cancer. *Histopathology*, *60*(4), 645–652. https://doi.org/10.1111/j.1365-2559.2011.04116.x

Bismar, T. a., Yoshimoto, M., Vollmer, R. T., Duan, Q., Firszt, M., Corcos, J., & Squire, J. a. (2011). PTEN genomic deletion is an early event associated with ERG gene rearrangements in prostate cancer. *BJU International*, *107*(3), 477–485. https://doi.org/10.1111/j.1464-410X.2010.09470.x

Bostwick, D. G., & Qian, J. (2004). High-grade prostatic intraepithelial neoplasia. *Modern Pathology*, *17*(3), 360–379. https://doi.org/10.1038/modpathol.3800053

Bruinsma, S. M., Bangma, C. H., Carroll, P. R., Leapman, M. S., Rannikko, A., Petrides, N., … Zhang, L. (2016). Active surveillance for prostate cancer: a narrative review of clinical guidelines. *Nature Reviews Urology*, *13*(3), 151–167. https://doi.org/10.1038/nrurol.2015.313

Bubien, V., Bonnet, F., Brouste, V., Hoppe, S., Barouk-Simonet, E., David, A., … Caux, F. (2013). High cumulative risks of cancer in patients with PTEN hamartoma tumour syndrome. *Journal of Medical Genetics*, *50*, 255–63. https://doi.org/10.1136/jmedgenet-2012-101339

Butler, M. G., Dasouki, M. J., Zhou, X., Talebizadeh, Z., Brown, M., Takahashi, T. N., … Eng, C. (2005). Subset of individuals with autism spectrum disorders and extreme macrocephaly associated with germline PTEN tumour suppressor gene mutations. *Journal of Medical Genetics* , *42*(4), 318–321. https://doi.org/10.1136/jmg.2004.024646

Carter, H. B., Albertsen, P. C., Barry, M. J., Etzioni, R., Freedland, S. J., Greene, K. L., … Zietman, A. L. (2013). American Urological Association (AUA) Guideline GUIDELINE American Urological Association Early Detection of Prostate Cancer, 1–28.

Carver, B. S., Chapinski, C., Wongvipat, J., Hieronymus, H., Chen, Y., Chandarlapaty, S., … Sawyers, C. L. (2011). Reciprocal Feedback Regulation of PI3K and Androgen Receptor Signaling in PTEN-Deficient Prostate Cancer. *Cancer Cell*, *19*(5), 575–586. https://doi.org/10.1016/j.ccr.2011.04.008

Caux, F., Plauchu, H., Chibon, F., Faivre, L., Fain, O., Vabres, P., … Longy, M. (2007). Segmental overgrowth, lipomatosis, arteriovenous malformation and epidermal nevus (SOLAMEN) syndrome is related to mosaic PTEN nullizygosity. *European Journal of Human Genetics : EJHG*, *15*(7), 767–773. https://doi.org/10.1038/sj.ejhg.5201823

Champion, B. R., Fisher, K., & Seymour, L. (2016). A PTENtial cause for the selectivity of oncolytic viruses? *Nature Publishing Group*, *17*(3), 2–3. https://doi.org/10.1038/ni.3394

Chen, L., & Guo, D. (2017). The functions of tumor suppressor PTEN in innate and adaptive immunity. *Cellular & Molecular Immunology*, *14*(April), 1–9. https://doi.org/ 10.1038/cmi.2017.30

Chen, Z., Trotman, L. C., Shaffer, D., Lin, H.-K., Dotan, Z. A., Niki, M., … Pandolfi, P. P. (2005). Crucial role of p53-dependent cellular senescence in suppression of Pten-deficient tumorigenesis. *Nature*, *436*(7051), 725–730. https://doi.org/10.3892/ijo

Choucair, K., Ejdelman, J., Brimo, F., Aprikian, A., Chevalier, S., & Lapointe, J. (2012). PTEN genomic deletion predicts prostate cancer recurrence and is associated with low AR expression and transcriptional activity. *BMC Cancer*, *12*(1), 543. https://doi.org/10.1186/1471-2407-12-543

Ciccarese, C., Massari, F., Iacovelli, R., Fiorentino, M., Montironi, R., Di Nunno, V., … Tortora, G. (2017). Prostate cancer heterogeneity: Discovering novel molecular targets for therapy. *Cancer Treatment Reviews*, *54*, 68–73. https://doi.org/10.1016/ j.ctrv.2017.02.001

Colby, S., Yehia, L., Niazi, F., Chen, J., Ni, Y., Mester, J. L., & Eng, C. (2016). Exome sequencing reveals germline gain-of-function EGFR mutation in an adult with Lhermitte-Duclos disease. *Cold Spring Harbor Molecular Case Studies*, *2*(6), a001230. https://doi.org/10.1101/mcs.a001230

Cooperberg, M. R., Freedland, S. J., Pasta, D. J., Elkin, E. P., Presti, J. C., Amling, C. L., … Carroll, P. R. (2006). Multiinstitutional validation of the UCSF cancer of the prostate risk assessment for prediction of recurrence after radical prostatectomy. *Cancer*, *107*(10), 2384–2391. https://doi.org/10.1002/cncr.22262

Cooperberg, M. R., Pasta, D. J., Elkin, E. P., Litwin, M. S., Latini, D. M., DuChane, J., & Carroll, P. R. (2005). The UCSF Cancer of the Prostate Risk Assessment (CAPRA) Score: a straightforward and reliable preoperative predictor of disease recurrence after radical prostatectomy. *Journal of Urology*, *173*(6), 1938–1942. https://doi.org/10.1097/ 01.ju.0000158155.33890.e7

Cuzick, J., Yang, Z. H., Fisher, G., Tikishvili, E., Stone, S., Lanchbury, J. S., … Sangale, Z. (2013). Prognostic value of PTEN loss in men with conservatively managed localised prostate cancer. *British Journal of Cancer*, *108*(12), 2582–9. https://doi.org/10.1038/ bjc.2013.248

Davoli, T., Xu, A. W., Mengwasser, K. E., Sack, L. M., Yoon, J. C., Park, P. J., & Elledge, S. J. (2013). XCumulative haploinsufficiency and triplosensitivity drive aneuploidy patterns and shape the cancer genome. *Cell*, *155*(4), 948–962. https://doi.org/10.1016/j.cell.2013.10.011

Deplus, R., Delliaux, C., Marchand, N., Flourens, A., Vanpouille, N., Leroy, X., … Duterque-Coquillaud, M. (2016). TMPRSS2-ERG fusion promotes prostate cancer metastases in bone. *Oncotarget*, *8*(7), 11827–11840. https://doi.org/10.18632/oncotarget.14399

Di Cristofano, A., Pesce, B., Cordon-Cardo, C., & Pandolfi, P. P. (1998). Pten is essential for embryonic development and tumour suppression. *Nature Genetics*, *19*(4), 348–355. https://doi.org/10.1038/1235

Draisma, G., Etzioni, R., Tsodikov, A., Mariotto, A., Wever, E., Gulati, R., … De Koning, H. (2009). Lead time and overdiagnosis in prostate-specific antigen screening: Importance of methods and context. *Journal of the National Cancer Institute*, *101*(6), 374–383. https://doi.org/10.1093/jnci/djp001

Drake, C. G. (2010). Immunotherapy for Prostate Cancer: An Emerging Treatment Modality. *Urologic Clinics of North America*, *37*(1), 121–129. https://doi.org/10.1016/j.ucl.2009.11.001

Edge, S. B., & Compton, C. C. (2010). The American Joint Committee on Cancer: the 7th edition of the AJCC cancer staging manual and the future of TNM. *Annals of Surgical Oncology*, *17*(6), 1471–4. https://doi.org/10.1245/s10434-010-0985-4

Eng, C. (2003). PTEN: One gene, Many syndromes. *Human Mutation*, *22*(3), 183–198. https://doi.org/10.1002/humu.10257

Epstein, J. I., Allsbrook, W. C., Amin, M. B., & Egevad, L. L. (2006). Update on the Gleason grading system for prostate cancer: results of an international consensus conference of urologic pathologists. In *Advances in anatomic pathology* (Vol. 13, pp. 57–59). https://doi.org/10.1097/01.pap.0000202017.78917.18

Epstein, J. I., Allsbrook, W. C., Amin, M. B., Egevad, L. L., & ISUP Grading Committee. (2005). The 2005 International Society of Urological Pathology (ISUP) Consensus Conference on Gleason Grading of Prostatic Carcinoma. *The American Journal of Surgical Pathology*, *29*(9), 1228–42. Retrieved from http://www.ncbi.nlm.nih.gov/pubmed/16096414

Epstein, J. I., & Herawi, M. (2006). Prostate Needle Biopsies Containing Prostatic Intraepithelial Neoplasia or Atypical Foci Suspicious for Carcinoma: Implications for Patient Care. *The Journal of Urology*, *175*(3), 820–834. https://doi.org/10.1016/S0022-5347(05)00337-X

Ericson, K. J., Wenger, H. C., Rosen, A. M., Kiriluk, K. J., Gerber, G. S., Paner, G. P., & Eggener, S. E. (2017). Prostate cancer detection following diagnosis of atypical small acinar proliferation. *The Canadian Journal of Urology*, *24*(2), 8714–8720.

Etzioni, R., Cha, R., Feuer, E. J., & Davidov, O. (1998). Asymptomatic incidence and duration of prostate cancer. *American Journal of Epidemiology*, *148*(8), 775–785. https://doi.org/10.1097/00005392-199907000-00083

Feilotter, H. E., Nagai, M. a, Boag, a H., Eng, C., & Mulligan, L. M. (1998). Analysis of PTEN and the 10q23 region in primary prostate carcinomas. *Oncogene*, *16*(13), 1743–1748. https://doi.org/10.1038/sj.onc.1200205

Feng, J., Liang, J., Li, J., Li, Y., Liang, H., Zhao, X., … Yin, Y. (2015). PTEN Controls the DNA Replication Process through MCM2 in Response to Replicative Stress. *Cell Reports*, *13*(7), 1295–1303. https://doi.org/10.1016/j.celrep.2015.10.016

Ferraldeschi, R., Nava Rodrigues, D., Riisnaes, R., Miranda, S., Figueiredo, I., Rescigno, P., … De Bono, J. (2015). PTEN protein loss and clinical outcome from castration-resistant prostate cancer treated with abiraterone acetate. *European Urology*, *67*(4), 795–802. https://doi.org/10.1016/j.eururo.2014.10.027

Fridman, W. H., Zitvogel, L., Sautès–Fridman, C., & Kroemer, G. (2017). The immune contexture in cancer prognosis and treatment. *Nature Reviews Clinical Oncology*, 5–8. https://doi.org/10.1038/nrclinonc.2017.101

Gannon, P. O., Poisson, A. O., Delvoye, N., Lapointe, R., Mes-Masson, A. M., & Saad, F. (2009). Characterization of the intra-prostatic immune cell infiltration in androgen-deprived prostate cancer patients. *Journal of Immunological Methods*, *348*(1–2), 9–17. https://doi.org/10.1016/j.jim.2009.06.004

Garnett, J. E., Oyasu, R., & Grayhack, J. T. (1984). The accuracy of diagnostic biopsy specimens in predicting tumor grades by Gleason's classification of radical prostatectomy specimens. *The Journal of Urology*, *131*(4), 690–3. Retrieved from http://www.ncbi.nlm.nih.gov/pubmed/6708183

Gerritsen, W. R. (2012). The evolving role of immunotherapy in prostate cancer. *Annals of Oncology*, *23*(SUPPL.8). https://doi.org/10.1093/annonc/mds259

Gleason, D. F. (1966). Classification of prostatic carcinomas. *Cancer Chemother Rep*, *50*, 125–128.

Gleason, D. F., & Mellinger, G. T. (1974). Prediction of prognosis for prostatic adenocarcinoma by combined histological grading and clinical staging. *J Urol*, *111*, 58--64.

Grasso, C. S., Wu, Y.-M., Robinson, D. R., Cao, X., Dhanasekaran, S. M., Khan, A. P., … Tomlins, S. A. (2012). The mutational landscape of lethal castration-resistant prostate cancer. *Nature*, *487*(7406), 239–43. https://doi.org/10.1038/nature11125

Guedes, L. B., Tosoian, J. J., Hicks, J., Ross, A. E., & Lotan, T. L. (2017). PTEN Loss in Gleason Score 3 + 4 = 7 Prostate Biopsies is Associated with Non-organ Confined Disease at Radical Prostatectomy. *Journal of Urology*, *197*(4), 1054–1059. https://doi.org/10.1016/j.juro.2016.09.084

Gumuskaya, B., Gurel, B., Fedor, H., Tan, H.-L., Weier, C. a, Hicks, J. L., … De Marzo, a M. (2013). Assessing the order of critical alterations in prostate cancer development and progression by IHC: further evidence that PTEN loss occurs subsequent to ERG gene fusion. *Prostate Cancer and Prostatic Diseases*, *16*(2), 209–15. https://doi.org/10.1038/pcan.2013.8

Gundem, G., Van Loo, P., Kremeyer, B., Alexandrov, L. B., Tubio, J. M. C., Papaemmanuil, E., … Bova, G. S. (2015). The evolutionary history of lethal metastatic prostate cancer. *Nature*, *520*(7547), 353–7. https://doi.org/10.1038/nature14347

Hand, T. W., Cui, W., Jung, Y. W., Sefik, E., Joshi, N. S., Chandele, A., … Kaech, S. M. (2010). Differential effects of STAT5 and PI3K/AKT signaling on effector and memory CD8 T-cell survival. *Proceedings of the National Academy of Sciences of the United States of America*, *107*(38), 16601–6. https://doi.org/10.1073/pnas.1003457107

Heijnsdijk, E. a M., der Kinderen, a, Wever, E. M., Draisma, G., Roobol, M. J., & de Koning, H. J. (2009). Overdetection, overtreatment and costs in prostate-specific antigen screening for prostate cancer. *British Journal of Cancer*, *101*(11), 1833–1838. https://doi.org/10.1038/sj.bjc.6605422

Hopkins, B. D., Hodakoski, C., Barrows, D., Mense, S. M., & Parsons, R. E. (2014). PTEN function: The long and the short of it. *Trends in Biochemical Sciences*, *39*(4), 183–190. https://doi.org/10.1016/j.tibs.2014.02.006

Hopkins, B. D., Hodakoski, C., Barrows, D., Mense, S., & Parsons, R. E. (2015). PTEN function, the long and the short of it. *Trends Biochem Sci*, *39*(4), 183–190. https://doi.org/10.1016/j.tibs.2014.02.006.PTEN

Horwitz, E. M., Thames, H. D., Kuban, D. a, Levy, L. B., Kupelian, P. a, Martinez, A. a, … Zietman, A. L. (2005). Definitions of biochemical failure that best predict clinical failure in patients with prostate cancer treated with external beam radiation alone: a multi-institutional pooled analysis. *The Journal of Urology*, *173*(3), 797–802. https://doi.org/10.1097/01.ju.0000152556.53602.64

Howlader, N., Noone, A. M., Krapcho, M., Miller, D., Bishop, K., C.L., K., … Cronin, K. A. (2017). SEER Cancer Statistics Review, 1975-2014, National Cancer Institute. Retrieved July 13, 2017, from http://seer.cancer.gov/statfacts/html/prost.html

Instituto Nacional de Cancer José Alencar Gomes da Silva. (2016). *INCA - Instituto Nacional de Câncer - Estimativa 2016*. *Ministério da Saúde Instituto Nacional de Cancer José Alencar Gomes da Silva*. https://doi.org/978-85-7318-283-5

Jiao, J., Wang, S., Qiao, R., Vivanco, I., Watson, P. A., Sawyers, C. L., & Wu, H. (2007). Murine cell lines derived from Pten null prostate cancer show the critical role of PTEN in hormone refractory prostate cancer development. *Cancer Research*, *67*(13), 6083–6091. https://doi.org/10.1158/0008-5472.CAN-06-4202

Kass, E. M., Moynahan, M. E., & Jasin, M. (2016). When Genome Maintenance Goes Badly Awry. *Molecular Cell*, *62*(5), 777–787. https://doi.org/10.1016/j.molcel.2016.05.021

Khani, F., Mosquera, J. M., Park, K., Blattner, M., O'Reilly, C., MacDonald, T. Y., … Robinson, B. D. (2014). Evidence for molecular differences in prostate cancer between african American and Caucasian Men. *Clinical Cancer Research*, *20*(18), 4925–4934. https://doi.org/10.1158/1078-0432.CCR-13-2265

Kluth, M., Harasimowicz, S., Burkhardt, L., Grupp, K., Krohn, A., Prien, K., … Schlomm, T. (2014). Clinical significance of different types of p53 gene alteration in surgically treated prostate cancer. *International Journal of Cancer*, *135*(6), 1369–1380. https://doi.org/10.1002/ijc.28784

Konishi, N., Nakamura, M., Kishi, M., Nishimine, M., Ishida, E., & Shimada, K. (2002). Heterogeneous methylation and deletion patterns of the INK4a/ARF locus within prostate carcinomas. *The American Journal of Pathology*, *160*(4), 1207–14. https://doi.org/10.1016/S0002-9440(10)62547-3

Krohn, A., Diedler, T., Burkhardt, L., Mayer, P. S., De Silva, C., Meyer-Kornblum, M., … Schlomm, T. (2012). Genomic deletion of PTEN is associated with tumor progression and early PSA recurrence in ERG fusion-positive and fusion-negative prostate cancer. *American Journal of Pathology*, *181*(2), 401–412. https://doi.org/10.1016/j.ajpath.2012.04.026

Krohn, A., Freudenthaler, F., Harasimowicz, S., Kluth, M., Fuchs, S., Burkhardt, L., … Minner, S. (2014a). Heterogeneity and chronology of PTEN deletion and ERG fusion in prostate cancer. *Modern Pathology*, *27*(12), 1612–1620. https://doi.org/10.1038/modpathol.2014.70

Krohn, A., Freudenthaler, F., Harasimowicz, S., Kluth, M., Fuchs, S., Burkhardt, L., … Minner, S. (2014b). Heterogeneity and chronology of PTEN deletion and ERG fusion in prostate cancer. *Modern Pathology : An Official Journal of the United States and Canadian Academy of Pathology, Inc*, 1–9. https://doi.org/10.1038/modpathol.2014.70

Kwabi-Addo, B., Giri, D., Schmidt, K., Podsypanina, K., Parsons, R., Greenberg, N., & Ittmann, M. (2001). Haploinsufficiency of the Pten tumor suppressor gene promotes prostate cancer progression. *Proceedings of the National Academy of Sciences of the United States of America*, *98*(20), 11563–8. https://doi.org/10.1073/pnas.201167798

Lee, J. O., Yang, H., Georgescu, M. M., Cristofano, A. Di, Maehama, T., Shi, Y., … Pavletich, N. P. (1999). Crystal structure of the PTEN tumor suppressor: Implications for its phosphoinositide phosphatase activity and membrane association. *Cell*, *99*(3), 323–334. https://doi.org/10.1016/S0092-8674(00)81663-3

Leslie, N. R., & Foti, M. (2011). Non-genomic loss of PTEN function in cancer: Not in my genes. *Trends in Pharmacological Sciences*, *32*(3), 131–140. https://doi.org/10.1016/j.tips.2010.12.005

Leslie, N. R., & Longy, M. (2016). Inherited PTEN mutations and the prediction of phenotype. *Seminars in Cell and Developmental Biology*, *52*, 30–38. https://doi.org/10.1016/j.semcdb.2016.01.030

Li, S., Zhu, M., Pan, R., Fang, T., Cao, Y.-Y., Chen, S., … Guo, D. (2015). The tumor suppressor PTEN has a critical role in antiviral innate immunity. *Nature Immunology*, *advance on*(December). https://doi.org/10.1038/ni.3311

Liaw, D., Marsh, D. J., Li, J., Dahia, P. L., Wang, S. I., Zheng, Z., … Parsons, R. (1997). Germline mutations of the PTEN gene in Cowden disease, an inherited breast and thyroid cancer syndrome. *Nature Genetics*, *16*(1), 64–67. https://doi.org/10.1038/ng0597-64

Lindquist, K. J., Paris, P. L., Hoffmann, T. J., Cardin, N. J., Kazma, R., Mefford, J. A., … Witte, J. S. (2016). Mutational landscape of aggressive prostate tumors in African American men. *Cancer Research*, *76*(7), 1860–1868. https://doi.org/10.1158/0008-5472.CAN-15-1787

Litwin, M. S., & Tan, H.-J. (2017). The Diagnosis and Treatment of Prostate Cancer. *JAMA*, *317*(24), 2532. https://doi.org/10.1001/jama.2017.7248

Liu, W., Laitinen, S., Khan, S., Vihinen, M., Kowalski, J., Yu, G., … Bova, G. S. (2009). Copy number analysis indicates monoclonal origin of lethal metastatic prostate cancer. *Nat Med*, *15*(5), 559–565. https://doi.org/10.1038/nm.1944

Lotan, T. L., Carvalho, F. L., Peskoe, S. B., Hicks, J. L., Good, J., Fedor, H. L., … Berman, D. M. (2014). PTEN loss is associated with upgrading of prostate cancer from biopsy to radical prostatectomy. *Modern Pathology : An Official Journal of the United States and Canadian Academy of Pathology, Inc*, *28*(1), 1–10. https://doi.org/10.1038/modpathol.2014.85

Lotan, T. L., Gumuskaya, B., Rahimi, H., Hicks, J. L., Iwata, T., Robinson, B. D., … De Marzo, A. M. (2012). Cytoplasmic PTEN protein loss distinguishes intraductal carcinoma of the prostate from high-grade prostatic intraepithelial neoplasia. *Modern Pathology*, *26*(10), 587–603. https://doi.org/10.1038/modpathol.2012.201

Lotan, T. L., Gurel, B., Sutcliffe, S., Esopi, D., Liu, W., Xu, J., … De Marzo, A. M. (2011). PTEN protein loss by immunostaining: Analytic validation and prognostic indicator for a high risk surgical cohort of prostate cancer patients. *Clinical Cancer Research*, *17*(20), 6563–6573. https://doi.org/10.1158/1078-0432.CCR-11-1244

Lotan, T. L., Wei, W., Ludkovski, O., Morais, C. L., Guedes, L. B., Jamaspishvili, T., … Squire, J. A. (2016). Analytic validation of a clinical-grade PTEN immunohistochemistry assay in prostate cancer by comparison with PTEN FISH. *Modern Pathology : An Official Journal of the United States and Canadian Academy of Pathology, Inc*, *29*(8), 904–14. https://doi.org/10.1038/modpathol.2016.88

Lu, X., Horner, J. W., Paul, E., Shang, X., Troncoso, P., Deng, P., … DePinho, R. A. (2017). Effective combinatorial immunotherapy for castration-resistant prostate cancer. *Nature*, *543*(7647), 728–732. https://doi.org/10.1038/nature21676

Lusky, K. (1997). Prostate pointers — PIN , ASAP , mimics , and markers, 40–46.

Maehama, T., & Dixon, J. E. (1998a). The tumor suppressor, PTEN/MMAC1, dephosphorylates the lipid second messenger, phosphatidylinositol 3,4,5-trisphosphate. *The Journal of Biological Chemistry*, *273*(22), 13375–8.

Maehama, T., & Dixon, J. E. (1998b). The tumor suppressor, PTEN/MMAC1, dephosphorylates the lipid second messenger, phosphatidylinositol 3,4,5-trisphosphate. *The Journal of Biological Chemistry*, *273*(22), 13375–8. Retrieved from http://www.ncbi.nlm.nih.gov/pubmed/9593664

Marsh, D. J., Dahia, P. L. M., Zheng, Z., Liaw, D., Parsons, R., Gorlin, R. J., & Eng, C. (1997). Germline mutations in PTEN are present in Bannayan-Zonana syndrome. *Nature Genetics*, *16*(4), 333–334. https://doi.org/10.1038/ng0897-333

Marzo, A. M. De, Platz, E. A., Sutcliffe, S., Xu, J., Grönberg, H., Drake, C. G., … Nelson, W. G. (2007). Inflammation in prostate carcinogenesis. *Nature Reviews. Cancer*, *7*(4), 256–69. https://doi.org/10.1038/nrc2090

May, M., Knoll, N., Siegsmund, M., Fahlenkamp, D., Vogler, H., Hoschke, B., & Gralla, O. (2007). Validity of the CAPRA Score to Predict Biochemical Recurrence-Free Survival After Radical Prostatectomy. Results From a European Multicenter Survey of 1,296 Patients. *Journal of Urology*, *178*(5), 1957–1962. https://doi.org/10.1016/j.juro.2007.07.043

McNeal, J. E., Bostwick, D. G., Kindrachuk, R. A., Redwine, E. A., Freiha, F. S., & Stamey, T. A. (1986). Patterns of progression in prostate cancer. *Lancet*, *1*(8472), 60–63. https://doi.org/10.1016/S0140-6736(86)90715-4

Mellinger, G. T., Gleason, D. F., & Bailar, J. (1967). The histology and prognosis of prostatic cancer. *J Urol*, *97*, 331–7.

Merrimen, J. L., Jones, G., Walker, D., Leung, C. S., Kapusta, L. R., & Srigley, J. R. (2009). Multifocal High Grade Prostatic Intraepithelial Neoplasia is a Significant Risk Factor for Prostatic Adenocarcinoma. *The Journal of Urology*, *182*(2), 485–490. https://doi.org/10.1016/j.juro.2009.04.016

Mester, J. L., Moore, R. A., & Eng, C. (2013). PTEN Germline Mutations in Patients Initially Tested for Other Hereditary Cancer Syndromes: Would Use of Risk Assessment Tools Reduce Genetic Testing? *The Oncologist*, *18*(10), 1083–1090. https://doi.org/10.1634/theoncologist.2013-0174

Mester, J. L., Tilot, A. K., Rybicki, L. A., Frazier, T. W., & Eng, C. (2011). Analysis of prevalence and degree of macrocephaly in patients with germline PTEN mutations and of brain weight in Pten knock-in murine model. *European Journal of Human Genetics*, *19*(7), 763–8. https://doi.org/10.1038/ejhg.2011.20

Minami, A., Nakanishi, A., Ogura, Y., Kitagishi, Y., & Matsuda, S. (2014). Connection between Tumor Suppressor BRCA1 and PTEN in Damaged DNA Repair. *Frontiers in Oncology*, *4*(November), 318. https://doi.org/10.3389/fonc.2014.00318

Mithal, P., Allott, E., Gerber, L., Reid, J., Welbourn, W., Tikishvili, E., … Freedland, S. J. (2014). PTEN loss in biopsy tissue predicts poor clinical outcomes in prostate cancer. *International Journal of Urology*. https://doi.org/10.1111/iju.12571

Morais, C. L., Guedes, L. B., Hicks, J., Baras, A. S., De Marzo, A. M., & Lotan, T. L. (2016). ERG and PTEN status of isolated high-grade PIN occurring in cystoprostatectomy specimens without invasive prostatic adenocarcinoma. *Human Pathology*, *55*, 117–125. https://doi.org/10.1016/j.humpath.2016.04.017

Morais, C. L., Han, J. S., Gordetsky, J., Nagar, M. S., Anderson, A. E., Lee, S., … Lotan, T. L. (2015). Utility of PTEN and ERG Immunostaining for Distinguishing High-grade PIN From Intraductal Carcinoma of the Prostate on Needle Biopsy. *American Journal of Surgical Pathology*, *39*(0), 169–178. https://doi.org/10.1097/PAS.0000000000000348

Moschini, M., Carroll, P. R., Eggener, S. E., Epstein, J. I., Graefen, M., Montironi, R., & Parker, C. (2017). Low-risk Prostate Cancer: Identification, Management, and Outcomes. *European Urology*, 1–12. https://doi.org/10.1016/j.eururo.2017.03.009

Mottet, N., Bellmunt, J., Bolla, M., Briers, E., Cumberbatch, M. G., De Santis, M., … Cornford, P. (2017). EAU-ESTRO-SIOG Guidelines on Prostate Cancer. Part 1: Screening, Diagnosis, and Local Treatment with Curative Intent. *European Urology*, *71*(4), 618–629. https://doi.org/10.1016/j.eururo.2016.08.003

Murphy, S. J., Karnes, R. J., Kosari, F., Castellar, B. E. R. P., Kipp, B. R., Johnson, S. H., … Cheville, J. C. (2016). Integrated analysis of the genomic instability of PTEN in clinically insignificant and significant prostate cancer. *Modern Pathology*, *29*(2), 143–156. https://doi.org/10.1038/modpathol.2015.136

Ness, N., Andersen, S., Valkov, A., Nordby, Y., Donnem, T., Al-Saad, S., … Richardsen, E. (2014). Infiltration of CD8+ lymphocytes is an independent prognostic factor of biochemical failure-free survival in prostate cancer. *Prostate*, *74*(14), 1452–1461. https://doi.org/10.1002/pros.22862

Ngeow, J., Sesock, K., & Eng, C. (2017). Clinical Implications for Germline PTEN Spectrum Disorders. *Endocrinology and Metabolism Clinics of North America*, *46*(2), 503–517. https://doi.org/10.1016/j.ecl.2017.01.013

Nguyen, K. B., Cousens, L. P., Doughty, L. a, Pien, G. C., Durbin, J. E., & Biron, C. a. (2000). Interferon alpha/beta-mediated inhibition and promotion of interferon gamma: STAT1 resolves a paradox. *Nature Immunology*, *1*(1), 70–76. https://doi.org/10.1038/76940

Ni, Y., Zbuk, K. M., Sadler, T., Patocs, A., Lobo, G., Edelman, E., … Eng, C. (2008). Germline Mutations and Variants in the Succinate Dehydrogenase Genes in Cowden and Cowden-like Syndromes. *American Journal of Human Genetics*, *83*(2), 261–268. https://doi.org/10.1016/j.ajhg.2008.07.011

Nieuwenhuis, M. H., Kets, C. M., Murphy-Ryan, M., Yntema, H. G., Evans, D. G., Colas, C., … Vasen, H. F. A. (2014). Cancer risk and genotype-phenotype correlations in PTEN hamartoma tumor syndrome. *Familial Cancer*, *13*(1), 57–63. https://doi.org/10.1007/s10689-013-9674-3

Okotie, O. T., Roehl, K. A., Han, M., Loeb, S., Gashti, S. N., & Catalona, W. J. (2007). Characteristics of prostate cancer detected by digital rectal examination only. *Urology*, *70*(6), 1117–1120. https://doi.org/S0090-4295(07)01833-X [pii]\r10.1016/j.urology.2007.07.019

Olschwang, S., Serova-Sinilnikova, O. M., Lenoir, G. M., & Thomas, G. (1998). PTEN germline mutations in juvenile polyposis coli. *Nature Genetics*, *18*(1), 12–4. https://doi.org/10.1038/ng0198-12

Orloff, M. S., & Eng, C. (2008). Genetic and phenotypic heterogeneity in the PTEN hamartoma tumour syndrome. *Oncogene*, *27*(41), 5387–5397. https://doi.org/10.1038/onc.2008.237

Orloff, M. S., He, X., Peterson, C., Chen, F., Chen, J. L., Mester, J. L., & Eng, C. (2013). Germline PIK3CA and AKT1 mutations in cowden and cowden-like syndromes. *American Journal of Human Genetics*, *92*(1), 76–80. https://doi.org/10.1016/j.ajhg.2012.10.021

Padberg, G. W., Schot, J. D. L., Vielvoye, G. J., Bots, G. T. A. M., & De Beer, F. C. (1991). Lhermitte-duclos disease and cowden disease: A single phakomatosis. *Annals of Neurology*, *29*(5), 517–523. https://doi.org/10.1002/ana.410290511

Pagliarulo, V., Bracarda, S., Eisenberger, M. A., Mottet, N., Schröder, F. H., Sternberg, C. N., & Studer, U. E. (2012). Contemporary role of androgen deprivation therapy for prostate cancer. *European Urology*. https://doi.org/10.1016/j.eururo.2011.08.026

Pencik, J., Schlederer, M., Gruber, W., Unger, C., Walker, S. M., Chalaris, A., … Kenner, L. (2015). STAT3 regulated ARF expression suppresses prostate cancer metastasis. *Nature Communications*, *6*, 7736. https://doi.org/10.1038/ncomms8736

Peng, W., Chen, J. Q., Liu, C., Malu, S., Creasy, C., Tetzlaff, M. T., … Hwu, P. (2016). Loss of PTEN promotes resistance to T cell–mediated immunotherapy. *Cancer Discovery*, *6*(2), 202–216. https://doi.org/10.1158/2159-8290.CD-15-0283

Pesche, S., Latil, a, Muzeau, F., Cussenot, O., Fournier, G., Longy, M., … Lidereau, R. (1998). PTEN/MMAC1/TEP1 involvement in primary prostate cancers. *Oncogene*, *16*(22), 2879–2883. https://doi.org/10.1038/sj.onc.1202081

Pettersson, a., Graff, R. E., Bauer, S. R., Pitt, M. J., Lis, R. T., Stack, E. C., … Mucci, L. a. (2012). The TMPRSS2:ERG Rearrangement, ERG Expression, and Prostate Cancer Outcomes: A Cohort Study and Meta-analysis. *Cancer Epidemiology Biomarkers & Prevention*, *21*, 1497–1509. https://doi.org/10.1158/1055-9965.EPI-12-0042

Picanço-Albuquerque, C. G., Morais, C. L., Carvalho, F. L. F., Peskoe, S. B., Hicks, J. L., Ludkovski, O., … Squire, J. A. (2016). In prostate cancer needle biopsies, detections of PTEN loss by fluorescence in situ hybridization (FISH) and by immunohistochemistry (IHC) are concordant and show consistent association with upgrading. *Virchows Archiv*, *468*(5), 607–617. https://doi.org/10.1007/s00428-016-1904-2

Pilarski, R., Burt, R., Kohlman, W., Pho, L., Shannon, K. M., & Swisher, E. (2013). Cowden syndrome and the PTEN hamartoma tumor syndrome: Systematic review and revised diagnostic criteria. *Journal of the National Cancer Institute*, *105*(21), 1607–1616. https://doi.org/10.1093/jnci/djt277

Planchon, S. M., Waite, K. a, & Eng, C. (2008). The nuclear affairs of PTEN. *Journal of Cell Science*, *121*(Pt 3), 249–253. https://doi.org/10.1242/jcs.022459

Poliseno, L., Salmena, L., Riccardi, L., Fornari, A., Song, M. S., Hobbs, R. M., … Pandolfi, P. P. (2010). Identification of the miR-106b~25 microRNA cluster as a proto-oncogenic PTEN-targeting intron that cooperates with its host gene MCM7 in transformation. *Science Signaling*, *3*(117), ra29. https://doi.org/10.1126/scisignal.2000594

Poliseno, L., Salmena, L., Zhang, J., Carver, B., Haveman, W. J., & Pandolfi, P. P. (2010). A coding-independent function of gene and pseudogene mRNAs regulates tumour biology. *Nature*, *465*(7301), 1033–1038. https://doi.org/nature09144 [pii]\r10.1038/nature09144

Pound, C. R., Partin, A. W., Epstein, J. I., & Walsh, P. C. (1997). Prostate-specific antigen after anatomic radical retropubic prostatectomy. Patterns of recurrence and cancer control. *The Urologic Clinics of North America*, *24*(2), 395–406. Retrieved from papers2://publication/uuid/5C7FB0FC-535D-407A-9CD9-BFCBF1874DC1

Pulido, R. (2015). PTEN: A yin-yang master regulator protein in health and disease. *Methods*, *77*, 3–10. https://doi.org/10.1016/j.ymeth.2015.02.009

Qian, J., & Bostwick, D. G. (1995). The Extent and Zonal Location of Prostatic Intraepithelial Neoplasia and Atypical Adenomatous Hyperplasia: Relationship with Carcinoma in Radical Prostatectomy Specimens. *Pathology - Research and Practice*, *191*(9), 860–867. https://doi.org/10.1016/S0344-0338(11)80969-6

Qu, X., Jeldres, C., Glaskova, L., Friedman, C., Schroeder, S., Nelson, P. S., … Fang, M. (2016). Identification of Combinatorial Genomic Abnormalities Associated with Prostate Cancer Early Recurrence. *The Journal of Molecular Diagnostics : JMD*, *18*(2), 215–224. https://doi.org/10.1016/j.jmoldx.2015.10.001

Quaranta, B. P., Marks, L. B., & Anscher, M. S. (2004). Comparing radical prostatectomy and brachytherapy for localized prostate cancer. *Oncology (Williston Park, N.Y.)*, *18*(10), 1284–1289,1309.

Rahdar, M., Inoue, T., Meyer, T., Zhang, J., Vazquez, F., & Devreotes, P. N. (2009). A phosphorylation-dependent intramolecular interaction regulates the membrane association and activity of the tumor suppressor PTEN. *Proceedings of the National Academy of Sciences of the United States of America*, *106*, 480–485. https://doi.org/10.1073/pnas.0811212106

Reid, A., Attard, G., Ambroisine, L., Fisher, G., Kovacs, G., Brewer, D., … Cooper, C. (2010). Molecular characterisation of ERG, ETV1 and PTEN gene loci identifies patients at low and high risk of death from prostate cancer. *British Journal of Cancer*, *102*, 678–684. https://doi.org/10.1038/sj.bjc.6605554

Reid, A. H. M., Attard, G., Brewer, D., Miranda, S., Riisnaes, R., Clark, J., … Cooper, C. S. (2012). Novel, gross chromosomal alterations involving PTEN cooperate with allelic loss in prostate cancer. *Modern Pathology*, *25*(8), 1179–1179. https://doi.org/10.1038/modpathol.2012.85

Reis, R. B., & Cassini, M. F. (2010). Antígeno Prostático Específico (PSA). In A. Nardoza-Junior, M. Zerati-Filho, & R. B. Reis (Eds.), *Urologia Fundamental* (pp. 190–194). São Paulo: Planmark Ed.

Robinson, D., Van Allen, E. M., Wu, Y. M., Schultz, N., Lonigro, R. J., Mosquera, J. M., … Chinnaiyan, A. M. (2015). Integrative clinical genomics of advanced prostate cancer. *Cell*, *161*(5), 1215–1228. https://doi.org/10.1016/j.cell.2015.05.001

Roehl, K. A., Han, M., Ramos, C. G., Antenor, J. A., & Catalona, W. J. (2004). Cancer progression and survival rates following anatomical radical retropubic prostatectomy in 3,478 consecutive patients: long-term results. *J Urol*, *172*(3), 910–914. https://doi.org/10.1097/01.ju.0000134888.22332.bb

Ross, a E., D'Amico, a V, & Freedland, S. J. (2015). Which, when and why? Rational use of tissue-based molecular testing in localized prostate cancer. *Prostate Cancer and Prostatic Diseases*, (May), 1–6. https://doi.org/10.1038/pcan.2015.31

Salmena, L., Carracedo, A., & Pandolfi, P. P. (2008). Tenets of PTEN Tumor Suppression. *Cell*, *133*(3), 403–414. https://doi.org/10.1016/j.cell.2008.04.013

Shen, M. M., & Abate-Shen, C. (2007). Pten inactivation and the emergence of androgen-independent prostate cancer. *Cancer Research*, *67*(14), 6535–6538. https://doi.org/10.1158/0008-5472.CAN-07-1271

Shen, W. H., Balajee, A. S., Wang, J., Wu, H., Eng, C., Pandolfi, P. P., & Yin, Y. (2007). Essential Role for Nuclear PTEN in Maintaining Chromosomal Integrity. *Cell*, *128*(1), 157–170. https://doi.org/10.1016/j.cell.2006.11.042

Si, T.-G., Wang, J.-P., & Guo, Z. (2013). Analysis of Circulating Regulatory T Cells (CD4+CD25+CD127-) after Cryosurgery in Prostate Cancer. *Asian Journal of Andrology*, *15*(4), 461–465. https://doi.org/10.1038/aja.2013.22

Siegel, R. L., Miller, K. D., & Jemal, A. (2017). Cancer Statistics, 2017. *CA Cancer J Clin*, *67*(1), 7–30. https://doi.org/10.3322/caac.21387

Simpson, L., & Parsons, R. (2001). PTEN: life as a tumor suppressor. *Experimental Cell Research*, *264*(1), 29–41. https://doi.org/10.1006/excr.2000.5130

Sircar, K., Yoshimoto, M., Monzon, F. A., Koumakpayi, I. H., Katz, R. L., Khanna, A., … Squire, J. A. (2009). PTEN genomic deletion is associated with p-Akt and AR signalling in poorer outcome, hormone refractory prostate cancer. *Journal of Pathology*, *218*(4), 505–513. https://doi.org/10.1002/path.2559

Solimini, N. L. (2013). Recurrent Hemizygous Deletions in Cancers May Optimize Proliferative Potential. *Science*, *104*(2012), 2012. https://doi.org/10.1126/science.1219580

Song, M. S., Salmena, L., & Pandolfi, P. P. (2012). The functions and regulation of the PTEN tumour suppressor. *Nat Rev Mol Cell Biol*, *13*(5), 283–296. https://doi.org/10.1038/nrm3330

Squire, J. a. (2009). TMPRSS2-ERG and PTEN loss in prostate cancer. *Nature Genetics*, *41*(5), 509–510. https://doi.org/10.1038/ng0509-509

Stamey, T. A., Kabalin, J. N., Mcneal, J. E., Johnstone, I. M., Freiha, F., Redwine, E. A., & Yang, N. (1989). Prostate Specific Antigen in the Diagnosis and Treatment of Adenocarcinoma of the Prostate. II. Radical Prostatectomy Treated Patients. *The Journal of Urology*, *141*(5), 1076–1083. https://doi.org/10.1016/S0022-5347(17)41175-X

Steck, P. a, Pershouse, M. a, Jasser, S. a, Yung, W. K., Lin, H., Ligon, a H., … Tavtigian, S. V. (1997). Identification of a candidate tumour suppressor gene, MMAC1, at chromosome 10q23.3 that is mutated in multiple advanced cancers. *Nature Genetics*, *15*(4), 356–362. https://doi.org/10.1038/ng0497-356

Stephenson, A. J., Kattan, M. W., Eastham, J. a, Dotan, Z. a, Bianco, F. J., Lilja, H., & Scardino, P. T. (2006). Defining biochemical recurrence of prostate cancer after radical prostatectomy: a proposal for a standardized definition. *Journal of Clinical Oncology : Official Journal of the American Society of Clinical Oncology*, *24*(24), 3973–8. https://doi.org/10.1200/JCO.2005.04.0756

Steurer, S., Mayer, P. S., Adam, M., Krohn, A., Koop, C., Ospina-Klinck, D., … Schlomm, T. (2014). TMPRSS2-ERG fusions are strongly linked to young patient age in low-grade prostate cancer. *European Urology*, *66*(6), 978–981. https://doi.org/10.1016/j.eururo.2014.06.027

Strasner, A., & Karin, M. (2015). Immune Infiltration and Prostate Cancer. *Frontiers in Oncology*, *5*(July). https://doi.org/10.3389/fonc.2015.00128

Tan, M.-H., Mester, J. L., Ngeow, J., Rybicki, L. A., Orloff, M. S., & Eng, C. (2012). Lifetime Cancer Risks in Individuals with Germline PTEN Mutations. *Clinical Cancer Research*, *18*(2), 400–407. https://doi.org/10.1158/1078-0432.CCR-11-2283

Tan, M.-H., Mester, J., Peterson, C., Yang, Y., Chen, J.-L., Rybicki, L. A., … Eng, C. (2011). A Clinical Scoring System for Selection of Patients for PTEN Mutation Testing Is Proposed on the Basis of a Prospective Study of 3042 Probands. *The American Journal of Human Genetics*, *88*(1), 42–56. https://doi.org/10.1016/j.ajhg.2010.11.013

Tan, M. H., Mester, J., Peterson, C., Yang, Y., Chen, J. L., Rybicki, L. A., … Eng, C. (2011). A clinical scoring system for selection of patients for pten mutation testing is proposed on the basis of a prospective study of 3042 probands. *American Journal of Human Genetics*, *88*(1), 42–56. https://doi.org/10.1016/j.ajhg.2010.11.013

Tapia-Laliena, M. A., Korzeniewski, N., Hohenfellner, M., & Duensing, S. (2014). High-risk prostate cancer: A disease of genomic instability. *Urologic Oncology: Seminars and Original Investigations*, *32*(8), 1101–1107. https://doi.org/10.1016/j.urolonc.2014.02.005

Tay, Y., Kats, L., Salmena, L., Weiss, D., Tan, S. M., Ala, U., … Pandolfi, P. P. (2011). Coding-independent regulation of the tumor suppressor PTEN by competing endogenous mRNAs. *Cell*, *147*(2), 344–357. https://doi.org/10.1016/j.cell.2011.09.029

Tosoian, J. J., Almutairi, F., Morais, C. L., Glavaris, S., Hicks, J., Sundi, D., … Lotan, T. L. (2017). Prevalence and Prognostic Significance of PTEN Loss in African-American and European-American Men Undergoing Radical Prostatectomy. *European Urology*, *71*(5), 697–700. https://doi.org/10.1016/j.eururo.2016.07.026

Tosoian, J. J., Mamawala, M., Epstein, J. I., Landis, P., Wolf, S., Trock, B. J., & Carter, H. B. (2015). Intermediate and longer-term outcomes from a prospective active-surveillance program for favorable-risk prostate cancer. *Journal of Clinical Oncology*, *33*(30), 3379–3385. https://doi.org/10.1200/JCO.2015.62.5764

Trotman, L. C., Niki, M., Dotan, Z. A., Koutcher, J. A., Di Cristofano, A., Xiao, A., … Pandolfi, P. P. (2003). Pten dose dictates cancer progression in the prostate. *PLoS Biology*, *1*(3), 385–397. https://doi.org/10.1371/journal.pbio.0000059

Troyer, D. a., Jamaspishvili, T., Wei, W., Feng, Z., Good, J., Hawley, S., … Squire, J. a. (2015). A multicenter study shows *PTEN* deletion is strongly associated with seminal vesicle involvement and extracapsular extension in localized prostate cancer. *The Prostate*, n/a-n/a. https://doi.org/10.1002/pros.23003

Venderbos, L. D. F., van den Bergh, R. C. N., Roobol, M. J., Schröder, F. H., Essink-Bot, M.-L., Bangma, C. H., … Korfage, I. J. (2015). A longitudinal study on the impact of active surveillance for prostate cancer on anxiety and distress levels. *Psycho-Oncology*, *24*(3), 348–354. https://doi.org/10.1002/pon.3657

Verhagen, P. C. M. S., van Duijn, P. W., Hermans, K. G. L., Looijenga, L. H. J., van Gurp, R. J. H. L. M., Stoop, H., … Trapman, J. (2006). The PTEN gene in locally progressive prostate cancer is preferentially inactivated by bi-allelic gene deletion. *The Journal of Pathology*, *208*(5), 699–707. https://doi.org/10.1002/path.1929

Wang, Y., & Dai, B. (2015). PTEN genomic deletion defines favorable prognostic biomarkers in localized prostate cancer: a systematic review and meta-analysis. *Int J Clin Exp Med*, *8*(4), 5430–5437. Retrieved from www.ijcem.com

Wein, A. J., Kavoussi, L. R., Partin, A. W., & Peters, C. A. (Eds.). (2016). *Campbell-Wash Urology* (Eleventh E). Philadelphia: Elsevier Ltd.

Welty, C. J., Cooperberg, M. R., & Carroll, P. R. (2014). Meaningful end points and outcomes in men on active surveillance for early-stage prostate cancer. *Current Opinion in Urology*, *24*(3), 288–292. https://doi.org/10.1097/MOU.0000000000000039

Williams, J. L., Greer, P. A., & Squire, J. A. (2014). Recurrent copy number alterations in prostate cancer: An in silico meta-analysis of publicly available genomic data. *Cancer Genetics*, *207*(10–12), 474–488. https://doi.org/10.1016/j.cancergen.2014.09.003

Wilt, T. J. T. J., Brawer, M. K., Jones, K. M., Barry, M. J. M. J., Aronson, W. J. W. J., Fox, S., … Wheeler, T. (2012). Radical prostatectomy versus observation for localized prostate cancer. *New England Journal of Medicine*, *367*(3), 203–213. https://doi.org/10.1056/NEJMoa1113162.Radical

Yehia, L., Niazi, F., Ni, Y., Ngeow, J., Sankunny, M., Liu, Z., … Eng, C. (2015). Germline heterozygous variants in SEC23B are associated with cowden syndrome and enriched in apparently sporadic thyroid cancer. *American Journal of Human Genetics*, *97*(5), 661–676. https://doi.org/10.1016/j.ajhg.2015.10.001

Yoshimoto, M., Cunha, I. W., Coudry, R. a, Fonseca, F. P., Torres, C. H., Soares, F. a, & Squire, J. a. (2007). FISH analysis of 107 prostate cancers shows that PTEN genomic deletion is associated with poor clinical outcome. *British Journal of Cancer*, *97*(5), 678–685. https://doi.org/10.1038/sj.bjc.6603924

Yoshimoto, M., Cutz, J. C., Nuin, P. a S., Joshua, A. M., Bayani, J., Evans, A. J., … Squire, J. a. (2006). Interphase FISH analysis of PTEN in histologic sections shows genomic deletions in 68% of primary prostate cancer and 23% of high-grade prostatic intra-epithelial neoplasias. *Cancer Genetics and Cytogenetics*, *169*(2), 128–137. https://doi.org/10.1016/j.cancergencyto.2006.04.003

Yoshimoto, M., Joshua, A. M., Cunha, I. W., Coudry, R. A., Fonseca, F. P., Ludkovski, O., … Squire, J. A. (2008). Absence of TMPRSS2:ERG fusions and PTEN losses in prostate cancer is associated with a favorable outcome. *Mod Pathol*, *21*(12), 1451–1460. https://doi.org/10.1038/modpathol.2008.96

Yoshimoto, M., Ludkovski, O., Degrace, D., Williams, J. L., Evans, A., Sircar, K., … Squire, J. A. (2012). PTEN genomic deletions that characterize aggressive prostate cancer originate close to segmental duplications. *Genes Chromosomes and Cancer*, *51*(2), 149–160. https://doi.org/10.1002/gcc.20939

Yu, H., Pardoll, D., & Jove, R. (2009). STATs in cancer inflammation and immunity: a leading role for STAT3. *Nature Reviews. Cancer*, *9*(11), 798–809. https://doi.org/10.1038/nrc2734

Zhao, D., Lu, X., Wang, G., Lan, Z., Liao, W., Li, J., … DePinho, R. A. (2017). Synthetic essentiality of chromatin remodelling factor CHD1 in PTEN-deficient cancer. *Nature*, *542*(7642), 484–488. https://doi.org/10.1038/nature21357

Zysman, M. a, Chapman, W. B., & Bapat, B. (2002). Considerations when analyzing the methylation status of PTEN tumor suppressor gene. *The American Journal of Pathology*, *160*(3), 795–800. https://doi.org/10.1016/S0002-9440(10)64902-4

12 Attachments

12.1 Attachment A – Protocol for FFPE FISH and technical considerations

January 2, 2013

Performing Formalin-Fixed Paraffin-Embedded Tissue Fluorescence In Situ Hybridization (FISH) Using the Four Colour PTEN Deletion Probe (Prostate Tissue)

The following protocol is designed to prepare Formalin Fixed Paraffin Embedded (FFPE) tissue samples for analysis by FISH. The sample should be cut into **5 µm sections** and affixed to a silanized or positively charged slide.

MATERIALS, EQUIPMENT AND FORM

Reagents & Solutions:	**Equipment:**	**Supplies:**
Xylene	Water bath (80°C and 37°C)	
100% EtOH	Coplin jars (plastic and glass)	Silanized or Positively charged slides
85% EtOH	Timer	Coverslips (22x22, 22x30, 22x40 and 22x50)
70% EtOH	Forceps	Rubber Cement
20x SSC	Diamond tipped scribe	1 mL tubes
2x SSC (pH 7.0-7.2)		Serological pipettes
Distilled H_2O	Micropipette with tips	pH indicator sticks or pH meter
Pepsin (Porcine Gastric Mucosa) (Sigma-Aldrich, Cat # P6887)	Vortex mixer	PPE recommended by your Health and Occupational Safety regulations
Pepsin stock solution (75000 U/mL)	Microcentrifuge	Laboratory Wipes
1N HCl	Calibrated thermometer	Razor blades
0.01N HCl	Graduated cylinder	
0.2N HCl	Fluorescence microscope equipped with recommended filters	

August 9, 2012

IGEPAL (Sigma-Aldrich, Cat # P6887)	Slide warmer (45°C)	
2x SSC/ 0.3% Igepal Solution	Stir bar	
Cymogen DX PTEN FISH probe	Magnetic stirrer	
DAPI II Counterstain (Abbott Cat# 06J50-001)	ThermoBrite Hybridization Instrument (Abbott Cat# 07J91-010)	
10mM NaCitrate (pH 6.4)	Incubators (37°C and 65°C)	
VECTASHIELD Mounting Medium For Fluorescence (Vector Laboratories H-1000)	Thermometer	
EDTA, 0.5M (pH 8.0) (Promega, Cat # V4233)	Phase contrast microscope	

August 9, 2012

REAGENTS

Pepsin stock solution

- 250 mg lyophilized powder (Sigma Cat # P6887).
- Order 5-6 bottles of the same lot number at a time, ensure that Pepsin stock does not run out.
- One person should prepare the solution to keep quality control.
- Method: take the number of units (in units/mg) on bottle and multiply by 250mg to get the total number of units. Required working solution of 75,000units total. Add appropriate volume of dH_2O to bottle and aliquot into 500µl aliquots (store -20ºC). Place in 49.5ml of 0.01N HCl making the final concentration 750U/ml. Aliquots can be stored for 6 to 9 months.

2x SSC (100 mL) pH 7.0 - 7.2
10 mL of 20x SSC.
90 mL of dH_2O.
Adjust pH with 1N HCL or 1N NaOH.

2x SSC/0.3% IGEPAL (500 mL)
498.5 mL 2xSSC (pH 7.0-7.2).
1.5 mL of IGEPAL (Sigma-Aldrich, Cat # P6887).

Add 1.5 mL of IGEPAL with a serological pipette. Pipette up and down to rinse the pipette. Mix thoroughly with a magnetic stir bar and heat the solution to 40-50°C until the IGEPAL has been completely dissolved. Store in the dark at room temperature for up to 30 days. If sediment appears during storage, discard and prepare a fresh wash solution.

0.01N HCl (50 mL)
0.5 mL of 1N HCl.
49.5 mL of dH_2O.

0.2N HCl (50 mL)
10 mL of 1N HCl.
40 mL of dH_2O.

1 M Sodium Citrate
• Measure out 500 mL of dH_20, and add half the water to a 1 L volumetric flask.
• Add 147 g of Sodium Citrate Powder (Sigma Cat# S1804).
• Mix well until completely dissolved, add remaining water until there is exactly 500 mL of solution.

August 9, 2012

• Adjust the pH to 6.4 using 1N HCl.
• Autoclave at 121°C for 20 minutes to sterilize.

10 mM Sodium Citrate/2mM EDTA (500 mL)
• 493 mL of dH_2O.
• 5 mL of 1M Sodium Citrate (pH 6.4) .
• 2 mL of 0.5M EDTA.
• Mix well.

70% EtOH
• Add 350 mL of 100% EtOH to a flask and fill with dH_20 to a final volume of 500 mL.

85% EtOH
• Add 425 mL of 100% EtOH to a flask and fill with dH_20 to a final volume of 500 mL.

PROCEDURES

SAMPLES
- Archived formalin fixed paraffin embedded (FFPE) tissue sections, **5 µm thickness** on silanized or positively charged slides.

QUALITY CONTROL
- Control slides must be run concurrently with patient slides to monitor assay performance and to assess the accuracy of signal enumeration. Samples (same tissue type or metaphase spreads) should be used as positive and negative controls for the FISH testing.
- Control slides should be used beginning with the de-paraffinization process onward. Controls should be run on each day of FISH testing.
- The criteria for slide adequacy must be satisfied and the signal enumeration results should be within the specific established guidelines.
- Ensure that all reagents have reached desired temperatures prior to initiating procedure.
- Ensure that the DNA probe has been validated with established cut off values.
- Each hybridized slide should be evaluated against quality parameters determined by the laboratory.

PREPARATIONS REQUIRED BEFORE STARTING PROCEDURE
- Bake the 5 µm tissue section overnight at 56 - 65°C.
- All reagents and stock solutions should be prepared prior to the start of the procedure.
- Label the slides correctly: probe ID, date, lab identification gene or chromosome location, etc., along with name of person doing the procedure.

August 9, 2012

- Prepare fresh solutions prior to each procedure.

Day 1:

- Preheat water baths to 37°C and 80°C.
- Preheat 0.01N HCl: ensure that the temperature of the solution is 37°C.
- Preheat 10 mM Sodium Citrate/2mM EDTA: ensure that the temperature of the solution is 80°C.
- Prepare, label and preheat the coplin jars for the prehybridization steps:

  Xylene (1), Xylene (2) and Xylene (3) at room temperature (in chemical fume hood)
  100% EtOH (1) and 100%EtOH (2) at room temperature (in chemical fume hood)
  10 mM Sodium Citrate/2mM EDTA at 80°C
  0.2N HCl at room temperature
  2x SSC at room temperature
  0.01N HCl at 37°C
  dH_2O at room temperature
  2x SSC at room temperature
  70% EtOH at room temperature
  85% EtOH at room temperature
  100% EtOH at room temperature

Day 2:

- Preheat water bath to 72°C.
- Prepare, label and preheat the coplin jars for the post-hybridization steps:

  2x SSC/0.3% Igepal: ensure that the temperature of the solution is 72°C
  2x SSC at room temperature
  dH2O at room temperature

PROTOCOL

Day 1:

Deparaffinizing tissue section

- Immerse the slide(s) in Xylene for 10 minutes.
- Repeat the step above twice using fresh Xylene each time. Air dry slides for 2-5 minutes.
- Dehydrate in 100% ETOH for 5 minutes. Repeat.
- Air dry slide(s).

Slide pre-treatment

August 9, 2012

- Incubate slide(s) in 0.2N HCl at room temperature for 30 minutes.
- Incubate slide(s) in 10mM NaCitrate (pH 6.4)/ 2mM EDTA (pH 8.0) at 80°C for 45 minutes.
- Immerse the slide in 2x SSC at room temperature for 2 minutes.
- Rinse in dH2O for 10 minutes.

Protease pre-treatment

- Pre-warm the 0.01N HCl solution to 37°C.
- Incubate slide(s) in 0.2N HCl at room temperature for 2 minutes.
- Immediately prior to use, add 0.5 mL of the 75000U/mL pepsin solution to 49.95 mL of 0.01N HCl.
- Incubate slide(s) in pepsin/ 0.01N HCl at 37°C for 15 minutes

Note: The optimal incubation time for some sections may be shorter or longer, depending on the size, tissue preservation and heterogeneous cell content

- Immediately, immerse the slide in dH_2O at room temperature for 10 minutes.
- Dehydrate the slide(s) in a series of EtOH solutions (70%, 85% and 100%, 2 minutes each) at room temperature.
- Air-dry the slide(s).
- Assess tissue morphology using phase contrast microscopy to ensure sufficient digestion of the stroma/matrix has occurred (i.e. nuclei should be visible with distinct cell borders from one another). If required, the pepsin step may be repeated. Hollows in the tissue or a “ghosty” appearance indicate overdigestion. Start again and decrease the pepsin pre-treatment incubation.

Probe dilution

- Warm up the probe at 37°C for 5 minutes
- Vortex an then briefly centrifuge the vial
- Before applying the probe warm up the slide(s) at 45°C for 5 minutes.
- Apply 10 µl of the probe mix to slide and immediately apply coverslip (22x40 or 22x30) or, apply 5 µl of the probe mix to smaller tissue section and immediately apply coverslip (22x22)
- Seal the coverslip with rubber cement.

Co-denaturation

- Once the probe and coverslip are applied to the slide, warm on a thermobrite at 75°C for 10 minutes (calibrate the temperature of the thermobrite) for denaturation of target and probe DNA.
- Hybridize for 16 hours at 37°C.

Day 2:
Washing the slide

August 9, 2012

- Carefully remove the rubber cement and coverslip by securing the coverslip between your index finger and thumb, slowly peeling off the rubber cement with forceps. Use a razor blade to carefully lift the coverslip off the slide without dragging it across the slide's surface.
- Immediately immerse the slide(s) in 2x SSC/ 0.3% Igepal at 72°C for 2 minutes (+ 0.2°C/ per slide, up to a maximum of 73°C).
- Immerse the slide(s) in 2x SSC at room temperature for 5 minutes.
- Immerse the slide(s) in dH_2O at room temperature for 5 minutes.
- Air dry in the dark keeping the slide in an upright position.
- Dilute Vysis DAPI II counterstain 1:1 with Vectashield Mounting Medium for Fluorescence.
- Apply 25µl of Vysis DAPI II counterstain to the target area and apply coverslip (22x50).
- Keep the slides at -20°C for at least 30 minutes.

PROCEDURE NOTES

- FFPE sections are prepared according to standard histological methods. Check slides for morphology under phase contrast before hybridization. Nuclei should be visible with distinct cell borders from one another. Hollows in the tissue or a "ghosty" appearance indicate overdigestion.
- Mark hybridization area(s) with a diamond tipped pencil on the backside of specimen slide(s).
- Prepare all reagents prior to starting procedure.
- Immediately prior to use, warm the probe to 37°C so that viscosity decreases sufficiently to allow accurate pipeting. Vortex to mix.
- Measure temperature(s) of solution(s) inside Coplin jar(s) with a calibrated thermometer.

CARE WHILE PERFORMING FISH

- FISH assay results may not be informative if the specimen quality and/or specimen slide preparation is inadequate. A rigorous quality check should be performed before scoring.
- Fluorophores are readily photobleached by exposure to light. To limit this degradation, handle all solutions and slides containing fluorophore labeled probes in reduced light.
- Perform all steps that do not require light for manipulation, such as incubations and washes, in low light.
- Probe should be stored at -20°C, protected from light.
- Do not use probe beyond expiration date shown on vial.

August 9, 2012

Table 2. Summary Protocol

	Action	**Temperature**	**Incubation time**
	Day 1 (slides baked overnight at 56-65ºC)		
1	Xylene (3 treatments)	RT	10 minutes each
2	Air dry slides	RT	
3	100% ETOH (2 treatments)	RT	5 minutes each
4	Air dry slides	RT	
5	Incubate in the 0.2N HCL	RT	30 minutes
6	Incubate in the pre-warmed 10mM NaCitrate /2mM EDTA	80°C	45 minutes
7	2x SSC	RT	2 minutes
8	dH_2O	RT	10 minutes
9	Incubate in the 0.2N HCL	RT	2 minutes
10	Incubate in the pre-warmed pepsin/ 0.01N HCl at 37°C	37°C	15 minutes
11	dH_2O	RT	10 minutes
12	2x SSC	RT	5 minutes
13	70%, 85% and 100% EtOH	RT	2 minutes each
14	Air dry slides	RT	
15	Assess tissue morphology using phase contrast microscopy		
16	Prepare the probe according to the appropriate protocol		
17	Warm up the slides	45°C	5 minutes

August 9, 2012

18	Apply probe mix to slide and immediately apply coverslip		
19	Seal the coverslip with rubber cement		
20	Place the slide on a thermobrite	75°C	10 minutes
21	Target and probe DNA hybridization	37°C	16 hours
	DAY 2		
22	Carefully remove the rubber cement and coverslip.		
23	2x SSC/0.3% Igepal	72°C	2 minutes
24	2x SSC	RT	5 minutes
25	dH_2O	RT	5 minutes
26	Air dry in dark		
27	Apply DAPI counterstain to the target area and apply coverslip		

Technical considerations for FISH deletion assays using FFPE tissue sections

1. FISH Test Validation should be performed according to the most appropriate Standards and Guidelines for Laboratories [1] [2] [3] [4] [5], and for monitoring and reporting data[6]. There are a number of reviews that address clinical applications of FISH [7] [8].
2. Standard controls in laboratory testing should be applied. The laboratory should periodically check assay performance (including control probes) as part of quality monitoring. Monitoring FISH testing over time to assess adverse technical trends is also recommended.
3. Assessment of several normal metaphase cells should be considered for validation that the correct probe was used for the study. In typical analytic validations the FISH probe is hybridized to metaphase and interphase cells from peripheral blood cultures of five karyotypically normal control males. For each specimen the number of FISH signals in 50 consecutive interphase cell is recorded, and then the hybridization sites in 20 metaphase cells are identified by banded chromosome morphology. The analytic sensitivity and specificity for metaphase cells, and the percentage of nuclei that meet the signal pattern criteria for normal cells are calculated as described [1]. This evaluation also ensures that there are no background signals or cross-hybridizations to related genes that could be misinterpreted in interphase FISH tissue section analyses.
4. The cut-off levels to be used to identify a sample as deleted should be established as part of the FISH test validation for the laboratory. The cut-off value used is established by analyzing a reference panel of histological tissue sections from normal healthy cases. The use of suitable normal control tissue with similar sized nucleus to the target tissue being analyzed can help to establish the expected percentage of signal losses due to signal truncation artefacts. In this context, setting up a normal database for each probe being used in the laboratory is suggested. The laboratory's cut-off database should address each type of target tissue and it should identify the thickness of samples used for FISH (the same thickness should be maintained for all specimen testing). Wiktor et al[1] published an excllent clinical FISH validation approach, which describes a cut-off method to establish an analytic sensitivity with a 95% confidence level. The ECA

guidelines also discuss various approches to establishing robust cutoffs [2]. Monitoring and revising existing cut-off values should also be considered as probes used and test approaches change with time.

5. Run positive and negative controls. For FISH deletion assays these will be samples with known homozygous, hemizygous and undeleted copies of the tumor suppressor gene of interest.
6. Use optimal filter set for the deletion assay probe combination and check there is no bleed-through between different filters.
7. Review slides for hybridization performance- should be >85% efficiency with minimal non-specific noise.
8. Pre-screen the tumour area selected by the pathologist using an adjacent hematoxylin and eosin section map for the following features:
    - the area is tumor rich
    - nuclei have a regular shape and uniform DAPI staining
    - nuclei do not have evidence of digestion damage such as "doughnut-like" appearance with empty epicentres
    - nuclei should not be covered by a cloudy typically yellowish layer or obscured by auto-fluorescent structures.
    - nuclei have hybridization signals with uniform intensity and similar patterns of granularity.
9. Ensure that the entire selected area of tumor has been pre-screened carefully before selecting nuclei to score. Sometimes a small area containing a clonal deletion may be missed without this pre-screen.
10. Only examine nuclei that are distinct and ideally separated from each other. Select cells in which the borders of individual nuclei can be clearly distinguished. Avoid scoring nuclei that are crowded, overlapping, or distorted.
11. When selecting nuclei focus up and down on the z-axis and make sure the entire volume of the chosen nucleus is present inside the section and that the FISH signals at all focal planes are enumerated. A bias in distribution to the upper or lower face of the section may indicate truncation.
12. The probes flanking the tumor suppressor gene can help distinguish between truncation losses and "real" interstitial deletions. Sometime the deletion may be larger and include one (or both) flanking probe sets.

13. All scores should be entered onto score sheets in an unbiased manner. A routine FISH evaluation should be scored by two technologists.
14. All scores should be entered onto score sheets together with comments that may be relevant concerning heterogeneity, signal quality etc.
15. Score appropriate number of nuclei according to the Standards and Guidelines for Laboratories. When inconsistent results are obtained a third reader is required or additional nuclei should be scored based on the laboratory director's guidance.
16. Be aware of the possibility of clonality of deletions (such as mixture of hemi-and homozygous deletion). Any clone should be visible once appropriate number of nuclei have been scored.
17. Sometimes in complex cases there are more than one type of clone. Each clone should be scored individually (score appropriate number of nuclei for each clone) and the location of the clone marked on the hematoxylin and eosin section map. In such complex tissue where there are more than one type of aberration, each clone should be scored individually (ideally scoring 100 cells for each).
18. Once completed the scoring, re-scan the marked tumor area to ensure nothing has been missed.
19. Typical scoring results for tumor suppressor gene FISH assays will describe the % of normal cells, the frequency of homozygous and /or hemizygous deletions or monosomies. In addition there may be a percentage of cells with ploidy alterations or gains of the chromosome. The criteria for scoring deletion FISH should in general be developed for the tumor supressor gene of interest after taking into account the previous experience of the laboratory and using data from the literature from other groups performing similar assays.
20. For quality control – ensure that signals from all probes are present in normal surrounding tissue adjacent to tumor areas on all slides to confirm successful FISH hybridization.

REFERENCES

1. Wiktor, A. E. *et al.* Preclinical validation of fluorescence in situ hybridization assays for clinical practice. *Genet. Med.* 8**,** 16–23 (2006).

2. European Cytogenetics Association. FISH ON HISTOLOGICAL SECTIONS OF SOLID TUMORS: E.C.A. RECOMMENDATIONS. *E.C.A. European*

Cytogeneticists Asscoiation Newsletter 28–30 (2012).

3. Wolff, D. J. *et al.* Guidance for fluorescence in situ hybridization testing in hematologic disorders. *J. Mol. Diagn.* 9**,** 134–143 (2007).

4. Ventura, R. A. *et al.* FISH analysis for the detection of lymphoma-associated chromosomal abnormalities in routine paraffin-embedded tissue. *J. Mol. Diagn.* 8**,** 141–151 (2006).

5. Mascarello, J. T. *et al.* Section E9 of the American College of Medical Genetics technical standards and guidelines: fluorescence in situ hybridization. *Genet. Med.* 13**,** 667–675 (2011).

6. Deutsch, E. W. *et al.* Minimum information specification for in situ hybridization and immunohistochemistry experiments (MISFISHIE). *Nat. Biotechnol.* **26,** 305–312 (2008).

7. Squire, J. A., Marrano, P. & Kolomietz, E. FISH in clinical cytogenetics. *FISH, Pract. approach. Ed. by B. Beatty, S. Mai, J. Squire. Oxford Univ. Press. New York, NY* 183–202 (2002).

8. Liehr, T. in *Fluorecence in situ hybridization (FISH) application guide* (2016).

12.2 Attachment B - Ethics Committee Approval

HOSPITAL DAS CLÍNICAS DA FACULDADE DE MEDICINA
DE RIBEIRÃO PRETO DA UNIVERSIDADE DE SÃO PAULO

FMRP-USP
RIBEIRÃO PRETO

Ribeirão Preto, 03 de setembro de 2015

Ofício nº 3151/2015
CEP/MGV

Prezados Senhores,

O trabalho intitulado **"CARACTERIZAÇÃO DO GENE PTEN COMO BIOMARCADOR PROGNÓSTICO NO CÂNCER DE PRÓSTATA" – Versão 2, de 03/08/2015**, foi analisado pelo Comitê de Ética em Pesquisa, em sua 414ª Reunião Ordinária realizada em 31/08/2015 e enquadrado na categoria: APROVADO, bem como a solicitação de dispensa do Termo de Consentimento Livre e Esclarecido, de acordo com o Processo HCRP nº 9499/2015.

Este Comitê segue integralmente a Conferência Internacional de Harmonização de Boas Práticas Clínicas (IGH-GCP), bem como a Resolução nº 466/12 CNS/MS.

Lembramos que devem ser apresentados a este CEP, o Relatório Parcial e o Relatório Final da pesquisa.

Atenciosamente.

DRª. MARCIA GUIMARÃES VILLANOVA
Coordenadora do Comitê de Ética em
Pesquisa do HCRP e da FMRP-USP

Ilustríssimos Senhores
CLARISSA GONDIM PICANÇO DE ALBUQUERQUE
PROF.DR.JEREMY A. SQUIRE(Orientador)
Depto. de Genética – FMRP-USP

12.3 Attachment C – Published manuscript

Virchows Arch
DOI 10.1007/s00428-016-1904-2

ORIGINAL ARTICLE

In prostate cancer needle biopsies, detections of PTEN loss by fluorescence in situ hybridization (FISH) and by immunohistochemistry (IHC) are concordant and show consistent association with upgrading

C. G. Picanço-Albuquerque[1] · C. L. Morais[2] · F. L. F. Carvalho[2] · S. B. Peskoe[3] · J. L. Hicks[2] · O. Ludkovski[4] · T. Vidotto[1] · H. Fedor[2] · E. Humphreys[5] · M. Han[5] · E. A. Platz[3,5,6] · A. M. De Marzo[2,5,6] · D. M. Berman[2,4,5] · T. L. Lotan[2,6] · J. A. Squire[1,4,7]

Received: 13 August 2015 / Revised: 15 December 2015 / Accepted: 12 January 2016

Abstract The prognostic value of phosphatase and tensin homolog (PTEN) loss in prostate cancer has primarily been evaluated by either fluorescence in situ hybridization (FISH) or immunohistochemistry (IHC). Previously, we found that PTEN loss by IHC was associated with increased risk of upgrading from biopsy (Gleason 3+3) to prostatectomy (Gleason 7+). Now, using an evaluable subset of 111 patients with adjacent biopsy sections, we analyzed the association between *PTEN* deletion in cancer and the odds of upgrading by a highly sensitive and specific four-color FISH assay. We also compared the concordance of PTEN loss by IHC and *PTEN* deletion by FISH. *PTEN* deletion was found in 27 % (12/45) of upgraded cases compared with 11 % (7/66) of controls ($P=0.03$). Cancers with *PTEN* deletions were more likely to be upgraded than those without deletions (adjusting for age odds ratio = 3.40, 95 % confidence interval 1.14–10.11). With respect to concordance, of 93 biopsies with PTEN protein detected by IHC, 89 (96 %) had no *PTEN* deletion by FISH, and of 18 biopsies without PTEN protein by IHC, 15 had homozygous or hemizygous *PTEN* deletion by FISH. Only 4 biopsies of the 93 (4 %) with PTEN protein intact had *PTEN* deletion by FISH. When the regions of uncertainty in these biopsies were systematically studied by FISH, intra-tumoral variation of *PTEN* deletion was found, which could account for variation in immunoreactivity. Thus, FISH provides a different approach to determining PTEN loss when IHC is uncertain. Both FISH and IHC are concordant, showing consistent positive associations between PTEN loss and upgrading.

Electronic supplementary material The online version of this article (doi:10.1007/s00428-016-1904-2) contains supplementary material, which is available to authorized users.

✉ J. A. Squire
jsquireinsp@gmail.com

[1] Department of Genetics, Ribeirão Preto Medical School, University of Sao Paulo, Ribeirão Preto, Brazil

[2] Department of Pathology, Johns Hopkins University School of Medicine, Baltimore, MD, USA

[3] Department of Epidemiology, Johns Hopkins Bloomberg School of Public Health, Baltimore, MD, USA

[4] Department of Pathology and Molecular Medicine, Queen's University, Kingston, ON, Canada

[5] Department of Urology and the James Buchanan Brady Urological Institute, Johns Hopkins University School of Medicine, Baltimore, MD, USA

[6] Department of Oncology, Johns Hopkins University School of Medicine, Baltimore, MD, USA

[7] Department of Pathology, Ribeirão Preto Medical School, University of Sao Paulo, Ribeirão Preto, Brazil

Published online: 09 February 2016

Keywords Gleason upgrade · Tumor suppressor gene · Prognostic biomarker assay · Hemizygous and homozygous genomic deletion

Introduction

Loss of the phosphatase and tensin homolog (*PTEN*) tumor suppressor gene by genomic deletion occurs in approximately 20–30 % of prostate cancers (PCas) [1–4]. *PTEN* loss at radical prostatectomy has been shown to correlate with early biochemical recurrence [2, 4, 5], extracapsular and seminal vesicle invasion [6], castrate-resistant disease, metastasis, and PCa-specific death [7, 8]. Differentiation of aggressive from indolent tumors remains a high priority for the appropriate management of prostate cancer and the avoidance of unnecessary treatment and side effects in patients with indolent disease [9]. Biomarker assays that determine whether or not *PTEN* has been deleted are therefore important for determining prognosis in PCa. However, to be of practical value for improving PCa management, PTEN assays performed using needle core biopsies must not only accurately determine whether PTEN function has been lost but also demonstrate that PTEN loss in the tumor on biopsy is associated with, and ultimately predictive for, upgrading of the Gleason score.

The clinical parameters currently available for prognostic assessment of PCa at the time of diagnosis include prostate-specific antigen (PSA) level, number of positive biopsy cores, percent of cores involved by tumor, and Gleason score. Various nomograms are used to integrate these data into an overall prognostic index to aid in initial treatment decision making after a positive biopsy [10]. The Gleason score of PCa in the needle biopsy is one of the most powerful prognostic markers, but its determination is inaccurate in a large percentage of cases, especially when only a small-volume tumor was sampled during biopsy. Thus, the presence of PTEN loss in the PCa of needle cores may provide useful additional prognostic information in the context of the biopsy, when there is uncertainty about the overall Gleason score in the detected tumor.

PTEN loss using clinical tissue samples may be determined by either immunohistochemistry (IHC) or by fluorescence in situ hybridization (FISH). Two recent studies using IHC showed a positive association between PTEN loss in tumor in needle biopsies at diagnosis and poor outcome [11, 13]. In the most recent study, Lotan et al. [12] using IHC showed that PTEN loss in Gleason 3+3=6 needle core biopsies was associated with upgrading to Gleason 7+ at radical prostatectomy.

Recently, a four-color FISH assay was developed that detects *PTEN* deletions with high sensitivity and specificity [14]. As yet, no systematic comparison of *PTEN* deletion detected by this FISH assay and PTEN protein loss detected by IHC on needle core biopsies has been done. Thus, to provide further support for the utility of PTEN loss as a biomarker for PCa through the use of this FISH assay, we analyzed 111 sections that were immediately adjacent to those previously studied by IHC [12]. We evaluated the association between *PTEN* loss by FISH and upgrading from Gleason 3+3=6 at biopsy to Gleason 7+ at radical prostatectomy and determined the concordance in PTEN loss between *PTEN* deletion by FISH and PTEN protein loss by IHC. In addition, we show how *PTEN* FISH can be used in areas of PCa where IHC is hard to interpret, either due to intra-tumoral heterogeneity or to marginally reduced levels of PTEN immunoreactivity.

Material and methods

Patients and tissue samples

The source population consisted of patients previously studied by PTEN IHC [12]. Use of the samples required informed consent and permission by the internal review board. Briefly, the 174 men had Gleason 6 (3+3) prostate cancer on needle biopsy and either were (71 cases) or were not (103 controls) upgraded to Gleason 7+ on radical prostatectomy. All radical prostatectomy tissues were entirely submitted for histologic analysis, and all biopsies and radical prostatectomy slides were re-reviewed and re-graded by trained uropathologists (DMB and TLL) using the 2005 modified International Society of Urologic Pathology (ISUP) grading system [15]. A single block (usually with two cores on one slide) that contained the largest percentage involvement by tumor was selected for PTEN immunostaining, and the immediate adjacent section was used for *PTEN* FISH.

It is not universally agreed upon whether a tumor with majority Gleason pattern 3 and <5 % Gleason pattern 4 should be graded as Gleason 3+3=6 with tertiary pattern 4 or Gleason 3+4=7. In favor of using a tertiary grade, the ISUP consensus paper noted that tumors with majority Gleason pattern 3 and <5 % pattern 4 generally have a lower pathologic stage than a Gleason score 3+4=7 where pattern 4 occupies >5 % of the tumor [15]. Overall, in the current study, 41 % (27/66) of the non-upgraded control radical prostatectomies had a component (<5 %) of tertiary Gleason pattern 4. However, because the inter-observer reproducibility of tertiary grading remains largely untested and because Gleason score 6 tumors have largely negligible lethality regardless of tertiary Gleason pattern [16], grading in the current study was defined solely by Gleason score without reference to a tertiary component.

PTEN FISH

In the current study, adjacent sections of biopsy tissue were successfully evaluated by FISH on 64 % of cases (45 cases and 66 controls). Part of the reason for the relatively low overall rate of FISH success was the difficulty we encountered

Table 1 Summary of the clinical characteristics and pathology of prostate needle biopsies and subsequent radical prostatectomies for upgraded cases and controls

	Cases ($n=45$)	Controls ($n=66$)	P value
Age at diagnosis (years, mean (SD))	62.2 (5.1)	59.1 (5.9)	0.005
Non-white (%)	31.1	19.7	0.17
Preoperative PSA (ng/ml, mean (SD))	6.19 (2.67)	5.46 (2.93)	0.18
PSA density[a] (ng/ml g, mean (SD))	0.12 (0.06)	0.11 (0.08)	0.23
Clinical stage (%)			
1–T1c	83.7	79.4	0.78
2–T2a	14.0	15.9	
3–T2b	2.3	4.8	
Percent missing	4.4	4.5	
PSA recurrence (%)	7.9	1.7	0.30
Percent missing	15.6	12.1	
Years of follow-up (mean (SD))	3.7 (3.0)	4.7 (3.5)	0.17
Percent missing	15.6	12.1	
Number of cores sampled (mean (SD))	11.8 (1.0)	12.1 (1.1)	0.25
Less than 12 cores sampled (%)	8.9	6.1	0.71
Number involved cores (mean (SD))	4.6 (2.5)	3.7 (2.0)	0.05
Mean percent of involved cores (mean % (SD))	40 (23)	32 (17)	0.05
Maximum percent tumor per core (mean (SD))	54 (26)	51 (26)	0.53
Bilateral positive cores (%)	57.8	40.0	0.07
Perineural invasion (%)	35.6	25.8	0.27
Post-operative pathology			
Gland weight (g, mean (SD))	55.0 (20.5)	57.9 (22.7)	0.51
Pathologic stage (%)			
1–T2	68.2	80.3	0.38
2–T3a	27.3	16.7	
3–T3b	4.5	3.0	
Percent missing	2.2	0.0	
Pathologic stage > T2 (%)	31.8	19.7	0.15
Percent missing	2.2	0.0	
Positive margins (%)	20.0	4.5	0.01
Tertiary Gleason pattern (%)			
0–no pattern	77.8	59.1	<0.0001
3	0.0	0.0	
4	6.7	40.9	
5	15.6	0.0	

[a] PSA density was calculated using the prostate weight at radical prostatectomy

in locating the same small area of carcinoma studied by immunohistochemistry in the adjacent section. In 24 % of samples, the same region of cancer could not be found due to alignment problems or because the carcinoma did not extend to the adjacent section. The actual FISH failure rate in the samples where the same region of cancer could be located was only 10 %. The PTEN Del TECT FISH assay chosen utilizes a four-color probe combination as described [7, 14]. Probes were supplied by CymoGenDx LLC (New Windsor, NY) as follows: centromeric copy control probe (CEP)—CYMO-pink, wings apart-like homolog (*WAPAL*)—CYMO-green, *PTEN*—CYMO-red, and *FAS*—CYMO-aqua. FISH analysis was performed using 4-μm sections of needle biopsies stained with 4′,6-diamidino-2-phenylindole dihydrochloride (DAPI) in areas selected by the pathologist using an immediately adjacent section stained with hematoxylin and eosin. *PTEN* copy number was evaluated by counting spots for all four probes using SemRock filters appropriate for the excitation and emission spectra of each dye in 50–100 non-overlapping, intact, inter-phase nuclei per tumor in each selected biopsy section. For each case, all areas selected by the pathologist were checked and two to four areas (depending on availability) were chosen for scoring based on overall technical variables such as the quality of FISH hybridization and the presences of sectioning artifacts (also called "nuclear truncation"). Artifacts in assessing *PTEN* deletion can arise when

Fig. 1 Analysis of PCa needle core biopsies by PTEN immunohistochemistry and FISH. **a** Representative hematoxylin and eosin images of a needle ▶ core biopsy (×10 original magnification) with region of PCa as an enlarged inset (*rectangle* ×63 original magnification) to show an area of PCa with Gleason score 3 + 3 = 6. **b** There is uniform retention of PTEN protein expression in all malignant glands within this needle core section (×10 original magnification). The enlarged inset (*rectangle* ×63 original magnification) shows detail of a Gleason score 3 + 3 = 6 with PTEN protein expression. Stromal cells and benign glands act as an internal control and exhibit a similar level of PTEN protein expression. **c** *PTEN* four-color FISH image (×63 original magnification) from an area of PCa showing a normal chromosome 10 disomy pattern—two copies of *PTEN*. Note that *PTEN* intact (*red*) as well as pericentromic control probes (CEPs) (*pink*) and flanking gene probes *WAPAL* (*green*) and *FAS* (*aqua*) are intact in all untrucated cells. The *yellow circled nucleus* has two clusters of signals in which all probes are represented, consistent with a normal undeleted *PTEN* FISH pattern. **d** PTEN immunohistochemistry image (×200 magnification) from an adjacent section of PCa needle core to the FISH findings shown in **c** to illustrate PTEN protein expression in both cytoplasm and nucleus (×200 magnification). **e** *PTEN* FISH image (×63 original magnification) captured from a tumor tissue showing homozygous *PTEN* submicroscopic deletions. The *yellow circled nucleus* has the typical signal configuration for interstitial homozygous deletion involving the *PTEN* gene (*red signals* missing). Since both flanking probes are retained, the deletions are interstitial with the proximal break point between *WAPAL* (*green*) and *PTEN* (*red*) and the distal break point between *PTEN* (*red*) and *FAS* (*aqua*). **f** PTEN immunohistochemistry image (×200 magnification) from an adjacent section of PCa needle core to the FISH findings to illustrate loss of PTEN protein expression as indicated in the PCa regions in which *PTEN* homozygous deletion is apparent in **e**. The relative level of reduced level of PTEN protein IHC can be appreciated by comparison to PTEN protein retention in adjacent benign glands (*blue arrow*). **g** *PTEN* four-color FISH image (×63 magnification) captured from a tumor tissue showing a complex homozygous *PTEN* deletion in a tetrasomic for chromosome 10 cells. Note that in *yellow circle*, there is no *red signal*. Two chromosomes have a submiscroscopic *PTEN* deletion, another one has *PTEN* and *FAS* deletion, and the last one was completely deleted. **h** PTEN immunohistochemistry image (×200 magnification) from an adjacent section of PCa needle core to the FISH findings shown in **g** to illustrate PTEN protein expression levels when *PTEN* is homozygously deleted, demonstrating PTEN protein loss with heterogeneous pattern in tumor gland Gleason 6 with a focal loss of PTEN protein in tumor glands (*blue arrow*) and an adjacent tumor gland stained positively (*blue circle*). **i** *PTEN* FISH image (×63 magnification) captured from a tumor tissue from an area of PCa showing a hemizygous *PTEN* deletion. The *yellow circled nucleus* has one intact chromosome 10 with four signals (*pink*, *green*, *red*, and *aqua*), and the other chromosome has a hemizygous *PTEN* deletion (one *red signal* missing) with three signals retained (*pink*, *green*, and *aqua*). **j** PTEN immunohistochemistry image (×200 magnification) from an adjacent section of PCa needle core to the FISH findings shown in **i** to illustrate PTEN protein expression levels when *PTEN* is present as one copy (hemizygous deletion). There is no appreciable reduction in PTEN protein expression in either the cytoplasm or the nucleus of PCa cores in comparison to the surrounding benign or stomal cells. **k** *PTEN* FISH image (×63 magnification) captured from a tumor tissue from an area of PCa showing hemizygous *PTEN* and *FAS* terminal deletions with the break point between *WAPAL* (*green*) and *PTEN* (*red*). The *yellow circled nucleus* has one intact chromosome 10 with four signs (*pink*, *green*, *red*, and *aqua*) and the other chromosome with hemizygous *PTEN* and *FAS* deletions showing two signals (*pink* and *green*). **l** PTEN immunohistochemistry image (×200 magnification) from an adjacent section of PCa needle core to the FISH findings shown in **k** to illustrate PTEN protein expression levels when PTEN is hemizygously deleted, demonstrating reduced PTEN protein in tumor gland Gleason score 3 + 3 = 6 and PTEN protein retention in adjacent benign glands (*blue arrow*)

histologic sectioning cuts away the *PTEN* locus in cells in the section while leaving other probes from chromosome 10 in place. We have shown previously that use of the two probes immediately bracketing *PTEN* improves the fidelity of assessments of *PTEN* deletion [14]. The results of scoring the same tissue sections by each observer using this probe set showed a high level of agreement for detection of deletion status (see Supplementary Table 1). In cases with different clonal deletions, all areas marked by the pathologist were included into FISH analysis. Hemizygous (single copy) *PTEN* deletion was assigned when >50 % of nuclei exhibited clonal loss of *PTEN* and adjacent probes. Homozygous *PTEN* deletion was defined by a simultaneous lack of both *PTEN* locus signals in 30 % of scored nuclei [17].

PTEN IHC and interpretation

PTEN IHC was performed manually and blindly scored by two uropathologists (TLL and DMB) using a validated dichotomous scoring system [18] as described previously [12]. In brief, 4-μm biopsy sections were deparaffinized and rehydrated under standard conditions. Antigen unmasking was performed by steaming in EDTA buffer (pH 8.0) for 45 min. Endogenous peroxidase activity was quenched by incubation with peroxidase block for 5 min at room temperature. Slides were incubated for 45 min at room temperature (RT) with a rabbit anti-human PTEN antibody (Clone D4.3 XP; Cell Signaling, Danvers, MA; 1:50 dilution). A horseradish peroxidase-labeled polymer (PowerVision, Leica Microsystems, Bannockburn, IL) was applied for 30 min at RT, and signal detection was performed using 3,3′-diaminobenzidine tetrahydrochloride (DAB) as the chromogen. Slides were counterstained with hematoxylin, dehydrated, and mounted. Cases were considered to have PTEN loss if the intensity of cytoplasmic and nuclear staining was markedly decreased or entirely negative across >10 % of tumor cells compared to surrounding benign glands and/or stroma. Previously, the inter-observer reproducibility of the dichotomous scoring system developed for cytoplasmic/nuclear PTEN was shown to remain high [18] with disagreements about the immunohistochemistry scoring in 17/174 cases in the original study [12] and in only 11/111 biopsies for which there were definitive FISH results in the current study. In cases of disagreement, a third uropathologist (AMD) blindly scored the case to break the tie [12].

Statistical analysis

Means and proportions of characteristics, including pre- and post-operative factors, of upgraded cases and controls, were

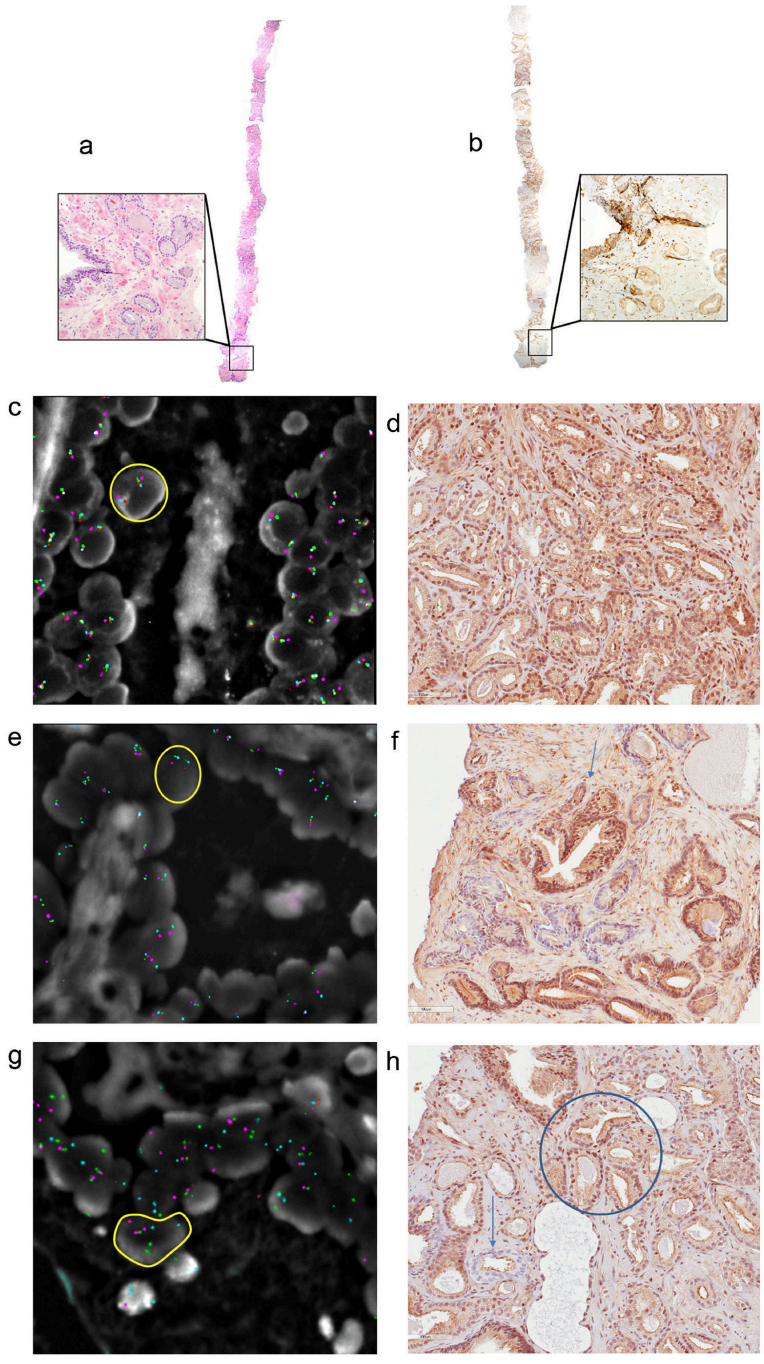
a
b
c
d
e
f
g
h

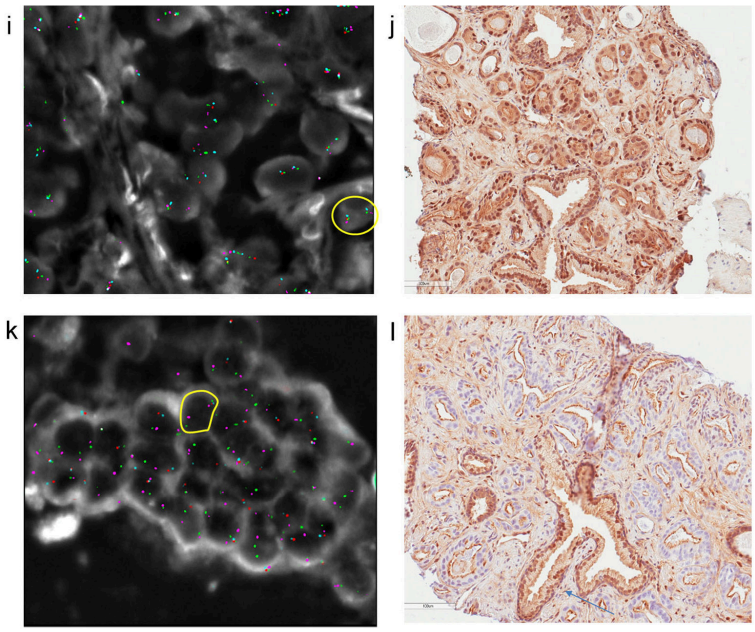

Fig. 1 (continued)

compared using the two-sample *t* test and the chi-squared test, respectively. Multivariable logistic regression was used to estimate the odds ratios (ORs) and 95 % confidence intervals (CIs) of upgrading for *PTEN* deletion. First, ORs were estimated adjusted for age at diagnosis. Next, ORs were adjusted for pre-operative PSA concentration (continuous, log-transformed) and clinical stage (binary, T2 or higher). ORs were further adjusted for race (binary, non-white), and finally, they were adjusted for the fraction of involved cores positive for tumor (continuous). Concordance for the presence and absence of PTEN was calculated as positive and negative agreements. Statistical analyses were performed using SAS 9.3 (Cary, NC, USA). Two-sided tests were conducted and a p value < 0.05 was considered to be statistically significant.

Results

Characteristics of upgraded cases and controls

Upgraded cases were slightly older at diagnosis than controls (62.2 vs. 59.1 years, $P = 0.005$; Table 1). The remaining characteristics, such as race, pre-operative serum PSA level, and clinical stage distribution, did not differ between the cases and controls. The majority of patients underwent radical prostatectomy within 3 months of biopsy diagnosis, and there was no significant difference in the pre-operative interval between the case and controls. Although the study was not designed to examine this, upgraded cases were non-statistically significantly more likely to subsequently experience PSA recurrence than controls (8 vs. 2 %). More than 90 % of both cases and controls had 12-core needle biopsies performed, with a comparable number of cores examined in cases and controls (11.8 vs. 12.1; Table 1). Both the number of involved cores (4.6 vs. 3.7) and the mean percentage of involved cores containing tumor (40 vs. 32 %) were higher in cases compared to controls ($P = 0.05$), although the maximum percent tumor per core was not significantly different. Tumor was present on bilateral cores (from the left and right prostate) in a higher percentage of the upgraded cases compared with controls (58 vs. 40 %, $P = 0.07$). However, the percentage of men with perineural invasion was not significantly different between the cases and controls. Upgraded cases and controls had similar prostate weights at radical prostatectomy (55 vs. 57.9 g, $P = 0.51$), and the post-operative pathologic stage distribution was not different between the two groups ($P = 0.38$). Upgraded cases were more likely to have positive margins at radical prostatectomy (20 vs. 5 %, $P = 0.01$).

PTEN FISH and PTEN IHC analysis

For each of the 111 samples, a uropathologist selected the histologic area(s) of the biopsy that contained PCa using the

corresponding hematoxylin and eosin-stained slide (Fig. 1a). Since each sample had previously been scored using PTEN IHC, it was necessary to identify the same regions of all biopsies containing PCa for FISH analysis using the adjacent section. Figure 1b illustrates an example of a biopsy with immunoreactivity for PTEN. The same area scored in an adjacent 4-μm section was used for *PTEN* FISH analysis (Fig. 1c). Within the region of interest, PCa cells selected for FISH analysis contained numerous intact, spherical, and non-overlapping cells with clear FISH signals for all four probes. The two probes *WAPAL* (green) and *FAS* (aqua) on either side of *PTEN* (red) provided information both also about the size of larger deletions (Table 2), and they were used to eliminate nuclei with sectioning truncation artifacts from the analysis. The centromere probe (pink) is an additional copy number control that is helpful when numerical changes affecting chromosome 10 are present in scored nuclei. In the example shown in Fig. 1c, there was no apparent *PTEN* deletion, which was in agreement with the strong immunoreactivity observed in the adjacent section (Fig. 1d).

In total, there were 19 biopsies with a *PTEN* deletion (15 homozygous and 4 hemizygous). Of the 92 biopsies scored as undeleted for *PTEN* by FISH, 89 were found to have intact PTEN protein by IHC (Table 3). There were three biopsies without PTEN immunoreactivity but with retention of both copies of the gene. Possibly, the *PTEN* gene in these samples underwent a submicroscopic deletion, point mutation, or epigenetic alteration that led to absence of protein expression. Alternatively, it is possible that misalignment of sections led to different regions of the biopsy being studied by FISH.

Homozygous *PTEN* deletion was readily detected by FISH analysis in these biopsies. A typical example of one of the 15 homozygous *PTEN* deletion is shown in Fig. 1e. In the adjacent section (Fig. 1f), the same area of carcinoma has no PTEN staining by IHC as expected, because both copies of the gene have been deleted. Among the 18 evaluable biopsies with decreased PTEN protein, 13 (72 %) showed a concurrent homozygous *PTEN* deletion by FISH in the same region of PCa scored for IHC (Table 3). The two biopsies that had a discordant finding of homozygous deletion by FISH but previously scored as PTEN protein intact by IHC were both from men who were not upgraded (i.e., controls). One biopsy had a discrete focal region of homozygous loss that had not been detected previously because it involved only a single gland (Fig. 1g, h). The other biopsy, which appeared to have a very low level of staining, was scored as PTEN protein indeterminate by two reviewers and the third reviewer scored it as intact.

Hemizygous *PTEN* deletion was of particular interest as the presence of one copy of an intact *PTEN* gene might be sufficient to maintain expression at levels indistinguishable to those typically observed by IHC in undeleted tumors. Four hemizygous deletions (three cases and one control) were detected (Tables 2 and 3). Among the 18 biopsies with decreased PTEN protein, two cases (11 %) had a hemizygous *PTEN* deletion by FISH that had been previously scored as PTEN protein intact by IHC. Figure 1i (FISH) and j (IHC) shows examples of an upgraded case with a hemizygous *PTEN* deletion in areas of PCa that did not lead to appreciable loss of PTEN immunoreactivity by IHC. Figure 1k, l shows adjacent sections from two hemizygous deletions (one case and one control) that were both scored as PTEN loss by IHC.

Comparison between PTEN IHC and *PTEN* FISH showed that the assays were highly concordant (Table 3), with 89/93 (96 %) of evaluated biopsies scored as having protein intact also showing undeleted *PTEN* by FISH. In total, 15/18 of the biopsies with PTEN loss showed homozygous or hemizygous *PTEN* deletion by FISH. Only 4 biopsies of the 93 (4 %) with PTEN intact had a deletion by FISH, and all 4 had biopsies in which intra-tumoral heterogeneity could explain assay discordancy.

Table 2 Types of *PTEN* deletions found in cases and controls

	Number
Homozygous *PTEN* deletion	15
PTEN homozygous	2
PTEN homozygous/*FAS* hemizygous	2
PTEN homozygous/*WAPAL* hemizygous	1
PTEN homozygous/*WAPAL* and *FAS* hemizygous	7
PTEN homozygous/*FAS* hemizygous/*WAPAL* and CEP gain	2
PTEN and *FAS* homo/*WAPAL* and CEP hemizygous	1
Hemizygous *PTEN* deletion	4
PTEN hemizygous	1
PTEN and *FAS* hemizygous	1
PTEN, *WAPAL*, and *FAS* hemizygous	2

FAS FISH genomic probe containing Fas cell surface death receptor gene, *WAPAL* FISH genomic probe containing wings apart-like homolog gene, *CEP* FISH pericentromeric region probe from chromosome 10

Variations of PTEN loss at the gene and protein levels

Some of the biopsies previously studied by IHC [12] exhibited intra-tumoral heterogeneity (18/174) or had staining results difficult to interpret where two reviewers disagreed (17/174), with substantial overlap between these groups. All regions of PCa showing different intensities of IHC immunoreactivity or exhibiting focal losses of PTEN were systematically scored using *PTEN* FISH. One control showed a heterogeneous result with a mixture of homozygous and hemizygous deletion areas. However, the IHC pattern for this biopsy indicated a uniform pattern PTEN loss in this region of PCa. Similarly, one case had a hemizygous deletion of *PTEN* (Fig. 2a), in which the same area

Table 3 Concordance in PTEN functionality between IHC and FISH in upgraded cases and controls combined, *n* (%)

IHC	FISH			Total
	PTEN deletion		No *PTEN* deletion	
	Homozygous	Hemizygous		
PTEN loss	13 (11.8 %)	2 (1.8 %)	3 (2.7 %)	18 (16.3 %)
PTEN intact	2 (1.8 %)	2 (1.8 %)	89 (80.1 %)	93 (83.7 %)
Total	15 (13.6 %)	4 (3.6 %)	92 (82.8 %)	111 (100 %)

containing PCa in the adjacent section showed reduced staining by IHC intermingled with discrete regions of tumor with PTEN-positive immunoreactivity (Fig. 2b).

The most common type of *PTEN* deletion observed was a homozygous deletion in which a large deletion on one chromosome was accompanied by interstitial loss affecting the other chromosome 10. In these biopsies, a proximal break point occurred between *WAPAL* and *PTEN* and a distal break point between *PTEN* and *FAS*. The other chromosome had a large proximal deletion involving *WAPAL*, *PTEN*, and *FAS*. Seven biopsies (four cases and three controls) exhibited this type of loss (see Table 2). In addition to the 19 biopsies with a

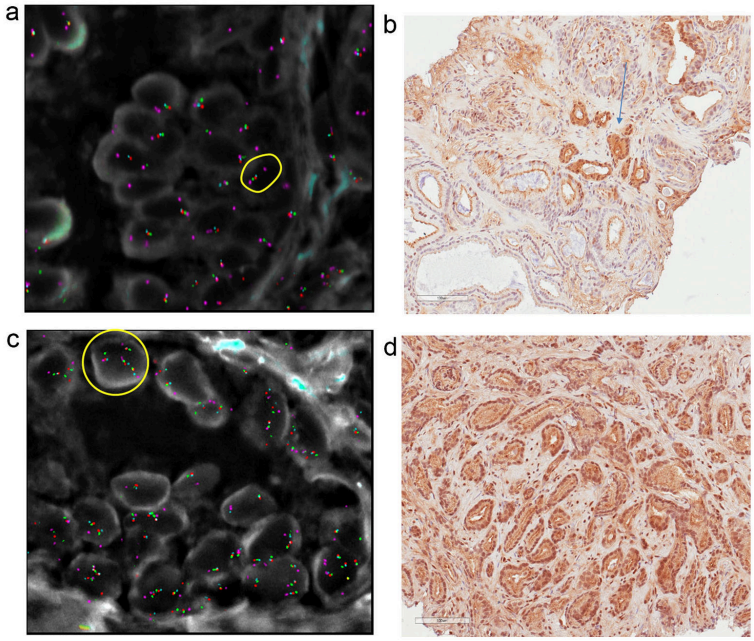

Fig. 2 Variables of PTEN copy number and heterogeneous protein expression by IHC. **a** *PTEN* four-color FISH image (×63 magnification) captured from a tumor tissue showing hemizygous PTEN large deletion of 10q with the breaking point between CEP (*pink*) and *WAPAL* (*green*). The *yellow circle* shows one intact chromosome 10 with four signs (*pink*, *green*, *red*, and *aqua*) and the other chromosome with just the centromere of chromosome 10 (*pink*). **b** PTEN immunohistochemistry image (×200 magnification) from an adjacent section of PCa needle core to the FISH findings shown in **a** to illustrate PTEN protein expression levels when *PTEN* is hemizygously deleted, demonstrating PTEN protein loss with heterogeneous pattern in tumor gland Gleason 6 with PTEN protein loss in tumor gland and an adjacent tumor gland stained positively (*blue arrow*). **c** *PTEN* FISH image (×63 magnification) of PCa shows gains of chromosome 10 without a *PTEN* deletion. The *yellow circled nucleus* has four clusters of signals in which all probes are represented, consistent with tetrasomy or four copies of all probes including *PTEN*. **d** PTEN immunohistochemistry image (×200 magnification) from an adjacent section of PCa needle core to the FISH findings shown in **c** to illustrate PTEN protein expression levels when *PTEN* has additional copies in each nucleus. The PTEN IHC demonstrates positive staining diffusedly in both the cytoplasm and nucleus in PCA Gleason score 3 + 3 = 6

PTEN deletion, there were 7 biopsies with extra copies of chromosome 10 and *PTEN* gain. In the example shown in Fig. 2c, there was chromosomal gain leading to additional copies of the *PTEN* gene in all tumor cells. This tumor also exhibited strong immunoreactivity of PTEN (Fig. 2d). In total, the seven biopsies (two cases and five controls) with chromosomal gain and extra copies of *PTEN* all had intact PTEN by IHC.

Association between *PTEN* deletion by FISH and Gleason upgrading

Prevalence of PTEN loss by IHC and *PTEN* deletion by FISH ($P = 0.03$) was significantly higher in upgraded cases than in controls (Table 4). After adjusting for age, the OR of upgrading for deletion of one or two copies of *PTEN* by FISH was 3.40 (95 % CI 1.14–10.11; Table 5). After further adjusting for known prognostic markers, the association was only modestly attenuated (Table 5). Results were similar when restricted to patients who all had at least 12 biopsy cores taken. In total, there were 36 samples that were upgraded from Gleason 3 + 3 = 6 to Gleason 3 + 4 = 7. Of these, 10 samples had a *PTEN* deletion by FISH. Only nine samples were upgraded from Gleason 3 + 3 = 6 to Gleason 4 + 3 = 7, and of these, two had *PTEN* deletions.

Discussion

The *PTEN* gene and PTEN protein show promise for identifying aggressive PCa. Loss of PTEN function is strongly associated with key properties of the aggressive cancer phenotype such as cell survival, proliferation, migration, adhesion, and invasion [19]. *PTEN* is almost always lost by genomic deletion in PCa, so that FISH has historically been the standard assay to detect in situ PTEN loss in tumor tissue. *PTEN* deletion detected by FISH has been reported to occur in 20–30 % of PCa cases [2–4], and PTEN loss is strongly associated with aggressive disease and PCa-specific death [3, 4, 6–8]. However, the majority of studies to date using either FISH or IHC have been performed retrospectively using prostatectomy tissue microarray sets. To be of practical value for improving PCa management in the clinic, PTEN assays, such as FISH and IHC, must be sensitive, specific, and reliable on needle core biopsy tissue sections at diagnosis. In this study, we compared the performance of FISH to IHC in needle core biopsies from 111 cases and controls, in whom it was recently shown that PTEN loss by IHC is associated with upgrading from Gleason 6 on biopsy to Gleason 7+ at radical prostatectomy [12].

Table 4 PTEN loss by IHC and *PTEN* deletion by FISH in upgraded cases and controls

	Cases ($n = 45$)	Controls ($n = 66$)	*P* value
PTEN loss by IHC, *n* (%)[a]	12 (26.7 %)	6 (9.1 %)	0.01
PTEN deletion by FISH, *n* (%)[a]	12 (26.7 %)	7 (10.6 %)	0.03

[a] Hemizygous or homozygous deletion

The main prognostic tool for newly diagnosed PCa is currently the Gleason score. However, upgrading of the Gleason score from the biopsy to the radical prostatectomy still occurs in 26–50 % of patients [20]. Difficulties encountered when determining the Gleason score of biopsies include inter-observer variability, particularly when assessing small-tumor foci in biopsies. In recent years, improvements in antibody specificity have led to an increasing interest in using IHC to evaluate the loss of PTEN expression as an additional prognostic biomarker to traditional assessment of risk. Two recent studies using prostate cancer needle biopsies have shown a positive association between PTEN loss, as determined by IHC, with Gleason upgrading [12] and poor outcome [11].

IHC has been shown to efficiently fit readily into the workflow of a routine diagnostic pathology clinical service at modest cost, allowing the assay to be performed in a timely way well suited to clinical service needs. IHC is an alternative method for detecting the consequences of *PTEN* genomic deletion as detected by FISH, since submicroscopic alterations such as point mutations or promoter methylation may lead to loss of protein expression, which can be readily detected by IHC. Since these molecular mutations cannot be detected by FISH assays, IHC is a more comprehensive method for loss of function screening. Another advantage of IHC is that PTEN loss may be genotypically heterogeneous, comprising of one or more distinct clones in primary PCa [21–23]. Thus, detection of *PTEN* deletion by FISH alone may be technically challenging, while systematic analysis with IHC to search for areas of PCa with reduced PTEN immunoreactivity provides an easy approach to initially screen for regions of focal loss.

FISH has some distinct advantages over IHC for detecting emerging clones of PCa in which a few hundred cells may have undergone a *PTEN* deletion against a background of PCa with undeleted *PTEN*. Since small areas of homozygous deletion are relatively easy to detect by FISH, we have shown the value of incorporating FISH when there is uncertainty about PTEN IHC, the Gleason score, or when there is intra-tumoral heterogeneity. In both cases and controls, a few cases showed a distinct "patchy presentation" of IHC staining within the glands that made it difficult to identify individual cells with PTEN loss without the additional information provided by *PTEN* FISH. In 11 of the 17 equivocal biopsies by

Table 5 Association between *PTEN* deletion by FISH and Gleason upgrading

Model	Number of cases/controls	Hemizygous or homozygous *PTEN* deletion[a]	
		OR (95 % CI)	*P* value
All men	45/66		
Age-adjusted		3.40 (1.14–10.11)	0.03
Multivariable-adjusted A[b]		3.08 (0.99–9.55)	0.05
Multivariable-adjusted B[c]		3.29 (1.03–10.53)	0.05
Multivariable-adjusted C[d]		2.77 (0.85–9.04)	0.09
Men with 12+ biopsy cores	41/62		
Age-adjusted		3.31 (1.06–10.37)	0.04
Multivariable-adjusted A[b]		3.05 (0.94–9.93)	0.06
Multivariable-adjusted B[c]		3.05 (0.92–10.09)	0.07
Multivariable-adjusted C[d]		2.72 (0.81–9.17)	0.11

[a] Hemizygous (single copy) *PTEN* deletion was assigned when >50 % of nuclei exhibited clonal loss of *PTEN* and adjacent probes. Homozygous *PTEN* deletion was defined by a simultaneous lack of both *PTEN* locus signals in 30 % of scored nuclei

[b] Additionally adjusted for preoperative PSA (continuous, log-transformed) and clinical stage (binary, T2 or higher)

[c] Additionally adjusted for preoperative PSA (continuous, log-transformed), clinical stage (binary, T2 or higher), and race (binary, nonwhite)

[d] Additionally adjusted for preoperative PSA (continuous, log-transformed), clinical stage (binary, T2 or higher), race (binary, nonwhite), and fraction of cores with tumor involvement (continuous)

IHC, we were able to show that an emerging subclonal homozygous or hemizygous deletion might account for the small foci of loss that were inconclusive by IHC. Another advantage of this four-color FISH assay is that hemizygous deletions can be readily detected. These deletions led to loss of PTEN in two cases, but in one case and one control, retention of PTEN was present, even though one copy of the gene was deleted. In these latter two examples of hemizygous deletion, the presence of PTEN indicates that the remaining unaffected *PTEN* gene is presumably expressing sufficient protein to be scored as PTEN intact by IHC. However, the presence of the hemizygous deletion might be an indication that both tumors are more likely to have an unfavorable prognosis, despite retaining what appears to be normal levels of PTEN protein. One technical limitation of this study was the difficulty in aligning the area to be studied by FISH with the same region studied previously by IHC. Alignment variation may have resulted in discordancy in a small proportion of cases and controls. This would be less likely problematic when sequential sections are processed specifically for FISH and IHC as part of a systematic clinical assay. Another technical challenge for future routine clinical use will be the high level of analytical expertise required to interpret the complex signal configurations that may be encountered when four-color FISH probes are used. However, the benefits with the *PTEN* probe design used in this study outweigh this disadvantage, as sectioning artifacts are less likely to bias interpretations.

If PTEN loss is independently associated with upgrading, it could be assayed alone or in combination with other emerging biomarkers such as TMPRSS-ERG that may add additional information [8]. Using HER-2 status in breast cancer as a model [24], the availabilities of both IHC and FISH assays for PTEN status offer the prospect of implementing the most informative biomarker combination in needle core biopsies of PCa. Collectively, the recent data using needle core biopsies [11, 12] and the findings of this present manuscript draw attention to the value of PTEN as a possible biomarker in men with biopsies indicative of lower-risk disease and suggest a possible clinical workflow for assessing PTEN status at first diagnosis. For example, initial analyses of PTEN expression could be carried out using IHC with established methods [12]. In biopsies with equivocal findings or histopathologic discordance, a reflex *PTEN* FISH test could be ordered with a specific request to analyze PCa in areas of uncertainty by IHC. Based on the number of cases and controls with inconclusive findings in this study, we estimate that no more than 10 % of samples would require reflex FISH testing. However, a larger study would be needed to determine more precisely the optimal use of both technologies in predicting Gleason upgrading.

In conclusion, our findings suggest that *PTEN* deletion by FISH in needle biopsies provides an important additional tool to assist urologists and patients making treatment decisions when faced with low- to intermediate-risk prostate cancer. In this study, FISH and immunohistochemistry were concordant,

showing consistent positive associations between PTEN loss and upgrading. Moreover, we showed that in some situations, FISH provided a more precise approach to the examination of areas of cancer with heterogeneous staining when immunohistochemistry was uncertain. Given the findings of this FISH study and the previous companion IHC study [12], determining loss of PTEN by FISH and IHC holds significant promise for improved patient care. Future studies will be needed to define optimal workflows using these methods to best provide the added prediction of PTEN loss for upgrading in the context of established markers such as PSA level, number of positive core biopsies, percent of cores involved by tumor, and Gleason score.

Acknowledgments Funding for this research was provided in part by a Prostate Cancer Foundation Young Investigator Award (TLL), a grant from David Koch administered by the Patrick C. Walsh Prostate Cancer Research Fund (TLL), and the NIH/NCI Prostate SPORE P50CA58236. TV was supported by Coordenação de Aperfeiçoamento de Pessoal de Nivel Superior (CAPES) in Brazil. JAS and CGPA were supported by the Conselho Nacional de Desenvolvimento Científico e Tecnológico (CNPq) in Brazil.

Compliance with ethical standards

Conflicts of interest Jeremy Squire has consulted for CymoGenDx LLC.

References

1. Verhagen PCMS, van Duijn PW, Hermans KGL et al (2006) The PTEN gene in locally progressive prostate cancer is preferentially inactivated by bi-allelic gene deletion. J Pathol 208(5):699–707. doi:10.1002/path.1929
2. Yoshimoto M, Cunha IW, Coudry a RA et al (2007) FISH analysis of 107 prostate cancers shows that PTEN genomic deletion is associated with poor clinical outcome. Br J Cancer 97(5):678–685. doi:10.1038/sj.bjc.6603924
3. Reida HM, Attard G, Ambroisine L et al (2010) Molecular characterisation of ERG, ETV1 and PTEN gene loci identifies patients at low and high risk of death from prostate cancer. Br J Cancer 102(4):678–684. doi:10.1038/sj.bjc.6605554
4. Krohn A, Diedler T, Burkhardt L et al (2012) Genomic deletion of PTEN is associated with tumor progression and early PSA recurrence in ERG fusion-positive and fusion-negative prostate cancer. Am J Pathol 181(2):401–412. doi:10.1016/j.ajpath.2012.04.026
5. Burdelski C, Reiswig V, Hube-Magg C et al. (2015) Cytoplasmic accumulation of sequestosome 1 (p62) is a predictor of biochemical recurrence, rapid tumor cell proliferation and genomic instability in prostate cancer. Clin Cancer Res 1. doi:10.1158/1078-0432.CCR-14-0620.
6. Troyer DA, Jamaspishvili T, Wei W et al. (2015) A multicenter study shows *PTEN* deletion is strongly associated with seminal vesicle involvement and extracapsular extension in localized prostate cancer. Prostate :n/a - n/a. doi:10.1002/pros.23003.
7. Sircar K, Yoshimoto M, Monzon FA et al (2009) PTEN genomic deletion is associated with p-Akt and AR signalling in poorer outcome, hormone refractory prostate cancer. J Pathol 218(4):505–513. doi:10.1002/path.2559
8. Cuzick J, Yang ZH, Fisher G et al (2013) Prognostic value of PTEN loss in men with conservatively managed localised prostate cancer. Br J Cancer 108(12):2582–2589. doi:10.1038/bjc.2013.248
9. Boström PJ, Bjartell AS, Catto JWF et al. (2015) Genomic predictors of outcome in prostate cancer. Eur Urol. doi:10.1016/j.eururo.2015.04.008.
10. Punnen S, Freedland SJ, Presti JC et al (2014) Multi-institutional validation of the CAPRA-S score to predict disease recurrence and mortality after radical prostatectomy. Eur Urol 65(6):1171–1177. doi:10.1016/j.eururo.2013.03.058
11. Mithal P, Allott E, Gerber L et al. (2014) PTEN loss in biopsy tissue predicts poor clinical outcomes in prostate cancer. Int J Urol.
12. Lotan TL, Carvalho FL, Peskoe SB et al (2014) PTEN loss is associated with upgrading of prostate cancer from biopsy to radical prostatectomy. Mod Pathol 28(1):1–10. doi:10.1038/modpathol.2014.85
13. Shah RB, Bentley J, Jeffrey Z, Demarzo AM (2015) Heterogeneity of PTEN and ERG expression in prostate cancer on core needle biopsies: implications for cancer risk stratification and biomarker sampling. Hum Pathol 46(5):698–706. doi:10.1016/j.humpath.2015.01.008
14. Yoshimoto M, Ludkovski O, Degrace D et al (2012) PTEN genomic deletions that characterize aggressive prostate cancer originate close to segmental duplications. Genes Chromosom Cancer 51(2):149–160. doi:10.1002/gcc.20939
15. Epstein JI, Allsbrook WC, Amin MB, Egevad LL (2006) Update on the Gleason grading system for prostate cancer: results of an international consensus conference of urologic pathologists. In: Advances in Anatomic Pathology 13:57–59. doi:10.1097/01.pap.0000202017.78917.18.
16. Pound CR, Partin AW, Eisenberger MA, Chan DW, Pearson JD, Walsh PC (1999) Natural history of progression after PSA elevation following radical prostatectomy. JAMA 281(17):1591–1597. doi:10.1097/00005392-199910000-00103
17. Ventura RA, Martin-Subero JI, Jones M et al (2006) FISH analysis for the detection of lymphoma-associated chromosomal abnormalities in routine paraffin-embedded tissue. J Mol Diagn 8(2):141–151. doi:10.2353/jmoldx.2006.050083
18. Lotan TL, Gurel B, Sutcliffe S et al (2011) PTEN protein loss by immunostaining: analytic validation and prognostic indicator for a high risk surgical cohort of prostate cancer patients. Clin Cancer Res 17(20):6563–6573. doi:10.1158/1078-0432.CCR-11-1244
19. Song MS, Salmena L, Pandolfi PP (2012) The functions and regulation of the PTEN tumour suppressor. Nat Rev Mol Cell Biol 13(5):283–296. doi:10.1038/nrm3330
20. Hoogland AM, Kweldam CF, Van Leenders GJLH (2014) Prognostic histopathological and molecular markers on prostate cancer needle-biopsies: a review. Biomed Res Int 2014:1–12. doi:10.1155/2014/341324
21. Krohn A, Freudenthaler F, Harasimowicz S et al. (2014) Heterogeneity and chronology of PTEN deletion and ERG fusion in prostate cancer. Mod Pathol :1–9. doi:10.1038/modpathol.2014.70.
22. Gumuskaya B, Gurel B, Fedor H et al (2013) Assessing the order of critical alterations in prostate cancer development and progression by IHC: further evidence that PTEN loss occurs subsequent to ERG gene fusion. Prostate Cancer Prostatic Dis 16(2):209–215. doi:10.1038/pcan.2013.8
23. Yoshimoto M, Ding K, Sweet JM et al. (2013) PTEN losses exhibit heterogeneity in multifocal prostatic adenocarcinoma and are associated with higher Gleason grade. Mod Pathol 1–13. doi:10.1038/modpathol.2012.162.
24. Wolff AC, Hammond MEH, Hicks DG et al (2013) Recommendations for human epidermal growth factor receptor 2 testing in breast cancer: American Society of Clinical Oncology/College of American Pathologists clinical practice guideline update. J Clin Oncol 31(31):3997–4013. doi:10.1200/JCO.2013.50.9984